The Pennsylvania State University

The Graduate School

PROTEIN AGGREGATION, FRAGMENTATION AND ITS ROLE IN NEURODEGENERATIVE DISEASES.

A Dissertation in

Chemistry

by

Ashlesha Bhide

Submitted in Partial Fulfillment of
the Requirements
for the Degree of

Doctor of Philosophy

December 2023

The dissertation of Ashlesha Bhide was reviewed and approved by the following:

Ayusman Sen
Verne M. Willaman Professor of Chemistry
Distinguished Professor of Chemistry
Professor of Chemical Engineering
Dissertation Advisor
Chair of Committee

Christine D. Keating
Distinguished Professor of Chemistry

Igor Aronson
Huck Chair Professor of Biomedical Engineering, Chemistry and Mathematics.

James Adair
Professor of Materials Science and Engineering, Biomedical Engineering, and Pharmacology

Philip Bevilacqua
Professor of Chemistry
Head of the Department of Chemistry

ABSTRACT

Aggregation refers to the accumulation or clumping together of proteins. Aggregates can be characterized based on the size of aggregates, reversibility, structure of the aggregate and the conformation of proteins within aggregates. Protein aggregation plays an important role in neurodegenerative diseases and it is important to understand it so that we can find cures to these diseases. It could also cause errors in experimental measurements if assumptions are made about the size of the protein. The work presented here clarifies various aspects of protein aggregation and its role in neurodegenerative diseases as well as its application in targeted drug delivery.

In Chapter 2, I investigate the aggregation and fragmentation of enzymes. Our lab has previously studied the enhanced diffusion of enzymes. Previous papers have shown that enzymes diffuse faster when the substrate of the enzyme is present. However, if the size of the enzyme changes, the diffusion will change inversely. So, if there is a change in the diameter of enzymes due to aggregation or fragmentation, it could cause artifacts in diffusion measurements. I investigated this phenomenon for enzymes in the presence of chemicals that are relevant to its catalysis such as the substrate of the enzyme, co-factor, product of the reaction etc. Using Fluorescence Resonance Energy Transfer (FRET), I showed that glucose oxidase fragments in the presence of its substrate, D-Glucose but not its non-substrate enantiomer, L-Glucose. I was also able to identify that a minimum of 0.3mM D-Glucose is needed to cause fragmentation. Interestingly, this is lower than the blood glucose concentration (4-6mM). This study showed that we cannot assume that the size of enzymes remains the same during catalysis.

It is known that the enzyme, alkaline phosphatase also plays a role in Alzheimer's disease (AD). Alkaline phosphatase activity increases in Alzheimer's disease but the cause for this increase in activity was not known. It is important to investigate this activity increase because alkaline phosphatase plays a role in neurodegeneration by dephosphorylating tau protein in the extracellular space which causes death of other neurons and helps the progression of the disease. Using various spectroscopic methods, I show that the activity of alkaline phosphatase increases in the presence of the peptide, amyloid - β and acetylcholinesterase. I also show that the activity increases occur in the presence of high concentrations of acetylcholine and choline. Using FRET, I also demonstrate that there is an interaction between amyloid - β and alkaline phosphatase. These conditions occur during the disease or might occur due to various drugs that are used for treating AD. By investigating this, we aim to clarify the role of alkaline phosphatase in the disease.

I also investigate the application of protein aggregation in targeted drug delivery systems in Chapter 4. Lipid-based delivery systems are commonly used for drug delivery due to their spherical compartmentalized structure and biocompatibility. In this work, using dynamic light scattering (DLS) and confocal microscopy, I demonstrate that we can obtain precise control over the aggregation of uncoated and protein-coated liposomes in the presence of salts such as zinc nitrate and calcium nitrate. The proteins we use are streptavidin and avidin. Our results show that liposome aggregation can be controlled selectively based on the protein attached to the outside of liposomes and the concentration of the salt solution added. I also demonstrate that we can control the aggregation of hard particles such as streptavidin-coated microspheres. By precisely controlling their aggregation in the presence of certain metal salts, we can improve the efficiency of lipid-based targeted drug delivery.

TABLE OF CONTENTS

LIST OF FIGURES

LIST OF TABLES

ACKNOWLEDGEMENTS

First and foremost, I want to thank my advisor, Ayusman Sen for his guidance and support during my time in grad school. Thank you for teaching me how to come up with research ideas, solve problems and be a good researcher. I also appreciate your support and willingness to let me pursue research ideas that I was interested in. I am grateful for my thesis committee members Dr. Christine Keating, Dr. Igor Aronson and Dr. James Adair. Dr. Keating, I appreciate all your advice during committee meetings and also your kindness for allowing me to use instruments in your lab. Dr. Aronson and Dr. Adair, thank you for your guidance and helpful advice during my grad school journey. I also want to thank Penn State and the chemistry department for providing the support that I needed throughout the last 5 years.

I want to thank both the past and present members of the Sen lab. Xi, Farzad, Allan, Alicia, Ben, Matt, Kayla, Josh and Ambika, thank you for welcoming me to the lab and teaching me various experimental and data analysis techniques as well as answering all my questions about graduate school life. Angus, Niladri, Jiaqi, Aditya, Sanjana, Yu-Ching, Errie, Shanid and Chamika, thank you for being great peers and friends. Thank you to everyone for being awesome lab mates and friends and for making the past 5 years enjoyable. I enjoyed all our discussions in the kitchen, group lunches, coffee runs, soccer games, attending events etc.

I also want to thank my friends outside of graduate school. I enjoyed being a part of various student organizations or groups such as Association for India's Development, Chemistry GSA and Graduate Women in Science (GWIS) and MRSEC. Thank you to Rohitha, Sanjana, Sujata, Mahaan, Shiva and many others for being an awesome part of AID and enriching my experience.

I also want to thank Kristin, Tiffany, Brooke and Sarah for giving me an opportunity to do science outreach. Thank you for all your support and guidance when I was a part of MRSEC.

I am also thankful to my professors and mentors at Institute of Chemical Technology (ICT) Mumbai as well as at my school and junior college for helping me identify my love for chemistry and supporting me in my journey to grad school. I also appreciate all my friends from ICT (Rucha, Patki, Vaidehi, Radhika, Apoorva, Suyash and many others) that were always a call away whenever I needed advice, encouragement or support. Thank you to my grad school friends Aishwarya, Rohitha, Pranav, Sanjana, Chinmay etc for always being there. I enjoyed all our potlucks, movie nights, hikes, trips and other activities.

I would also like to thank my parents, Baba (Dhananjay) and Aai (Mrudula) for everything that they have done for me that has helped me get to this stage. I appreciate all the long calls and your support when I faced difficulties and was anxious about things. Thank you to my extended family for all their help, guidance and blessings. I also enjoyed all our meet-ups when I got a chance to go back to India. I also want to thank my partner, Aditya Lele for being a constant source of support during this entire grad school journey. I appreciate all the love, laughter, encouragement and joy that you brought to my life.

I want to thank the funding agencies for their support. The work in this thesis is funded by the Air Force Office of Scientific Research FA9550-20-1-0393. Any findings or conclusions expressed in this dissertation are those of the authors and do not necessarily reflect the views of the Air Force Office of Scientific Research.

Chapter 1

1 Introduction

1.1 Background and Motivations

Proteins are essential for our survival due to the important role that they play in various cellular functions. They are also used extensively in the pharmaceutical, textile and food industry for various commercial processes[1,2]. Protein aggregation refers to the accumulation or clumping together of proteins. It is generally believed that it occurs due to abnormal associations formed between them due to degradation or misfolding[3]. Based on the conditions and the proteins studied, aggregates of various structures, sizes and compositions have been observed. Due to its critical role in neurodegenerative diseases[4], the aggregation of proteins has been studied extensively. However, numerous questions related to its cause and nature remain unanswered. Solving these problems would have enormous benefits for not only improving human health, but also for optimizing these commercial processes and avoiding artifacts in experimental observations. In this work, I focus particularly on the aggregation of proteins that catalyze reactions, also known as enzymes as well as protein aggregation in neurodegenerative diseases and the role of protein

aggregation in drug delivery. To understand protein aggregation, it is important to understand the mechanism behind the phenomenon as well the challenges associated with studying this topic.

1.1.1 Mechanism of protein aggregation

Aggregation of proteins can be caused by a variety of external and internal factors[5]. External factors include stress-causing processes such as changes in temperature, agitation, change in solvent etc[6] and the extent to which certain stresses cause aggregation will depend on the individual protein. These stresses must be taken into consideration while using proteins for laboratory research or industrial processes. However, it is possible that aggregation can also occur without any external stresses. If the native protein has a tendency to associate with itself due to its structure, it can aggregate without the presence of any external stress. This tendency could occur due to presence of certain hydrophobic residues on the outer structure, that increase its 'stickiness' to other proteins. Other mechanisms for aggregation include nucleation or surface-induced aggregation[5]. Nucleation-induced aggregation occurs due to the formation of a small core known as a nucleus of aggregated proteins which then promotes the association of other proteins to it[7] while surface-induced aggregation occurs due to the association of proteins with a structure[8]. Observed aggregation could be a combination of any of these factors. Understanding these mechanisms can help us identify the ones that play a role in our system.

1.1.2 Challenges associated with studying protein aggregation

Accurate and reliable determination of protein aggregation is challenging. Experimental characterization of aggregates is done using various methods such as particle size determination,

chromatographic techniques and use of fluorescent dyes that show a spectral change upon interaction with aggregates[9]. Particle size determination of aggregates in the nanometer to micrometer range is usually done using scattering techniques such as Dynamic Light Scattering (DLS)[10]. With DLS, accurate detection of particle size is difficult for non-monodisperse samples. For chromatographic or spectroscopic techniques[11], sample alteration due to dilution, ionization or interaction with components used while using these methods could cause problems[12]. For fluorescent dyes, interaction with these dyes can alter the chemistry nature of proteins. Morphology of aggregates can be identified using microscopy techniques such as Atomic Force Microscopy (AFM) or Transmission Electron Microscopy (TEM)[9,13]. However, these methods could involve staining the sample with heavy metals or adhering the sample to a surface which could interfere with the aggregation process.

All the problems mentioned above could lead to incorrect or inconsistent results in the determination of protein aggregates. Recent research has delved into improving some of these methods. While these techniques are being developed, to ensure that there are no artifacts in the measurements, using a combination of various techniques will help eliminate some problems and validate results.

1.2 Enzyme Powered Motion and Assembly

Enzymes are defined as proteins that can act as biological catalysts. Enzyme powered motion and assembly is an emerging field of research and significant progress has been achieved so far. It has been shown that enzymes in solution can act as nano-sized motors while catalyzing reactions. In the presence of their substrate, they show both enhanced diffusion and chemotaxis, which could

lead to the formation of metabolons. In this section, I provide a brief overview of the work that is done in the field of enzyme powered motion and assembly.

1.2.1 Enzyme Enhanced Diffusion

Enzyme enhanced diffusion states that free-swimming enzymes in solution diffuse faster when their substrate is present in solution as opposed to when their substrate is absent. The first study of enzyme enhanced diffusion was carried out by Muddana et. al[14]. They showed that the diffusion coefficient of urease enhances when it is in a solution of its substrate, urea (Figure 1-1(a)). Since then, people have observed that multiple enzymes show this phenomenon[15,16,17]. However, these observations are highly debated[18]. There have been reports of contradictions in experimental observations (Figure 1-1 (b)). Multiple studies performed on the same enzyme show different amounts of enhanced diffusion. For example, Riedel et. al. observed an 80% increase in diffusion for alkaline phosphatase in the presence of its substrate while Günther et. al. observed 0% enhanced diffusion for alkaline phosphatase[15,19]. It has been suggested that dissociation, substrate binding or quenching of fluorescence could cause artifacts in Fluorescence Correlation Spectroscopy (FCS) measurements that are commonly used to study enhanced diffusion[19].

We know that the diffusion of particles in liquids is given by the Stokes-Einstein equation. This equation is given below (Equation 1-1),

$$D = \frac{k_B T}{6\pi\mu r} \tag{1-1}$$

where D is diffusion coefficient, T is the temperature k_B is the Boltzmann's constant, μ is the solvent viscosity and r is the particle radius,

According to this equation, there is an inverse correlation between diffusion and size. Changes in the size of enzymes due to aggregation or fragmentation could affect diffusion measurements. Thus, it is important to know and understand protein aggregation so that these problems can be solved.

(a) (b)

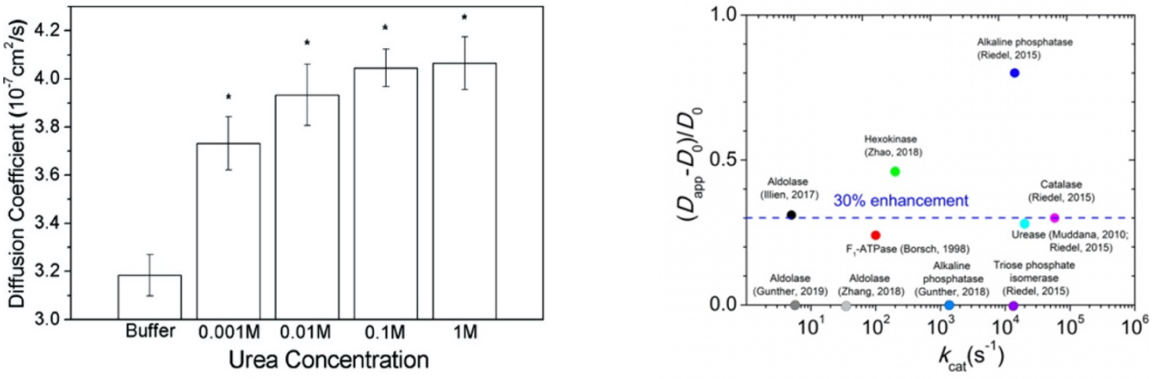

Figure 1- 1: (a) Diffusion coefficient of urease measured in the presence of different concentrations of urea. As urease converts urea to ammonium ions and bicarbonate, the diffusion coefficient of urease increases. This increase corresponds to the concentration of urea. As the concentration of urea increases, the diffusion coefficient also shows an increase. Reprinted with permission from J Am Chem Soc 2010 Feb 24;132(7):2110-1 Copyright 2010 American Chemical Society. (b) Differences in enhanced diffusion measurements observed in different studies compared with the turnover rate of the enzyme. It can be observed that the enhancements ranging from 0% to almost 100% have been observed in the reported studies. Reprinted from ACS Cent. Sci. 2019, 5, 939−948 https://doi.org/10.1021/acscentsci.9b00228 Copyright 2019.

1.2.2 Enzyme Chemotaxis and Metabolon Formation

Enzyme chemotaxis is defined as the movement of enzymes along a gradient of a corresponding species. Along with enhanced diffusion, researchers have shown that enzymes show

chemotaxis towards their substrate. In 2013, Sengupta et. al. showed that two enzymes, catalase and urease moved towards hydrogen peroxide and urea when subjected to their gradient in a microfluidic channel (Figure 1-2 (a))[20]. Since then, there has been considerable interest in this phenomenon. It has been demonstrated that chemotaxis can be used for separation of active and inactive enzymes in a 2-inlet-5 outlet channel[21]. The phenomenon has also been extended to enzyme-coated liposomes. Based on the compound added and the enzyme that was used for coating of liposomes, Somasundar et. al. demonstrated that liposomes coated with enzymes could undergo both positive and negative chemotaxis[22].

Enzymes that are part of a cascade and catalyze sequential reactions can form metabolons to achieve substrate channeling. Enzyme clusters or metabolons can occur in both animal and plant cells[23,24]. In recent years, it was discovered that chemotaxis could play a role in metabolon formation. Through experiments and theory, Zhao et. al. demonstrated that the first four enzymes of the glycolysis cascade form a metabolon due to enzyme chemotaxis[25] (Figure 1-2 (b)). These results demonstrate that chemotaxis plays an important role in the formation of enzyme aggregates.

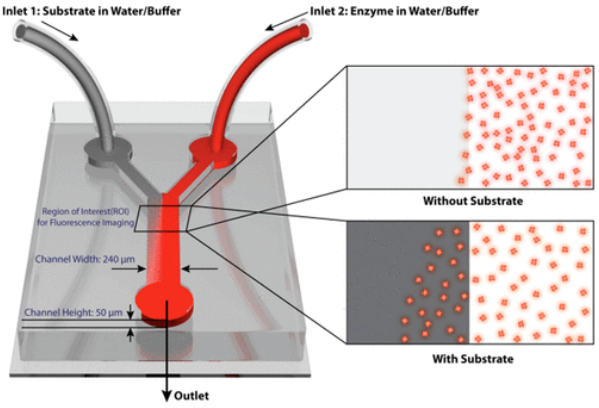

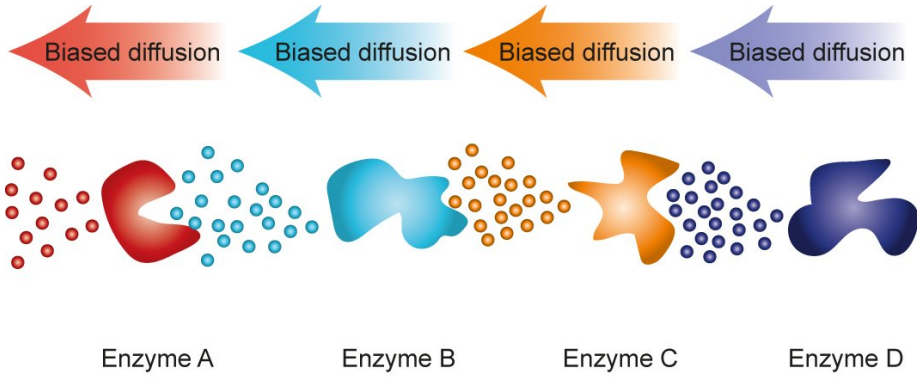

Figure 1- 2 (a) Microfluidic setup used to study chemotaxis of enzymes. It is a 2-inlet 1 outlet set up. The two inlets contain enzyme in water or buffer and either substrate in water or buffer or just water or buffer. In the presence of substrates, enzyme show movement towards their substrate. Reprinted with permission from *J. Am. Chem. Soc.* 2013, 135, 4, 1406–1414. Copyright 2013 American Chemical Society. (b) Schematic showing chemotaxis in enzyme metabolons. Enzymes A, B, C and D form metabolons. Since the product of the enzyme A reaction is a substrate for enzyme B reaction, enzyme B will show chemotaxis towards Enzyme A. Similar mechanism for enzyme C and D is also shown. Reproduced from Nature Chemistry. 2018, *10*, 311-317, Copyright 2018 with permission from Springer Nature.

1.3 Protein Aggregation in Neurodegenerative Diseases

Protein aggregation plays a crucial role in various neurodegenerative disease such as Alzheimer's disease, Parkinson's disease, Huntington's disease and amyotrophic lateral sclerosis (ALS). As life expectancy increases, the prevalence of these diseases continues to rise. In the US, costs associated with these diseases was $655 billion dollars in 2020[26]. Formation of protein aggregates in these diseases can be toxic to neurons and other cells and this plays a key role in the pathogenesis of these diseases. Figure 1-3 shows a summary of the protein aggregates observed in neurodegenerative diseases. In Huntington's disease, mutation in the huntingtin gene has been observed. Aggregates of huntingtin protein called inclusion bodies are observed in certain regions of the brain[27]. In Alzheimer's disease, there are two types of protein aggregates present in the brain, namely amyloid - β plaques and neurofibrillary tau tangles[28]. α- synuclein aggregates to

form clumps called Lewy bodies and have been implicated as a cause of Parkinson's disease[29]. Inclusions and aggregates in the brain have also been observed in ALS[30]. Although it is known that protein aggregation plays a major role, the mechanism of pathogenesis for these diseases is not well understood. In order to understand the underlying mechanisms and find cures to these diseases, it is important for us to study the aggregation of proteins such as amyloid- β.

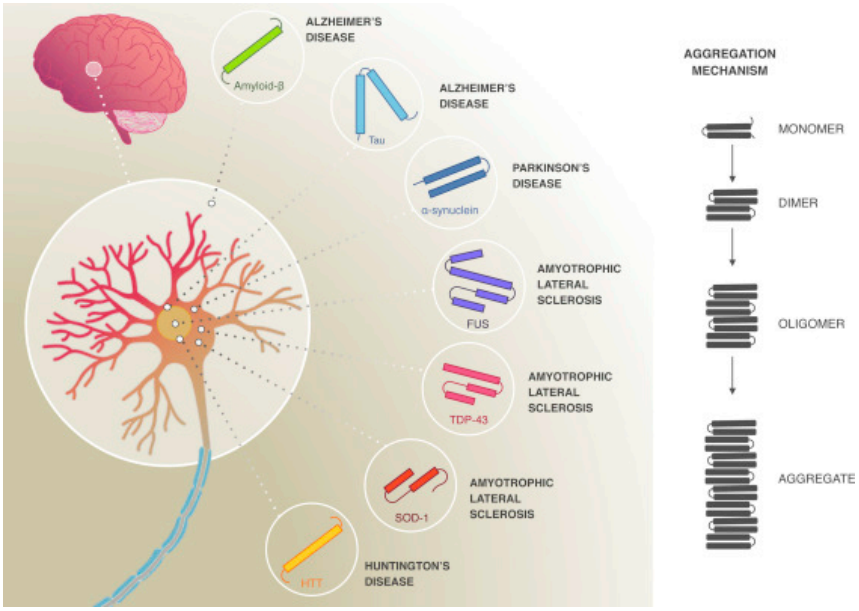

Figure 1- 3: Illustration showing the various proteins whose aggregation plays a role in neurodegenerative diseases such as Alzheimer's disease, Parkinson's disease, ALS and Huntington's disease. It also shows the aggregation mechanism where the protein goes from monomer to dimer, then oligomer and aggregate. Reprinted from *Mechanisms of ageing and development*, *156*, Author(s), Eftekharzadeh, B., Hyman, B.T. and Wegmann, pp.1-13., Copyright 2016, with permission from Elsevier.

In this work, we explore the role of proteins, specifically the enzymes in Alzheimer's disease. Alzheimer's disease is a progressive disease that affects millions of people. According to

the Alzheimer's Association, 6.7 million Americans aged 65 and older suffer from Alzheimer's dementia[31]. This disease can be either sporadic or familial. The important characteristics of Alzheimer's disease include the aggregation of amyloid - β and tau protein. Formation of amyloid - β aggregates occur when its precursor protein is cleaved due to certain secretases. This buildup of aggregates can then block the transfer of information from in between neurons and also cause other problems. Inside neurons, tau protein gets hyperphosphorylated and forms neurofibrillary tangles[32]. The formation of these tangles affects the microtubules inside neurons. This causes neuron death and the hyperphosphorylated tau is then released outside the neuron. Together, these aggregates of amyloid - β and tau protein play a role in the neurodegeneration and pathogenesis of the disease.

1.3.1 Role of Alkaline Phosphatase in Alzheimer's disease

Alkaline phosphatase is an enzyme that is found in various parts of the body such as the liver, bones, kidney, intestine, brain etc. Since it has the ability to remove a phosphate group, when combined with kinases, it is useful for regulating phosphorylated compounds in the body. Although abnormal levels of alkaline phosphatase are usually indications of altered liver activity, recent studies have shown that higher levels of various alkaline phosphatases are also associated with cognitive decline or Alzheimer's disease[33]. This was shown by Kellett et. al. in 2011 (Figure 1-4). They observed that plasma alkaline phosphatase activity increases in cases of mild cognitive impairment and Alzheimer's disease[34]. In 2012, Vardy et. al. observed higher levels of tissue non-specific alkaline phosphatase (TNAP) in AD[35]. A similar observation was made in 2020 where researchers observed that higher levels of serum alkaline phosphatase activity as a function of cognitive decline[36].

This increase in activity is significant because higher alkaline phosphatase can contribute to the progression of Alzheimer's disease. In neurofibrillary tangles, tau is hyperphosphorylated and it is released outside the neurons after the neuron dies. Alkaline phosphatase dephosphorylates this protein which then contributes to further neurotoxicity[37]. In 2008, it was discovered that tau protein in the extracellular environment promotes calcium uptake in other neuronal cells through muscarinic receptors M1 and M3[38]. This is toxic for other neurons. By dephosphorylating tau protein, increased activity of alkaline phosphatase contributes to this toxicity[39]. This implies that alkaline phosphatase plays a role in a positive feedback loop and contributes to the pathogenesis of the disease.

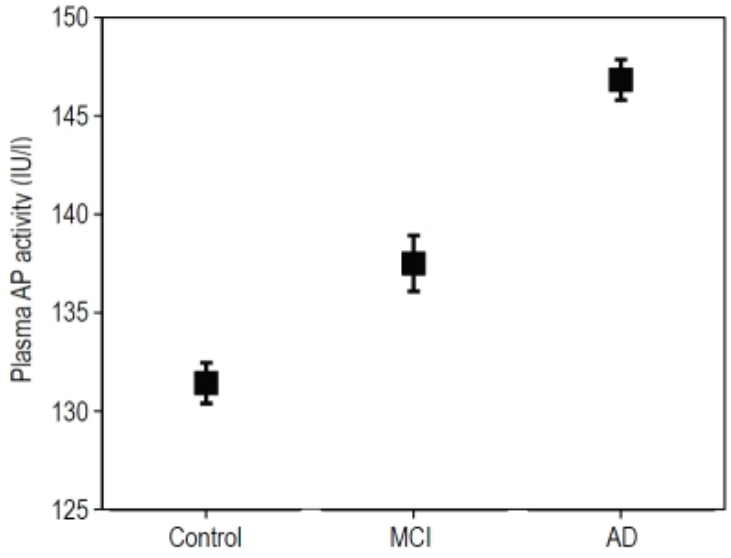

Figure 1- 4: Activity of plasma alkaline phosphatase in control, mild cognitive impairment and Alzheimer's disease cases. The plasma alkaline phosphatase activity increases for mild cognitive impairment cases and increases even more for Alzheimer's disease cases. Reprinted from Int J Mol Epidemiol Genet 2011:2(2):114-121 Copyright 2011.

1.3.2 Acetylcholinesterase reaction in Alzheimer's Disease

Acetylcholinesterase is a serine hydrolase that catalyzes the conversion of acetylcholine to choline and acetic acid. (Equation 1-2). These components of the acetylcholinesterase reaction are crucial to the functioning of the central nervous system[40].

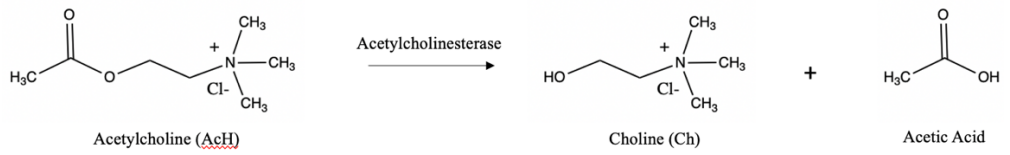

(1-2)

Acetylcholine is a neurotransmitter that helps transmit signal between various neurons. It has been shown that it plays an important role for learning and memory[41]. It is synthesized in the brain by the activity of choline acetyltransferase. At the axon terminal, it is packaged into vesicles and sent to the synaptic cleft. It ultimately binds to certain receptors (muscarinic or nicotinic) to transmit signals, unbinds and is then hydrolyzed by acetylcholinesterase[42].

This cholinergic signaling is extremely important and disruption of these processes due to AD is a major cause of concern[43]. Clinical studies show that patients with neurodegeneration due to AD have an acetylcholine deficiency when compared with healthy individuals[44]. This implies that this process of signaling is disrupted in AD patients. One of the early hypotheses for AD was the cholinergic hypothesis which suggests that the disruption of cholinergic signaling is directly associated with the decline of cognition in AD. Extensive research conducted since then has cast doubts about whether this is the main cause of AD, however it is still widely accepted that this plays a major role in the disease[45]. To combat this deficiency, cholinesterase inhibitors which inhibit acetylcholinesterase are widely used for alleviation of symptoms of AD[46]. These inhibitors are the most commonly used treatment for AD worldwide and there are several clinically approved inhibitors such as rivastigmine (Exelon®), donepezil (Aricept®), galantamine (Razadyne®)

available in the market[47]. Thus, this reaction is considered to be an important factor and has to be considered in the study of Alzheimer's disease. In our study, we are particularly interested in the acetylcholinesterase reaction due to the important role that it plays in this disease.

1.4 Targeted Drug Delivery using Protein Aggregation

Protein aggregation can also be used for targeted drug delivery. Targeted drug delivery is an idea that has fascinated researchers worldwide. It involves using a medium to transport a drug straight to the location of the disease. The advantages of using a targeted drug delivery system are immense and include minimizing side effects since the drug will not interact with healthy cells[48]. It can also help reduce the quantity of drug required to treat a disease which will help reduce healthcare costs significantly. However, the challenges to designing this system are also significant. The requirements include the considerations that it has to be biocompatible, it should be able to identify diseased cells and release the right amount of drug at the right time. There has been significant progress in this field in recent years and some of the commonly used carriers that have been investigated include liposomes[49], micelles[50], microalgae[51], DNA nanostructures[52], peptides[53] and other biodegradable nanoparticles[54]. In this section, I am going to focus on the use of liposomes as targeted drug delivery vehicles and also talk about how protein aggregation can be used to provide functionality to these vehicles. While developing liposome formulations for drug delivery, it is important to understand how they interact with each other and also with chemicals that are present in our body.

1.4.1 Liposomes for targeted drug delivery

Liposomes are compartment-like spherical structures that resemble cell membranes and are formed due to the self-assembly of phospholipid bilayers[55]. Altering synthesis methods can give a variety of sizes of liposomes. The lamellarity can also be controlled using processes such as extrusion. By using natural phospholipids to make these bilayers, they can be made biocompatible. All of these factors have played a role in the extensive use of liposomes for drug delivery applications. Based on the database for drugs, Liu et. al. found that 14 liposome-based products have been currently authorized by the Food and Drug Administration (FDA) and European Medicines Agency (EMA)[49]. These include cancer drugs such as Doxil® and Vyxeos® along with medications for infection, lung disease and so on. Most common components of these liposomes include phospholipids, sphingomyelin, cholesterol, etc. The components and the structure are chosen based on the drug that it needs to deliver. Liposomal drug delivery systems can be used to deliver both hydrophilic and hydrophobic drugs[56]. To improve the efficiency of these liposomal delivery systems, synthesizing 'smart' liposomes with multiple functionalities is critical. Liposomes that can identify diseases cells, move towards them and aggregate at a particular spot, selectively release the drug are important functionalities to have if they are to be used for targeted drug delivery.

1.4.2 Liposome Aggregation

Controlling liposome aggregation is important to control the stability as well as the functionality of liposome formulations. Various strategies have been used for controlling the aggregation of liposomes. A recent paper coated liposomes with DNA and used photoinduced

crosslinking to control the aggregation of liposomes[57]. Superparamagnetic nanoparticles that can be triggered by an external radiofrequency have been used to control the aggregation of liposomes with them as well as their movement[58]. However, the aggregation in these systems is controlled using external triggers. Controlling aggregation using triggers that are present inside the body is useful for improving these drug delivery systems. For example, cancer cells have been shown to have high concentration of zinc[59] ions. Further, high calcium concentrations in blood are observed for people with cancer[60]. Thus, using proteins that aggregate in the presence of zinc and calcium ions and designing liposomes coated with these proteins that can aggregate at high concentrations of zinc and calcium ions is a useful technique to design targeting vesicles.

1.5 Research Goals

In this thesis, I aim to answer questions related to various aspects of protein aggregation. In Chapter 2, I demonstrate the aggregation and fragmentation of individual enzymes in the presence of catalysis relevant species. Specifically, I investigate the fragmentation of glucose oxidase in the presence of its substrate and products of the reaction. Through Fluorescence Resonance Energy Transfer (FRET) measurements, I found that glucose oxidase fragments upon addition of D-Glucose which is the substrate. In the presence of L-Glucose, this fragmentation did not occur. Concentration-dependent experimental measurements and calculations showed that glucose oxidase fragments in the presence of a concentration of at least 0.3mM D-Glucose. I also show that glucose oxidase fragments not only from itself, but also from other enzymes such as invertase and maltase in the presence of D-Glucose. I also demonstrate the aggregation of glucose oxidase

in the presence of adenosine triphosphate (ATP) and magnesium ions. These measurements indicate that the size of enzymes does not remain constant during catalysis and enzyme aggregation or fragmentation should be taken into account while studying enzyme catalysis.

In Chapter 3, the role of alkaline phosphatase in Alzheimer's disease is investigated. It is known previously that higher alkaline phosphatase levels are observed in cognitive impairment or in Alzheimer's disease. In this work, we investigate the reason for increased alkaline phosphatase levels. We do so by probing its activity in the presence of amyloid - β and the acetylcholinesterase reaction. Both of these play a key role in Alzheimer's disease. The increases that we have seen correspond to the increases observed in cases of cognitive impairment or AD in literature. We also show that, at concentrations higher than physiological concentrations, acetylcholine and choline can also increase alkaline phosphatase activity. Our experiments show that higher levels are observed because the activity of alkaline phosphatase increases due to its interaction with these components.

Chapter 4 delves into the use of protein aggregation in drug delivery applications. In this work, I synthesize liposomes and study their aggregation upon addition of different amounts of metal salts before and after coating with proteins. To study this aggregation, I use techniques such as confocal microscopy and DLS. We show that uncoated liposomes show aggregation in the presence of lower concentration of zinc and calcium salts while liposomes coated with streptavidin and avidin show aggregation in the presence of higher concentration of those salts. On the other hand, streptavidin-coated nano-sized spheres only aggregate in the presence of zinc nitrate and not calcium nitrate. Thus, by varying the coating and the salt concentrations, we can obtain specific control over liposome aggregation. These results demonstrate that interactions between proteins that cause aggregation can be used for designing systems that can achieve targeted drug delivery.

Lastly, Chapter 5 is a summary of all the relevant conclusions and future directions for my research. Through this summary, I aim to elucidate my findings and give a perspective on how they help address certain unanswered questions in the field of protein aggregation. I also provide my broad perspective on the field and give specific examples about the challenges and questions that remain and need to be addressed in the future.

1.6 References

1. Motta, J. F. G., de FREITAS, B. C. B., de ALMEIDA, A. F., Martins, G. A. de S. & Borges, S. V. Use of enzymes in the food industry: a review. *Food Sci. Technol.* **43**, 1–14 (2023).
2. Polaina, J. & MacCabe, A. P. *Structure , Function and Applications*. *Springer* (2007).
3. Mahler, H. C., Friess, W., Grauschopf, U. & Kiese, S. Protein aggregation: Pathways, induction factors and analysis. *J. Pharm. Sci.* **98**, 2909–2934 (2009).
4. Ross, C. A. & Poirier, M. A. Protein aggregation and neurodegenerative disease. *Nat. Med.* **10**, S10 (2004).
5. Philo, J. & Arakawa, T. Mechanisms of Protein Aggregation. *Curr. Pharm. Biotechnol.* **10**, 348–351 (2009).
6. Weids, A. J., Ibstedt, S., Tamás, M. J. & Grant, C. M. Distinct stress conditions result in aggregation of proteins with similar properties. *Sci. Rep.* **6**, 1–12 (2016).
7. Das, T. K., Chou, D. K., Jiskoot, W. & Arosio, P. Nucleation in Protein Aggregation in Biotherapeutic Development: A look into the Heart of the Event. *J. Pharm. Sci.* **111**, 951–959 (2022).

8. Kopp, M. R. G. *et al.* Surface-Induced Protein Aggregation and Particle Formation in Biologics: Current Understanding of Mechanisms, Detection and Mitigation Strategies. *J. Pharm. Sci.* **112**, 377–385 (2023).

9. Housmans, J. A. J., Wu, G., Schymkowitz, J. & Rousseau, F. A guide to studying protein aggregation. *FEBS J.* **290**, 554–583 (2023).

10. Lorber, B., Fischer, F., Bailly, M., Roy, H. & Kern, D. Protein analysis by dynamic light scattering: Methods and techniques for students. *Biochem. Mol. Biol. Educ.* **40**, 372–382 (2012).

11. Wilkosz, N. *et al.* Molecular spectroscopic markers of abnormal protein aggregation. *Molecules* **25**, 1–26 (2020).

12. Marchi, I. *et al.* Characterization and classification of matrix effects in biological samples analyses. *J. Chromatogr. A* **1217**, 4071–4078 (2010).

13. Zhou, L. & Kurouski, D. Structural Characterization of Individual α-Synuclein Oligomers Formed at Different Stages of Protein Aggregation by Atomic Force Microscopy-Infrared Spectroscopy. *Anal. Chem.* **92**, 6806–6810 (2020).

14. Muddana, H. S., Sengupta, S., Mallouk, T. E., Sen, A. & Butler, P. J. Substrate catalysis enhances single-enzyme diffusion. *J. Am. Chem. Soc.* **132**, 2110–2111 (2010).

15. Riedel, C. *et al.* The heat released during catalytic turnover enhances the diffusion of an enzyme. *Nature* **517**, 227–230 (2015).

16. Jee, A. Y., Dutta, S., Cho, Y. K., Tlusty, T. & Granick, S. Enzyme leaps fuel antichemotaxis. *Proc. Natl. Acad. Sci. U. S. A.* **115**, 14–18 (2018).

17. Illien, P. *et al.* Exothermicity Is Not a Necessary Condition for Enhanced Diffusion of Enzymes. *Nano Lett.* **17**, 4415–4420 (2017).

18. Zhang, Y. & Hess, H. Enhanced Diffusion of Catalytically Active Enzymes. *ACS Cent. Sci.* **5**, 939–948 (2019).

19. Günther, J. P., Börsch, M. & Fischer, P. Diffusion Measurements of Swimming Enzymes with Fluorescence Correlation Spectroscopy. *Acc. Chem. Res.* **51**, 1911–1920 (2018).

20. Sengupta, S. *et al.* Enzyme molecules as nanomotors. *J. Am. Chem. Soc.* **135**, 1406–1414 (2013).

21. Dey, K. K. *et al.* Chemotactic separation of enzymes. *ACS Nano* **8**, 11941–11949 (2014).

22. Somasundar, A. *et al.* Positive and negative chemotaxis of enzyme-coated liposome motors. *Nat. Nanotechnol.* **14**, 1129–1134 (2019).

23. Dahmani, I., Qin, K., Zhang, Y. & Fernie, A. R. The Formation and Function of Plant Metabolons. *Plant J.* 1080–1092 (2023) doi:10.1111/tpj.16179.

24. Wu, F. & Minteer, S. Krebs cycle metabolon: Structural evidence of substrate channeling revealed by cross-linking and mass spectrometry. *Angew. Chemie - Int. Ed.* **54**, 1851–1854 (2015).

25. Zhao, X. *et al.* Substrate-driven chemotactic assembly in an enzyme cascade. *Nat. Chem.* **10**, 311–317 (2018).

26. Thorpe, K. E., Levey, A. I. & Thomas, J. U.S. Burden of Neurodegenerative Disease. *Emory Univ.* 13 (2021).

27. Spada, A., Weydt, P. & Pineda, V. Huntington's Disease Pathogenesis. 29–53 (2010) doi:10.1201/ebk0849390005-c2.

28. Ju, Y. & Tam, K. Pathological mechanisms and therapeutic strategies for Alzheimer's disease. *Neural Regen. Res.* **17**, 543–549 (2022).

29. Wakabayashi, K. *et al.* The Lewy body in Parkinson's disease and related

neurodegenerative disorders. *Mol. Neurobiol.* **47**, 495–508 (2013).

30. Blokhuis, A. M., Groen, E. J. N., Koppers, M., Van Den Berg, L. H. & Pasterkamp, R. J. Protein aggregation in amyotrophic lateral sclerosis. *Acta Neuropathol.* **125**, 777–794 (2013).

31. Report, S., Patient, T. H. E., In, J., Era, A. N. & New, O. F. 2023 Alzheimer's disease facts and figures. *Alzheimer's Dement.* (2023) doi:10.1002/alz.13016.

32. Gendron, T. F. The role of tau in neurodegeneration. *Mol. Neurodegener.* **4**, 1–19 (2009).

33. Nho, K. *et al.* Association of Altered Liver Enzymes With Alzheimer Disease Diagnosis, Cognition, Neuroimaging Measures, and Cerebrospinal Fluid Biomarkers. *JAMA Netw. Open* **2**, 1–20 (2019).

34. Kellett, K. A. B., Williams, J., Vardy, E. R. L. C., Smith, A. D. & Hooper, N. M. Plasma alkaline phosphatase is elevated in Alzheimer's disease and inversely correlates with cognitive function. *Int. J. Mol. Epidemiol. Genet.* **2**, 114–121 (2011).

35. Vardy, E. R. L. C., Kellett, K. A. B., Cocklin, S. L. & Hooper, N. M. Alkaline Phosphatase Is Increased in both Brain and Plasma in Alzheimer's Disease. *Neurodegener. Dis.* **9**, 31–37 (2011).

36. Boccardi, V. *et al.* Serum alkaline phosphatase is elevated and inversely correlated with cognitive functions in subjective cognitive decline: results from the ReGAl 2.0 project. *Aging Clin. Exp. Res.* **33**, 603–609 (2020).

37. Díaz-Hernández, M. *et al.* Tissue-nonspecific alkaline phosphatase promotes the neurotoxicity effect of extracellular tau. *J. Biol. Chem.* **285**, 32539–32548 (2010).

38. Gómez-Ramos, A., Díaz-Hernández, M., Rubio, A., Miras-Portugal, M. T. & Avila, J. Extracellular tau promotes intracellular calcium increase through M1 and M3 muscarinic

receptors in neuronal cells. *Mol. Cell. Neurosci.* **37**, 673–681 (2008).

39. Miguel Diaz-Hernandez, Felix Hernandez, M. T. M.-P. and J. A. Neuronal Tissue-Nonspecific Alkaline Phosphatase (TNAP). in *Neuronal Tissue-Nonspecific Alkaline Phosphatase (TNAP)* (2015).

40. Talesa, V. N. Acetylcholinesterase in Alzheimer's disease. *Mech. Ageing Dev.* **122**, 1961–1969 (2001).

41. Hasselmo, M. E. The role of acetylcholine in learning and memory. *Curr. Opin. Neurobiol.* **16**, 710–715 (2006).

42. Sam, C.; Bordoni, B. *Physiology, acetylcholine.* (In StatPearls [Internet]. StatPearls Publishing, 2022).

43. Chen, Z. R., Huang, J. B., Yang, S. L. & Hong, F. F. Role of Cholinergic Signaling in Alzheimer's Disease. *Molecules* **27**, 1–23 (2022).

44. Croxson, P. L., Kyriazis, D. A. & Baxter, M. G. Cholinergic modulation of a specific memory function of prefrontal cortex. *Nat. Neurosci.* **14**, 1510–1512 (2011).

45. Giacobini, E., Cuello, A. C. & Fisher, A. Reimagining cholinergic therapy for Alzheimer's disease. *Brain* **145**, 2250–2275 (2022).

46. Marucci, G. *et al.* Efficacy of acetylcholinesterase inhibitors in Alzheimer's disease. *Neuropharmacology* **190**, 2013 (2021).

47. Sharma, K. Cholinesterase inhibitors as Alzheimer's therapeutics (Review). *Mol. Med. Rep.* **20**, 1479–1487 (2019).

48. Singh, R. & Lillard, J. W. Nanoparticle-based targeted drug delivery. *Exp. Mol. Pathol.* **86**, 215–223 (2009).

49. Liu, P., Chen, G. & Zhang, J. A Review of Liposomes as a Drug Delivery System :

Current. *Molecules* **27**, 1372 (2022).

50. Kotta, S., Aldawsari, H. M., Badr-Eldin, S. M., Nair, A. B. & YT, K. Progress in Polymeric Micelles for Drug Delivery Applications. *Pharmaceutics* **14**, 1–32 (2022).

51. Khavari, F., Saidijam, M., Taheri, M. & Nouri, F. Microalgae: therapeutic potentials and applications. *Mol. Biol. Rep.* **48**, 4757–4765 (2021).

52. Hu, Q., Li, H., Wang, L., Gu, H. & Fan, C. DNA Nanotechnology-Enabled Drug Delivery Systems. *Chem. Rev.* **119**, 6459–6506 (2019).

53. Berillo, D., Yeskendir, A., Zharkinbekov, Z., Raziyeva, K. & Saparov, A. Peptide-Based Drug Delivery Systems. (2021).

54. Gagliardi, A. *et al.* Biodegradable Polymeric Nanoparticles for Drug Delivery to Solid Tumors. *Front. Pharmacol.* **12**, 1–24 (2021).

55. Vemuri, S. & Rhodes, C. T. Preparation and characterization of liposomes as therapeutic delivery systems: a review. *Pharm. Acta Helv.* **70**, 95–111 (1995).

56. Akbarzadeh, A., Rezaei-sadabady, R., Davaran, S., Joo, S. W. & Zarghami, N. Liposome : classification , prepNew aspects of liposomesaration , and applications. *Nanoscale Res. Lett.* **8**, 1–9 (2013).

57. Fujimoto, K., Ichikawa, M. & Nakamura, S. Photoinduced aggregation of liposome modified with DNA containing ultrafast DNA photo-cross-linker. *J. Chem. Technol. Biotechnol.* **97**, 295–298 (2022).

58. Haša, J., Hanuš, J. & Štěpánek, F. Magnetically Controlled Liposome Aggregates for On-Demand Release of Reactive Payloads. *ACS Appl. Mater. Interfaces* **10**, 20306–20314 (2018).

59. Rusch, P. *et al.* Zinc distribution within breast cancer tissue of different intrinsic subtypes.

Arch. Gynecol. Obstet. **303**, 195–205 (2021).

60. Seccareccia, D. & Mclsc, C. E. M. Palliative Care Files Cancer-related hypercalcemia Dori Seccareccia MD CCFP(EM) MClSc. *Palliat. Care Files* **56**, 244–246 (2010).

Chapter 2

2 Enzyme Aggregation and Fragmentation in the Presence of Catalysis Relevant Species.

Parts of this chapter are reproduced from Gentile, K.; Bhide, A.; Kauffman, J.; Ghosh, S.; Maiti, S.; Adair, J. Lee, T.H.; Sen, A. Enzyme Aggregation and Fragmentation Induced by Catalysis Relevant Species. Phys. Chem. Chem. Phys. 2021, 23, 20709-20717 with permission from the Royal Society of Chemistry.

2.1 Introduction

Enzyme catalysis plays an important role in various biological functions such as digestion, respiration, muscle movement and many more[1]. Additionally, enzymes are also used for producing textiles, paper as well as various food products[2,3]. In these applications, it is generally assumed that the size of the enzyme remains constant during catalysis. Furthermore, various enzymatic studies where measurements that rely on the size of enzymes are conducted assume no change in structure during catalysis. Aggregation or fragmentation of enzymes during catalysis could affect

these observations and incorrect conclusions can be drawn from these studies. Change in size due to the formation of aggregates or fragments should also be taken into account while using enzymes for various industrial processes.

One such example is the study of enhanced diffusion of enzymes. Enhanced diffusion is studied using methods such as Fluorescence Correlation Spectroscopy (FCS), Nuclear Magnetic Resonance Spectroscopy (NMR), DLS and so on[4,5,6]. However, some of these observations are highly debated since conflicting results have been observed in multiple studies[7]. We know from the Stokes-Einstein equation (given in Chapter 1) that size and diffusion are inversely correlated. Hence, if there is a change in the hydrodynamic diameter of the enzymes due to the presence of the substrate of the enzyme or the product of the reaction, then it could cause artifacts in these measurements[8,9]. To prevent these errors, it is necessary to understand how enzymes aggregate or fragment as the enzymatic reaction proceeds.

In this work, we use a technique known as Fluorescence Resonance Energy Transfer (FRET) study the aggregation and fragmentation of the enzyme, glucose oxidase in the presence of chemicals relevant to its catalysis such as its substrate, the product of the reaction and so on. We also study the effect of other aggregators such as ATP and Mg^{2+} on glucose oxidase. We also study its interaction with other enzymes such as invertase and maltase. These results help us find out crucial information about the aggregation and fragmentation of these enzymes and consequently their functions.

2.2 Results

2.2.1 Fragmentation of Glucose Oxidase

The enzyme glucose oxidase (GOx) from *Aspergillus niger* is a dimeric enzyme and its molecular weight is 160kDa. For these experiments, we purchased this enzyme from Millipore Sigma. The PDB structure of glucose oxidase is shown in Figure 2-1[10]. As the name suggests, it oxidizes D-glucose (D-Glu) to form hydrogen peroxide and gluconic acid. (Equation 2-1).

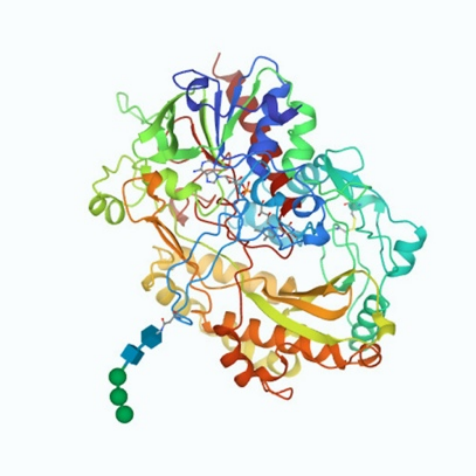

Figure 2- 1: Protein Data Bank structure of glucose oxidase from *Aspergillus niger. Reproduced from Physical Chemistry Chemical Physics. 2021, 23, 20709-20717, Copyright 2021.*

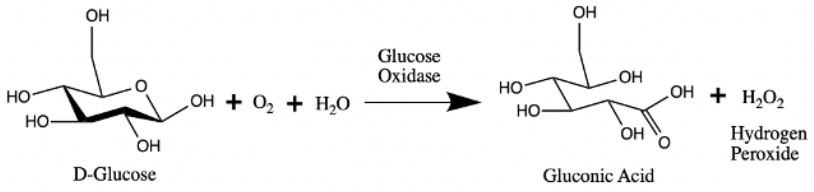

(2-1)

To study its aggregation, we used FRET to examine its aggregation state in the presence of various components of the reaction such as its substrate D-Glucose and the products hydrogen

peroxide and gluconic acid together as well as each of the products individually. We also tested its aggregation state in the presence of L-Glucose which is an enantiomer of D-Glucose but not a substrate of the enzyme. For these experiments, we took 2 batches of glucose oxidase and fluorescently tagged one of them with the donor dye (Alexa Fluor 488) and the other with the acceptor dye (Alexa Fluor 532). Then, we mixed these two and using a fluorimeter, excited the sample at 488 nm and recorded emission between 500-600 nm. We then calculated the ratio of the emission of the acceptor to the total emission to calculate FRET efficiency. More details about these experiments are given in the Materials and Methods section (section 2.4) This FRET Efficiency with respect to time is shown in Figure 2-2.

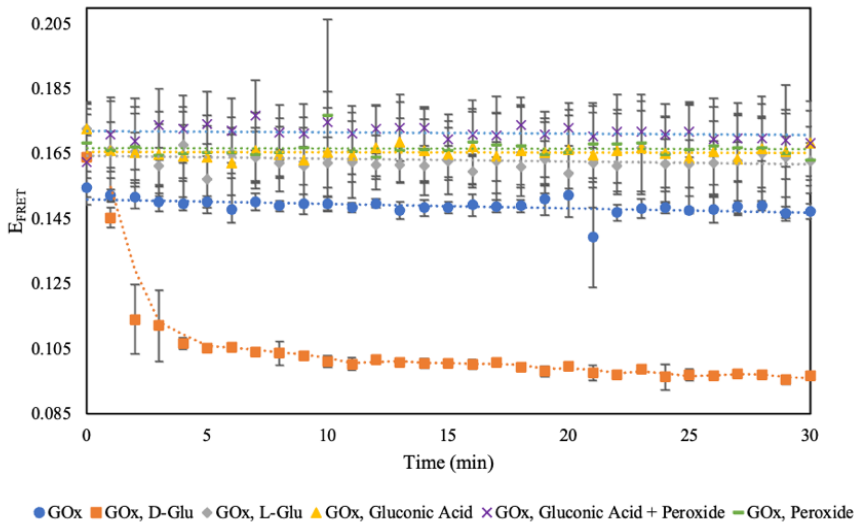

Figure 2- 2: FRET efficiency with respect to time for 0.2 µM Gox tagged with AF 488 and AF 532 (blue circles); 0.2 µM Gox tagged with AF 488 and AF 532, 1 mM D-Glu (orange squares), .2 µM Gox tagged with AF 488 and AF 532,1 mM L-Glu (gray diamonds); .2 µM Gox tagged with AF 488 and AF 532, 1 mM gluconic acid (yellow triangles); 0.2 µM Gox tagged with AF 488 and AF 532, 1 mM gluconic acid and 1 mM hydrogen peroxide (purple crosses); .2 µM Gox tagged with AF 488 and AF 532, 1 mM hydrogen peroxide (green dashes). The buffer that was used to make all solutions for the experiment was 50 mM MES (pH 6). The dashed lines are shown to guide the eye. Values are the average and error bars are the standard deviation from three trials. *Reproduced from Physical Chemistry Chemical Physics. 2021, 23, 20709-20717, Copyright 2021.*

FRET efficiency is a measure of aggregation and the higher the FRET efficiency, the higher the aggregation in the sample. Interestingly, we found that the FRET efficiency goes down in the presence of D-Glucose which means the enzyme is fragmenting when its substrate D-Glucose is added. Enzymes molecules have multimeric structures that are formed by the assembly of polypeptide subunits[11]. Thus, it is possible that these multimeric structures can aggregate or fragment and form individual monomers or large assemblies of monomers[12]. Here, we hypothesize that the observed fragmentation of glucose oxidase is due to its dissociation into individual subunits. However, it is also possible that fragmentation is observed due to conformational changes in the structure of glucose oxidase while catalyzing the reaction. L-Glucose which is not a substrate of the enzyme does not cause fragmentation which indicates that the fragmentation has something to do with the catalytic reaction of the enzyme. Interestingly, the products of the reaction, namely gluconic acid and hydrogen peroxide did not cause fragmentation as well.

Next, we also studied the effect of D-glucose not being present in the reaction mixture initially but being gradually produced over time. This was done by using the enzyme invertase. Invertase is also known as sucrase and is obtained from baker's yeast (*S. cerevisiae*). The PDB structure of the enzyme is shown in Figure 2-3[13]. For our experiments, we purchased invertase from Millipore Sigma. Invertase converts sucrose to glucose and fructose. (Equation 2-2)

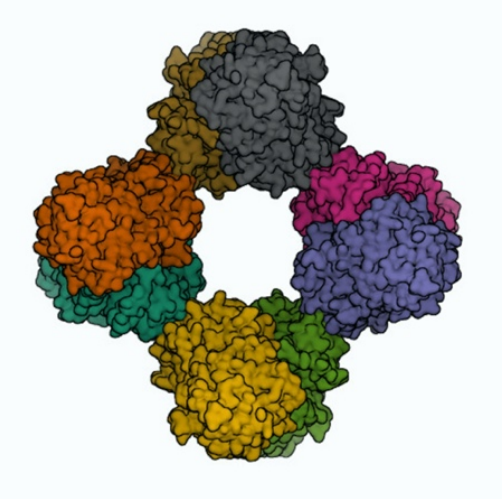

Figure 2- 3: Protein Data Bank structure of invertase (also known as sucrase) from Saccharomyces cerevisiae. *Reproduced from Physical Chemistry Chemical Physics. 2021, 23, 20709-20717, Copyright 2021.*

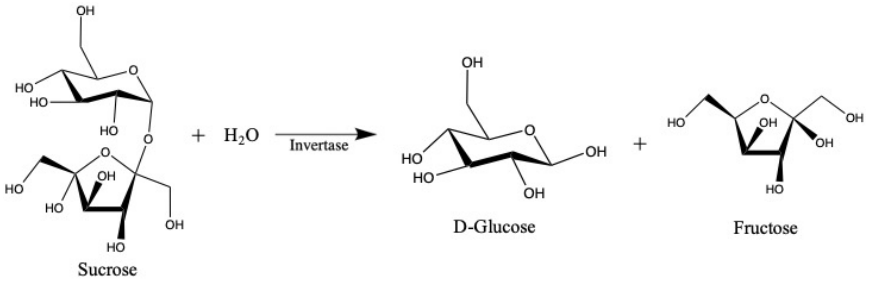

(2-2)

For this experiment, we added 0.1uM invertase that was not tagged with any dye to the FRET sample that contained glucose oxidase-Alexa Fluor 488 and glucose oxidase- Alexa Fluor 532. Using FRET, we studied the aggregation state of glucose oxidase in the presence of invertase and sucrose. Initially, we were expecting a time delay and a gradual onset of glucose oxidase fragmentation since D-Glucose is formed slowly in the solution due to the conversion of sucrose by invertase. These results are shown in Fig. 2-4.

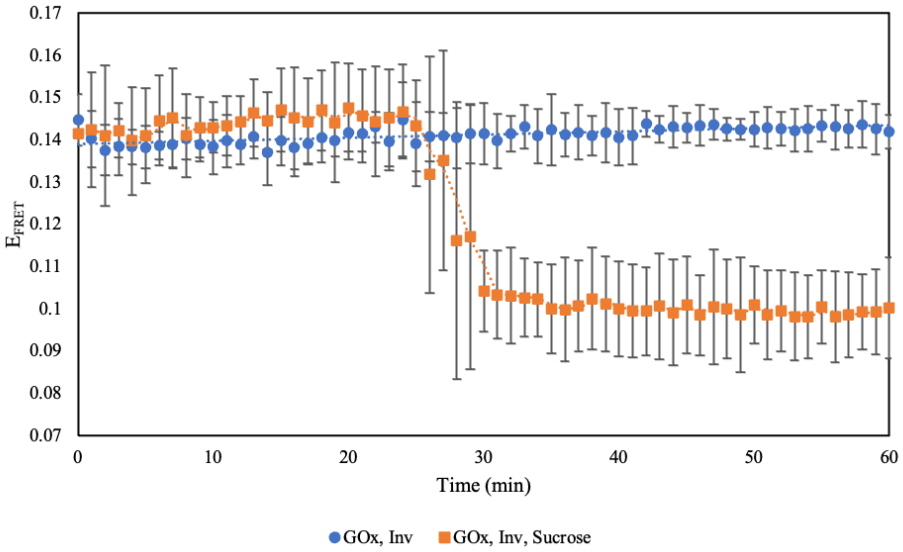

Figure 2- 4: FRET efficiency with respect to time for 0.2 µM Gox tagged with AF 488 and AF 532, 0.1 µM untagged Inv (blue circles); 0.2 µM Gox tagged with AF 488 and AF 532, 0.1 µM Inv, 1 mM sucrose (orange squares). The buffer that was used to make all solutions for the experiment was 50 mM MES (pH 6). The dashed lines are shown to guide the eye. Values are the average and the error bars represent the standard deviation from three trials. *Reproduced from Physical Chemistry Chemical Physics. 2021, 23, 20709-20717, Copyright 2021.*

Instead, we observed that, at a time period between 30-40 minutes, there was a sudden drop in the FRET efficiency which indicated that the fragmentation occurred at a particular concentration of D-Glucose.

2.2.2 Concentration required for Fragmentation of D-Glucose

To figure out the concentration required for fragmentation of D-Glucose, we did some experiments and calculations. First, we did concentration-dependent experiments to identify the concentration of D-Glucose that causes fragmentation. The results for these experiments are shown in Figure 2-5.

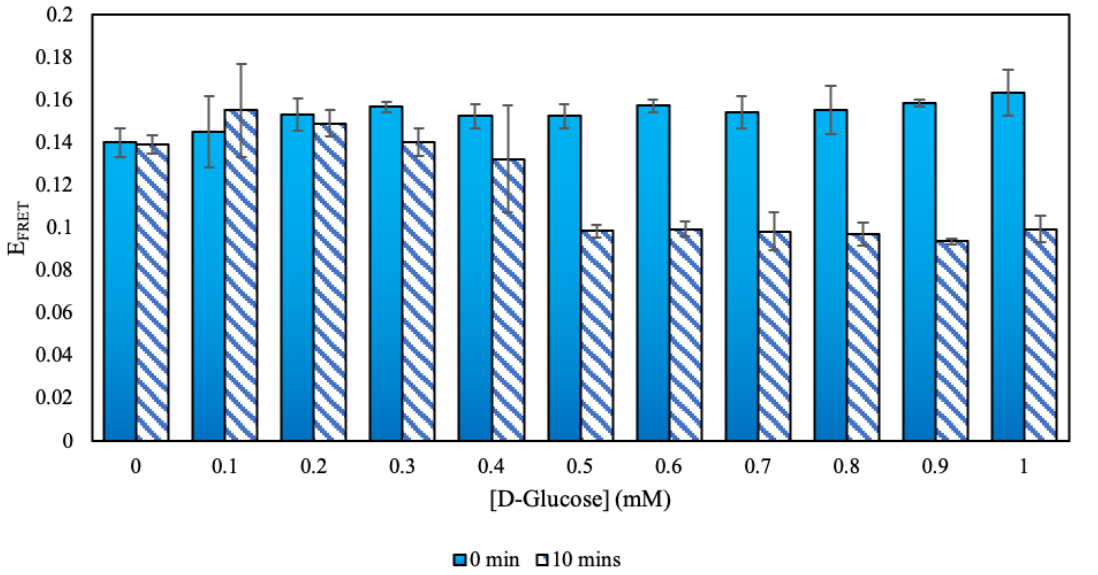

Figure 2- 5: FRET efficiency for fragmentation using 0.2 µM GOx tagged with AF 488 and AF 532 and different quantities of added D-Glucose. FRET efficiency at 0 min is represented by the blue bars and FRET efficiency 10 minutes after the addition of D-Glucose is represented by the striped bars. The buffer that was used to make all solutions for the experiment was 50 mM MES (pH 6). Values are the average and error bars represent the standard deviation from three trials of these experiments. The FRET efficiencies for 0.3 and 0.5 – 1 mM D-Glu at 10 mins are statistically different from the FRET efficiencies at 0 min (P value is less than 0.05). *Reproduced from Physical Chemistry Chemical Physics. 2021, 23, 20709-20717, Copyright 2021.*

These results indicated that concentrations above approximately 0.3mM D-Glucose caused fragmentation. This result was very interesting because 0.3mM is significantly lower than the blood glucose concentration which is about 4-6 mM[14]. To figure out if 0.3mM D-Glucose is produced in the invertase experiment after about 30-40 minutes, we performed some calculations.

This calculation for the concentration of D-Glucose present in the solution that contains glucose oxidase tagged with the two dyes, invertase and sucrose after 40 minutes was done as shown below.

For each experiment with invertase and sucrose, we used 760 µL of the stock solution that contained 0.1 µM of invertase. Hence, the number of moles of the enzyme invertase present in the solution can be calculated as

$$= 0.1 \times 10^{-6} \frac{moles}{L} \times 760\mu L$$

$$= 7.6 \times 10^{-11}\, moles$$

The invertase molecular weight is 270 kilo Daltons. Thus, the amount of invertase in the solution is

$$= 7.6 \times 10^{-11} moles \times 270 \times 10^{3} \frac{g}{mol}$$

$$= 2.1 \times 10^{-5} g$$

It is important to note that according to the website of Sigma Aldrich, the invertase that we use contains ≥ 300 units/ mg solid,

Thus, minimum number of units of invertase in our solution

$$= 2.1 \times 10^{-5} g \times 300 \frac{units}{mg}$$

$$= 6.3\, units$$

We know that one unit of invertase converts 1 µM of sucrose to 1 µM of D-Glucose per min at 4.5 pH of 4.5 with a temperature of 55°C. Thus, in our case, in one minute, 6.3 units of invertase will hydrolyze 6.3 µM of sucrose.

Thus, in a period of 40 minutes, the amount of sucrose hydrolyzed is

$$= 6.3 \frac{units}{min} \times 40\, min$$

$$= \sim 0.3 \times 10^{-3}\, moles$$

Therefore, in the experiment, 0.3 millimoles of D-Glucose have been produced.

As shown above, our calculations corresponded with our experimental observations and we prove that 0.3mM of D-Glucose can cause fragmentation of glucose oxidase.

2.2.3 Interaction of Glucose Oxidase with other Enzymes (Two Enzyme Experiments)

We also performed experiments to ascertain whether de-aggregation due to D-Glucose occurs only when glucose oxidase is aggregated with itself or if it also occurs when it is aggregated with other enzymes, such as invertase (Inv) or maltase (Mal). In these experiments, we tagged glucose oxidase with Alexa Fluor 488 and invertase/maltase with Alexa Fluor 532. Thus, the FRET efficiency is a measure of the aggregation of the two enzymes with each other, rather than by themselves. We measured the FRET efficiency after addition of substrates of both the enzymes. The results of the glucose oxidase-invertase experiment is shown in Figure 2-6 while the results of the glucose oxidase-maltase experiment are shown in Figure 2-8.

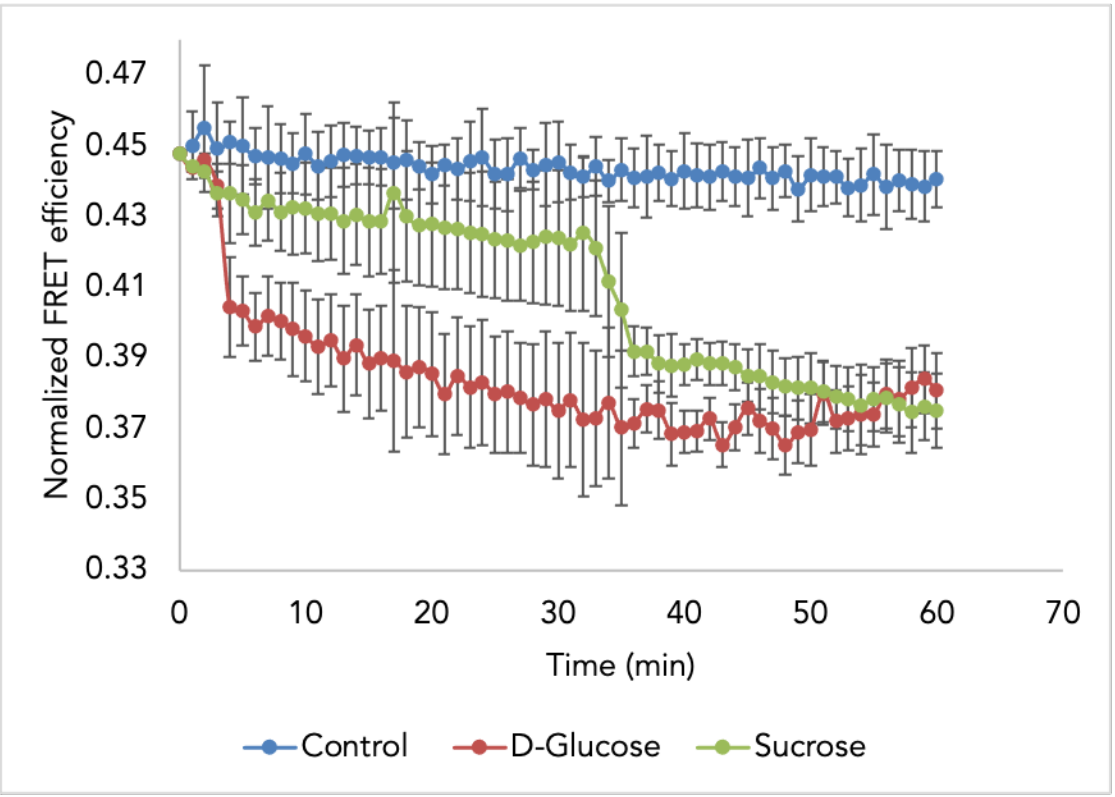

Figure 2- 6: FRET efficiency with respect to time for 0.1 µM GOx tagged with AF 488 and 0.1 µM Inv tagged with AF 532 (blue circles); 0.1 µM GOx tagged with AF 488 and 0.1 µM Inv tagged with AF 532, 1mM D-Glu (red circles), 0.1 µM GOx tagged with AF 488 and 0.1 µM Inv tagged with AF 532, 1mM Sucrose (green circles). The buffer that was used to make all solutions for the experiment was 50 mM MES (pH 6). Values are the average and error bars are the standard deviation from three trials.

As seen from Figure 2-6, glucose and invertase de-aggregate right away upon addition of D-Glucose. However, de-aggregation due to sucrose takes longer. We believe that this occurs due to the time required to form 0.3mM or higher of D-Glucose in the system.

Maltase, also known as α- glucosidase from *Saccharomyces cerevisiae* is a hexameric enzyme that catalyzes the conversion of maltase to D-Glucose (Equation 2-3). We have

purchased this enzyme from Millipore Sigma The PBD structure of maltase is shown in Figure 2-7[15].

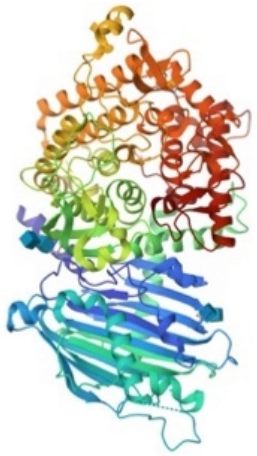

Figure 2- 7: Protein Data Bank structure of α- glucosidase (also known as maltase) from *Saccharomyces cerevisiae.*

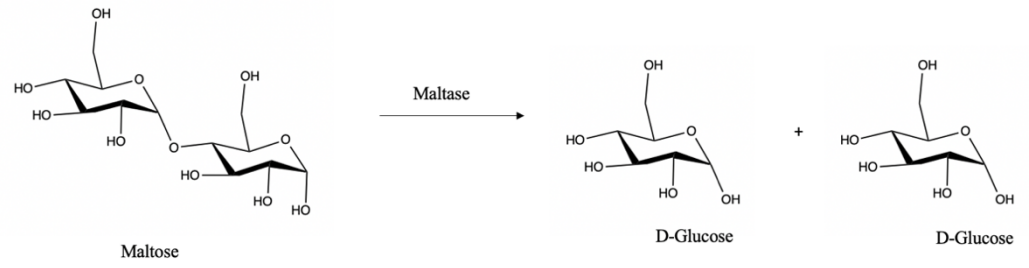

(2-3)

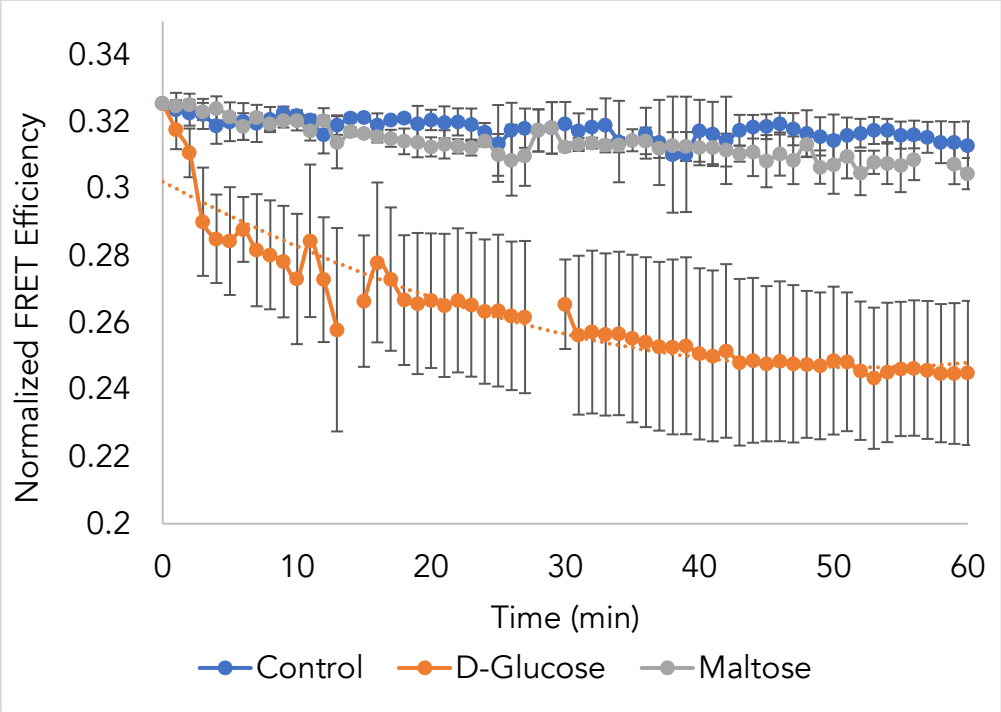

Figure 2- 8: FRET efficiency with respect to time for 0.1 µM GOx tagged with AF 488 and 0.1 µM Mal tagged with AF 532 (blue circles); 0.1 µM GOx tagged with AF 488 and 0.1 µM Mal tagged with AF 532, 1mM D-Glu (orange circles), 0.1 µM GOx tagged with AF 488 and 0.1 µM Mal tagged with AF 532, 1mM Maltose (gray circles). The buffer that was used to make all solutions for the experiment was 50 mM MES (pH 6). Values are the average and error bars are the standard deviation from three trials. Outliers have been removed from this graph. Appendix B has the version of this graph with the outliers.

As seen from Figure 2-8, glucose and maltase show de-aggregation when 1mM D-Glucose is added to the solution. However, unlike invertase, glucose oxidase and maltase do not show de-aggregation after a certain period of time. We hypothesize that this occurs because maltase is a slower enzyme as compared to invertase and thus, 60 minutes is not enough time for it to form 0.3mM or higher concentrations of D-Glucose in the solution.

2.2.4 Aggregation of Glucose Oxidase

Similar to glucose oxidase, hexokinase is also a glucose acting enzyme. While studying the aggregation and fragmentation of multiple enzymes, we also looked at the aggregation and fragmentation of hexokinase. We found that hexokinase aggregates in the presence of ATP, Mg^{2+} and low pH and fragments in the presence of D-Glucose[16]. Since its fragmentation is similar to glucose oxidase, we also wanted to test whether the aggregation pattern is similar. We found that, similar to hexokinase, glucose oxidase also aggregates upon addition of ATP and Mg^{2+} or ADP and Mg^{2+}. The results are shown in Figure 2-9. These results suggest that there is a similarity between the aggregation patterns of glucose oxidase and hexokinase which are both glucose-acting enzymes.

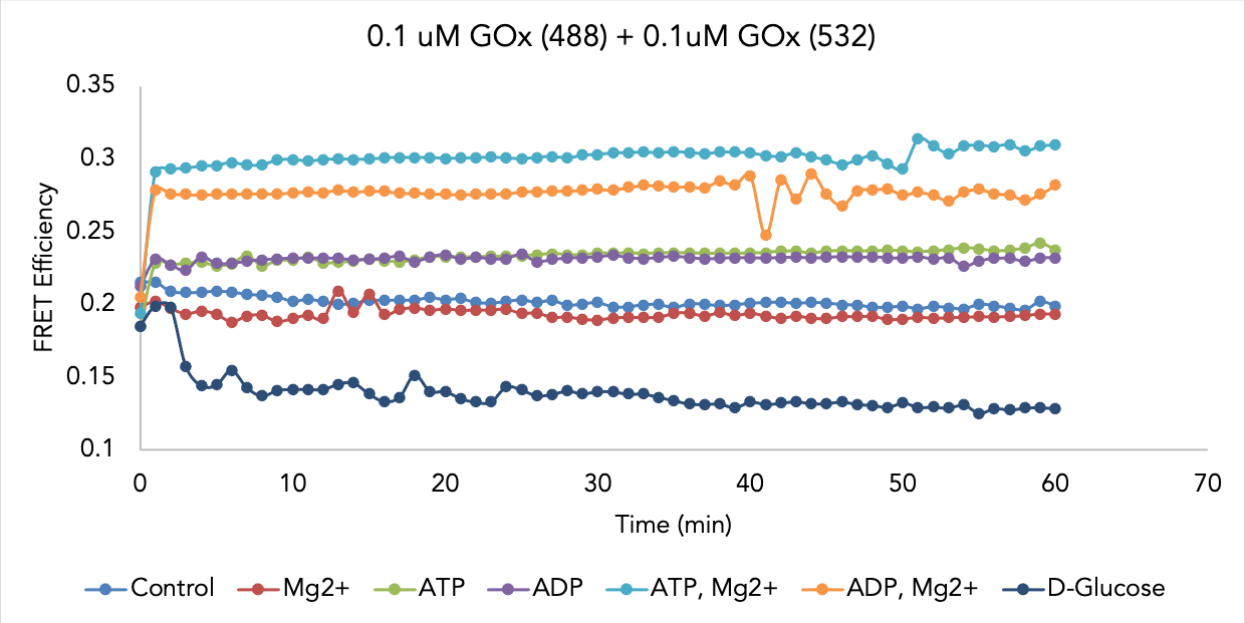

Figure 2- 9**:** FRET efficiency with respect to time for 0.1 µM GOx tagged with AF 488 and AF 532 (blue circles); 0.1 µM GOx tagged with AF 488 and AF 532, 1mM D-Glu (dark blue circles), 0.1 µM GOx tagged with AF 488 and AF 532, 40mM $MgCl_2$ (red circles), 0.1 µM GOx tagged with AF 488 and AF 532, 20mM ATP (green circles), 0.1 µM GOx tagged with AF 488 and AF 532, 20mM ADP (purple circles), 0.1 µM GOx tagged with AF 488 and AF 532, 20mM ATP, 40mM $MgCl_2$ (light blue circles), 0.1 µM GOx tagged with AF 488 and AF 532, 40mM $MgCl_2$, 20mM ADP (orange circles). The buffer that was used to make all solutions for the

experiment was 50 mM MES (pH 6). Values are the average and error bars are the standard deviation from three trials.

2.3 Conclusion and Discussion

This work identifies compounds which are responsible for aggregation or fragmentation of glucose oxidase. Based on our results, we observe that D-Glucose causes fragmentation of glucose oxidase at a concentration of more than 0.3mM, which is lower than the blood glucose concentration. We also study its interaction with other cascade enzymes. We observe that glucose oxidase de-aggregates from other enzymes such as invertase and maltase in the presence of D-Glucose. Also, similar to hexokinase, glucose aggregates in the presence of ATP and Mg^{2+} which suggests that there are some similarities between these glucose acting enzymes.

Based on our observations, we can conclude that the size of enzymes does not remain constant during catalysis and they undergo aggregation and fragmentation in the presence of chemicals that are relevant to their catalysis. They also interact with other enzymes in the presence of these chemicals. Thus, we cannot assume that the enzyme retains its native structure during catalysis. There are two possible mechanisms for this to occur. The first mechanism involves a conformational change. We hypothesize that a change in the conformation of the enzyme due to substrate binding or while catalyzing the reaction could cause aggregation or fragmentation. It is also possible that dissociation and association of the multimeric structure of the enzyme during catalysis could also be the reason for our observations. Future studies could look into investigating this mechanism. Interestingly, a separate study has also shown that ATP can cause solubilization and fragmentation of proteins[17].

2.4 Materials and Methods

2.4.1 Materials

Glucose oxidase (from *Aspergillus niger*), and invertase (from baker's yeast (*S. cerevisiae*) and α- glucosidase (from *Saccharomyces cerevisiae*), MES, D-(+)-Glucose, L-(-)- Glucose, D-(+)-Gluconic acid – lactone, Sucrose, D-(+)-maltose monohydrate, Adenosine 5′-triphosphate disodium salt hydrate, 99% were all purchased from Sigma Aldrich. Magnesium chloride anhydrous was purchased from Alfa Aesar. Alexa Fluor™ 488 NHS Ester (Succinimidyl Ester) and Alexa Fluor™ 532 NHS Ester (Succinimidyl Ester) were purchased from Thermo Fisher Scientific. Hydrogen peroxide, 30% was purchased from VWR.

2.4.2 Methods

2.4.2.1 Labeling of Glucose Oxidase, Invertase and Maltase with fluorescent dyes

For the single-enzyme experiments, the enzyme glucose oxidase was split into two halves. Alexa Fluor was added to one half and Alexa Fluor 532 was added to the other half along with 100mM sodium bicarbonate. This solution was rotated for 1 hour and then stored in the 2-8 degrees C fridge overnight. The next morning, these solutions were rotated for 2-3 hours and then purified according to the procedure given in the Antibody Conjugate Purification Kit for 0.5-1 mg (Thermo Fisher Scientific). For the column, the buffer was replaced with 50mM MES buffer (pH 6). After the enzyme-dye conjugate was obtained, the concentration of enzyme, dye and the enzyme: dye

ratio was measured using UV-Visible spectroscopy. The starting enzyme: dye ratio for all the three enzymes (glucose oxidase, invertase and maltase are given in Appendix B).

For the two enzyme experiments, a similar procedure was followed. Glucose oxidase was tagged with Alexa Fluor 488 and invertase or maltase was tagged with Alexa Fluor 532.

2.4.2.2 Glucose Oxidase FRET Experiments

For these experiments, we make a stock solution of 0.1 μM glucose oxidase tagged with AF 488 and 0.1 μM glucose oxidase tagged with AF 532 in MES buffer. The excitation and emission spectra are captured using a Fluorolog Jobin Yvon Horiba spectrofluorometer. The settings for the fluorimeter involve setting the integration time to 0.5 seconds, slit width is 5nm and the detector is capturing S1/R1. We take scans in increments of 5nm. For the FRET experiments, the sample containing the enzyme tagged with the two dyes is excited at 488 nm and emission is captured between 500 to 600 nm. The control experiment contains just the enzyme while for all the other experiments, the necessary chemicals in the correct quantities are added after the first scan at 0 min. For the invertase experiment, 0.1 μM of untagged invertase is added to all the samples. For the two enzyme experiments, the stock solution contains 0.1 μM glucose oxidase tagged with AF 488 and 0.1 μM invertase or maltase tagged with AF 532. The sample shows FRET when the two dyes are less than 6 nm apart from each other. The calculation of this distance as well as the details about the calculation of FRET efficiency is shown in Appendix B.

2.4.2.3 Calculation of normalized FRET efficiency

To calculate the normalized (baseline corrected) FRET efficiencies for the two enzyme experiments we use the FRET efficiency at 0 min of the trial that shows the highest FRET efficiency as a reference. For all the other trials with all the different substrates, we calculated

$$\alpha_i = F_0 - RE_0$$

Where i denotes the experiment or trial, F_0 denotes the FRET Efficiency at 0 min for that particular experiment and RE_0 denotes the FRET efficiency at 0 min for the reference experiment.

After calculating alpha value for all the experiments, we added this value to all FRET efficiencies at all the time points for that particular trial/ experiment. This was considered to the normalized/ baseline corrected FRET efficiency. We plotted these with respect to time to ensure that all the experiments start at the same time and the differences between the experiments can be seen clearly.

2.4.2.4 Statistical Analysis

To calculate the statistical significance, an unpaired t-test was performed. (Figure 2-5). For the test, alpha level is 0.05 (5%). If the two-tailed p-value was <0.05, then the results were considered statistically different from each other.

2.5 Acknowledgements

We would like to thank Dr. Christine Keating from Penn State Chemistry for letting us use the fluorimeter in her lab for the FRET measurements. We also thank Professor Henry Hess from Columbia University for helpful discussions. We gratefully acknowledge funding of the research by the Air Force Office of Scientific Research FA9550-20-1-0393 (AS). Any findings or conclusions expressed in this dissertation are those of the authors and do not necessarily reflect the views of the Air Force Office of Scientific Research.

2.6 References

1. Ringe, D., Petsko, G. A. & Phillips, D. How Enzymes Work. *Science (80-.).* **320**, 1428–1429 (2008).
2. Motta, J. F. G., de FREITAS, B. C. B., de ALMEIDA, A. F., Martins, G. A. de S. & Borges, S. V. Use of enzymes in the food industry: a review. *Food Sci. Technol.* **43**, 1–14 (2023).
3. Haki, G. D. & Rakshit, S. K. Developments in industrially important thermostable enzymes: A review. *Bioresour. Technol.* **89**, 17–34 (2003).
4. Muddana, H. S., Sengupta, S., Mallouk, T. E., Sen, A. & Butler, P. J. Substrate catalysis enhances single-enzyme diffusion. *J. Am. Chem. Soc.* **132**, 2110–2111 (2010).
5. Jee, A. Y., Dutta, S., Cho, Y. K., Tlusty, T. & Granick, S. Enzyme leaps fuel antichemotaxis. *Proc. Natl. Acad. Sci. U. S. A.* **115**, 14–18 (2018).

6. Riedel, C. *et al.* The heat released during catalytic turnover enhances the diffusion of an enzyme. *Nature* **517**, 227–230 (2015).

7. Zhang, Y. & Hess, H. Enhanced Diffusion of Catalytically Active Enzymes. *ACS Cent. Sci.* **5**, 939–948 (2019).

8. Günther, J. P., Börsch, M. & Fischer, P. Diffusion Measurements of Swimming Enzymes with Fluorescence Correlation Spectroscopy. *Acc. Chem. Res.* **51**, 1911–1920 (2018).

9. Zhang, Y., Armstrong, M. J., Bassir Kazeruni, N. M. & Hess, H. Aldolase Does Not Show Enhanced Diffusion in Dynamic Light Scattering Experiments. *Nano Lett.* **18**, 8025–8029 (2018).

10. Wohlfahrt, G. *et al.* 1.8 and 1.9 Å resolution structures of the Penicillium amagasakiense and Aspergillus niger glucose oxidases as a basis for modelling substrate complexes. *Acta Crystallogr. Sect. D Biol. Crystallogr.* **55**, 969–977 (1999).

11. Fernandez-Lafuente, R. Stabilization of multimeric enzymes: Strategies to prevent subunit dissociation. *Enzyme Microb. Technol.* **45**, 405–418 (2009).

12. Conrado, R. J., Varner, J. D. & DeLisa, M. P. Engineering the spatial organization of metabolic enzymes: mimicking nature's synergy. *Curr. Opin. Biotechnol.* **19**, 492–499 (2008).

13. Sainz-Polo, M. A. *et al.* Three-dimensional structure of Saccharomyces invertase: Role of a non-catalytic domain in oligomerization and substrate specificity. *J. Biol. Chem.* **288**, 9755–9766 (2013).

14. Wang, J. Electrochemical glucose biosensors. *Electrochem. Sensors, Biosens. their Biomed. Appl.* 57,I-69,I (2008) doi:10.1016/B978-012373738-0.50005-2.

15. Barker, M. K. & Rose, D. R. Specificity of processing α-glucosidase I is guided by the

substrate conformation: Crystallographic and in silico studies. *J. Biol. Chem.* **288**, 13563–13574 (2013).

16. Gentile, K. *et al.* Enzyme aggregation and fragmentation induced by catalysis relevant species. *Phys. Chem. Chem. Phys.* **23**, 20709–20717 (2021).
17. Patel, A. *et al.* Biochemistry: ATP as a biological hydrotrope. *Science (80-.).* **356**, 753–756 (2017).

Chapter 3

3 Interactions with amyloid beta peptide and acetylcholinesterase increase alkaline phosphatase activity

This chapter is reproduced from Bhide, A. and Sen, A., 2023. Interactions with amyloid beta peptide and acetylcholinesterase increase alkaline phosphatase activity. *Physical Chemistry Chemical Physics* with permission from the Royal Society of Chemistry.

3.1 Introduction

Alzheimer's disease (AD) is a progressive, neurodegenerative disease that affects more than 6 million Americans[1]. AD is characterized by the aggregation of two components in the brain, the extracellular amyloid-β peptides and intracellular tau protein[2]. Amyloid-β peptides are produced in the brain when the precursor protein breaks down due to the activity of β and γ -secretases. Although peptides of different lengths are formed, the longer forms, specifically

amyloid β-42, is deposited in the brain[3,4]. These peptides aggregate to form plaques. Recent evidence has shown that these amyloid peptides are associated with hyperphosphorylation of tau protein, which is present inside the neurons[5]. This hyperphosphorylated tau forms neurofibrillary tangles which ultimately leads to neuron death and AD[6,7].

In recent years, it has come to light that liver enzymes could play a role in AD. A recent study found that there is an association of increased liver alkaline phosphatase activity with poor cognition[8]. Multiple studies have also shown that increased activity of plasma, serum, and tissue non-specific alkaline phosphatase are associated with cognitive decline or AD[9,10,11]. Alkaline phosphatase is an enzyme that removes a phosphate group from its substrate. It is known that alkaline phosphatase is present in the central nervous system and its function is to regulate the amount of phosphorylated compounds present[12]. Upon neuron death, the hyperphosphorylated tau is released and alkaline phosphatase removes the phosphate groups from it. This could have a cascading effect since extracellular tau can be toxic for neurons. Extracellular dephosphorylated tau activates the muscarinic receptors and causes the influx of calcium into the cell which causes neuron death[13,14]. This suggests that alkaline phosphatase plays a role in this positive feedback loop that causes neurodegeneration. However, the cause of its increased activity remains unclear.

3.2 Results and Discussion

In this work, we investigated changes in the activity of alkaline phosphatase (AkP) under different AD-relevant conditions. Upon reaction with p-nitrophenyl phosphate (PNPP), this enzyme forms p-nitrophenol (PNP) which absorbs at 405 nm. We conduct these experiments at pH 7 since it is close to the physiological pH and we use 50 mM HEPES buffer since it does not contain any phosphate salts that could affect alkaline phosphatase activity. We monitor this

absorption to assay the enzyme activity. Our study reveals that alkaline phosphatase activity is affected by two species involved in Alzheimer's disease: 1) Amyloid β and 2) acetylcholinesterase.

3.2.1 Effect of Amyloid β

As shown in Figure 3-1(a), the activity of alkaline phosphatase increases upon addition of amyloid β. In this work, we used custom synthesized amyloid β (42 amino acids long). The peptide sequence and characterization are given in Appendix B, Section B.1. We used concentrations close to 10 μM, since at that concentration, amyloid β causes neurotoxicity[15]. This increase in activity is concentration dependent and increases with increasing concentration of amyloid β as shown in Figure 3-1(b).

(a)

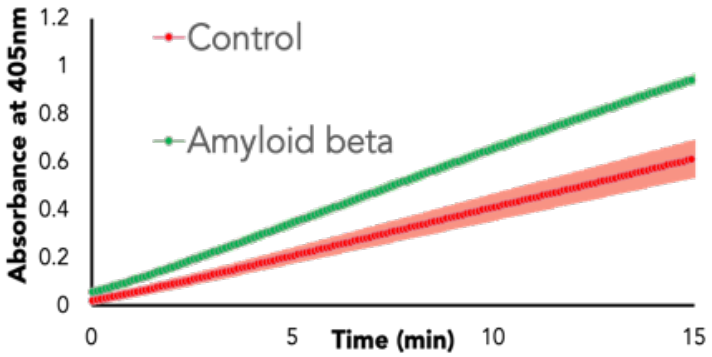

(b)

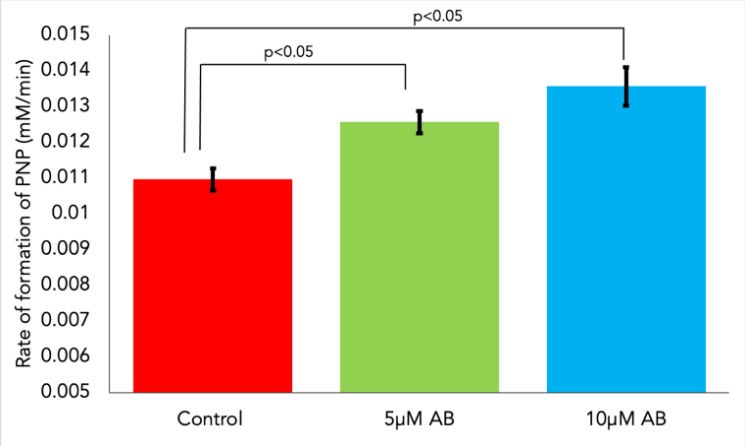

Figure 3- 1: Absorbance due to PNP formation at 405 nm measured using UV Visible spectroscopy in the presence and absence of 12.4 μM amyloid β (AB) for 0.2 μM alkaline phosphatase. Results show that the rate of increase of absorbance at 405nm with respect to time is faster in the presence of AB. (b) Effect 5 and 10 μM of concentration of amyloid β on the rate of formation of PNP due to 0.2μM alkaline phosphatase. Rate of formation of PNP increases as the concentration of AB increases. Results are the average of three trials and error bars represent the standard deviation from three trials. Experiment is performed in 50mM HEPES buffer.

The increase that we observed is comparable to the increases observed in cases of cognitive impairment or AD reported in the literature (Figure 3-2). This indicates that the increase in alkaline phosphatase activity observed in these studies could be due to the accumulation of amyloid β in the brain and its interaction with alkaline phosphatase.

In order to study this specific interaction, we performed a fluorescence resonance energy transfer (FRET) experiment to probe the aggregation state of alkaline phosphatase in the presence of amyloid β. A FRET experiment involves tagging one batch of alkaline phosphatase with the donor dye (Alexa Fluor 488) and one batch with the acceptor dye (Alexa Fluor 532). Upon aggregation (dyes separated by < 6 nm), energy transfer occurs between the two dyes. We excited the sample at 488 nm and recorded emission between 500-600 nm. Based on the emission of the acceptor and the total emission, we calculated FRET Efficiency, which is a

measure of how much of the sample is aggregated. The FRET efficiency varies between 0 and 1 with 0 indicating no aggregation and 1 indicating complete aggregation. More details about the FRET experiment and analysis are given in Section 3.4. We found that amyloid β de-aggregates alkaline phosphatase present in solution. (Figure 3-3) Although amyloid β does not de-aggregate alkaline phosphatase by a large amount, the difference between the two FRET efficiencies after 5 minutes is statistically significant ($p<0.05$). This is a clear indication that amyloid β interacts with alkaline phosphatase.

To test if this phenomenon is general, we also repeated this experiment with alkaline phosphatase from *E. coli*, which is a different source than bovine intestinal mucosa, which was used previously. We found that alkaline phosphatase from *E. coli* showed a 17% increase in activity due to 10 μM amyloid β, suggesting that this phenomenon is general for alkaline phosphatase enzymes. (Figure 3-4) Interestingly, for alkaline phosphatase from *E. coli,* we don't see as much of a concentration dependence of the activity as the alkaline phosphatase from bovine intestinal mucosa.

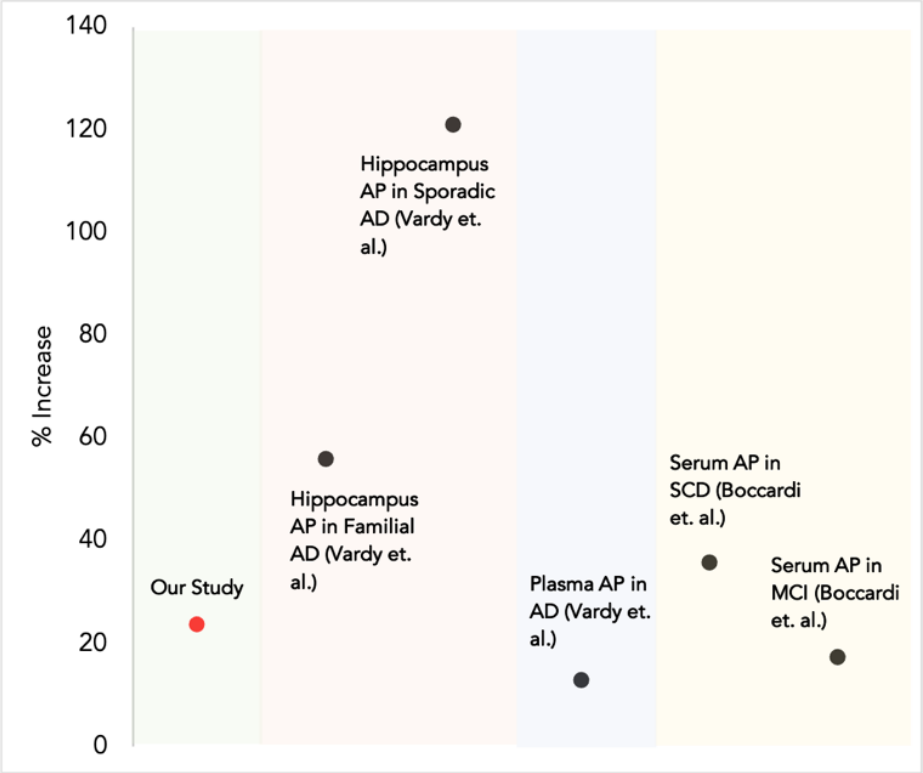

Figure 3- 2: Comparison of increase in alkaline phosphatase activity observed in our study with familial and sporadic AD by Vardy et.al[11], and subjective cognitive decline (SCD) and mild cognitive impairment (MCI) by Boccardi et. Al[10]. For Vardy et. al., % increases are between the TNAP activities in hippocampus and plasma AP as compared to age matched controls. For Boccardi et. al, % increases are between the adjusted means of ALP serum levels in healthy controls vs SCD and healthy controls vs MCI. These results show that the increase that we observe in our study is comparable to the increases in alkaline phosphatase observed in the literature due to Alzheimer's disease or cognitive decline.

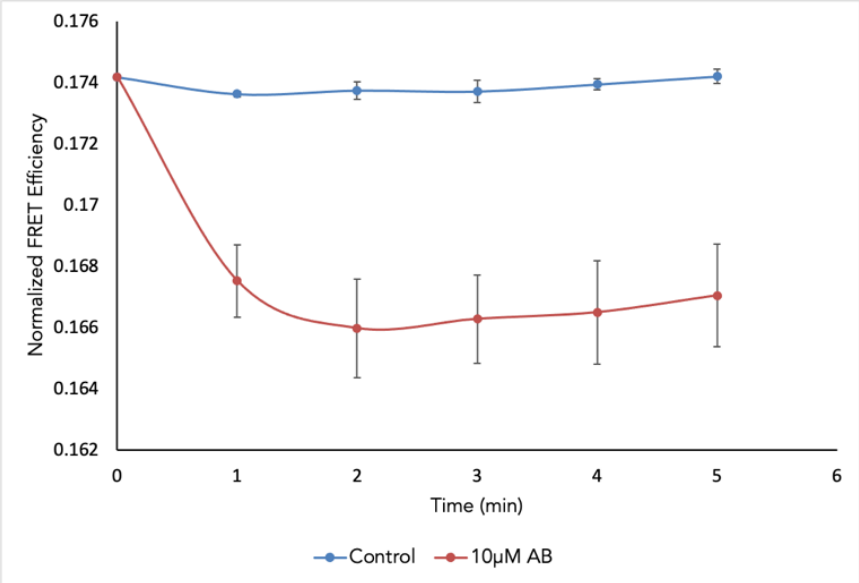

Figure 3- 3: Normalized FRET efficiency vs time graph showing the de-aggregation of 0.2 μM alkaline phosphatase in the absence of (blue) and presence of amyloid β (AB) (red). Results are the average of three trials and error bars represent the standard deviation from three trials. Experiments are performed in 50mM HEPES buffer.

We tested if the activity of alkaline phosphatase increases due to other proteins such as bovine serum albumin (BSA). We found that the activity does not show a significant increase with the same concentration (10 μM) as well as the same amount by mass (0.7 μM) of BSA (Appendix B, Figure B-3). This indicates that the interaction between amyloid β and alkaline phosphatase is specific and is not observed with all proteins.

Taken together, these results indicate that, due to a specific interaction between alkaline phosphatase and amyloid β, the activity of alkaline phosphatase increases.

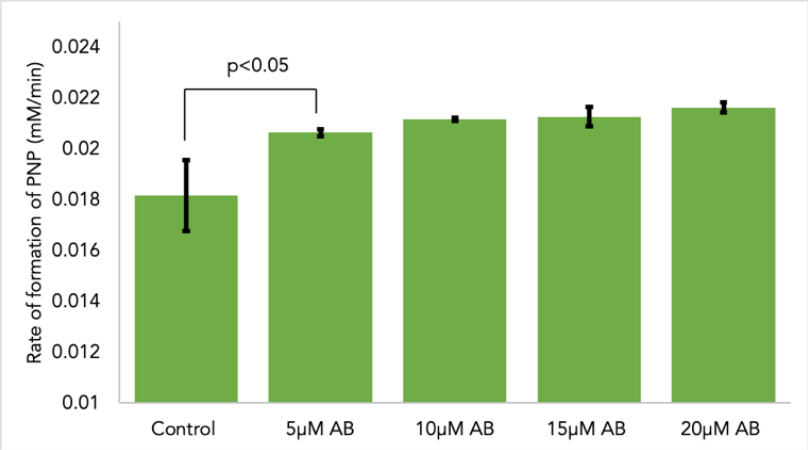

Figure 3- 4: Rate of formation of PNP by 0.2μM alkaline phosphatase from *E. coli* in the presence of amyloid β (AB). Results are the average of three trials and error bars represent the standard deviation from three trials. Results show that the rate of formation of PNP increases upon addition of AB. Rate of formation of PNP in the presence of 5 μM AB is significantly different ($p<0.05$) from the control. Experiments are performed in 50mM HEPES buffer.

3.2.1 Effect of Acetylcholinesterase Reaction

We also examined the effects of treatment procedures for AD. Cholinesterase inhibitors are commonly used for AD treatment[16,17]. Acetylcholinesterase (AchE) is an enzyme that converts the neurotransmitter acetylcholine to acetic acid and choline. It is present outside the neurons at synaptic junctions and is used to regulate the amount of acetylcholine[18]. There is a lowering of the amount of acetylcholine during AD. Thus, several approved drugs that are currently used, such as donepezil (Aricept®), rivastigmine (Exelon®), galantamine (Razadyne®), for treatment of AD are cholinesterase inhibitors. By inhibiting acetylcholinesterase, they ensure that the acetylcholine levels are maintained[16,19]. In our study, we found that the activity of alkaline phosphatase also increases in the presence of

acetylcholinesterase from *Electrophorus electricus* (electric eel) (Figure 3-5). This increase is also concentration-dependent.

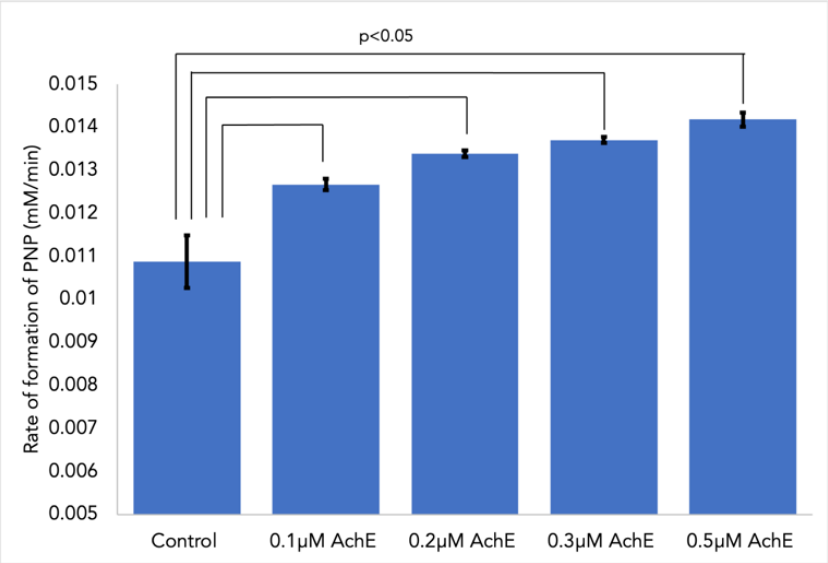

Figure 3- 5: Rate of formation of PNP measured using UV Visible Spectroscopy in the presence of different concentrations of acetylcholinesterase (AchE) due to 0.2 μM alkaline phosphatase. Results are the average of three trials and error bars represent the standard deviation from three trials. 0.1, 0.2, 0.3 and 0.5μM AchE values are significantly different ($p<0.05$) from the control. Results show that as the concentration of acetylcholinesterase increases, the rate of formation of PNP increases. All the different concentrations of AchE are significantly different ($p<0.05$) from each other. Experiments are performed in 50mM HEPES Buffer.

We also performed concentration dependent experiments to examine whether the activity of alkaline phosphatase also increases due to acetylcholine and choline at different physiological concentrations (Figures 3-6(a)(b)). For acetylcholine, the physiological concentration is very low. The concentration of acetylcholine in extracellular brain fluid is 0.1-6 nM[20]. The concentration of choline in human cerebrospinal fluid determined by Haubrich et. al. ranged from 1.8-31.2 μM with a mean of 5.7 μM[21]. We found that, at these concentrations, acetylcholine and choline do not affect the activity of alkaline phosphatase. However, at higher concentrations, both acetylcholine and choline increase the activity of alkaline phosphatase.

(Appendix B, Figure B-4). This is concerning because it means that if the concentration of acetylcholine increases due to cholinesterase inhibitor drugs, they could have a negative effect on AD. All these activity increases are summarized in Table 3-1. As expected, acetic acid did not increase alkaline phosphatase activity (Appendix B, Figure B-5).

We also studied whether these interactions affect acetylcholinesterase activity. Using Ellman's assay, we monitored the formation of 5-thio 2-nitrobenzoic acid (TNB) which absorbs at 412 nm. We found that alkaline phosphatase and amyloid β do not have any effect on acetylcholinesterase activity. (Figure 3-7).

(a)

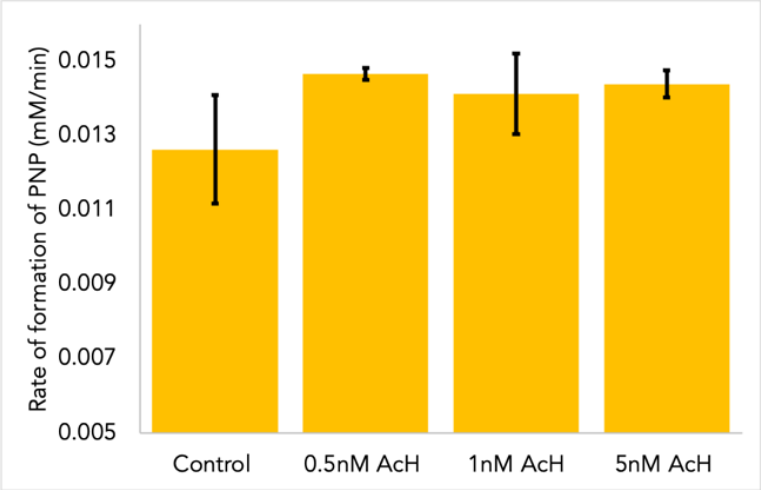

(b)

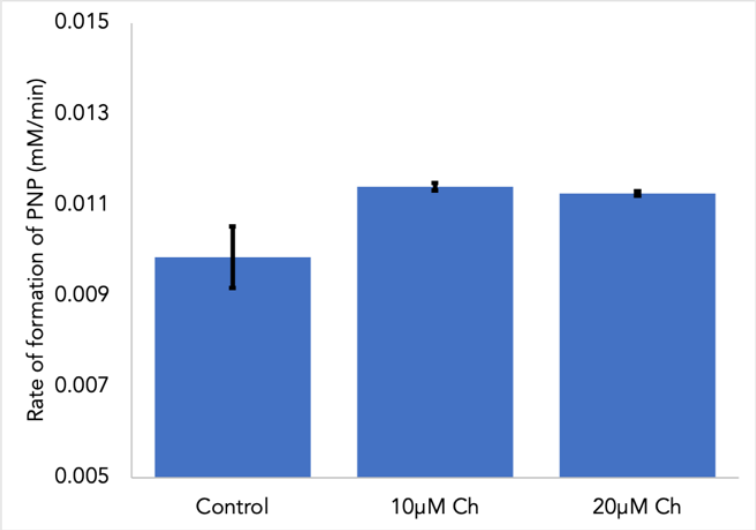

Figure 3- 6: Rate of formation of PNP due to 0.2μM alkaline phosphatase measured using UV Visible spectroscopy in the presence of (a) nanomolar concentrations of acetylcholine chloride (AcH) and (b) micromolar concentrations of choline chloride (Ch). Results show that the rate of formation of PNP does not change upon addition of acetylcholine and choline chloride. Results are the average of three trials and error bars represent the standard deviation from three trials. For both figures, none of the concentrations of AcH or Ch are significantly different ($p<0.05$) from the control. Experiments are performed in 50mM HEPES buffer.

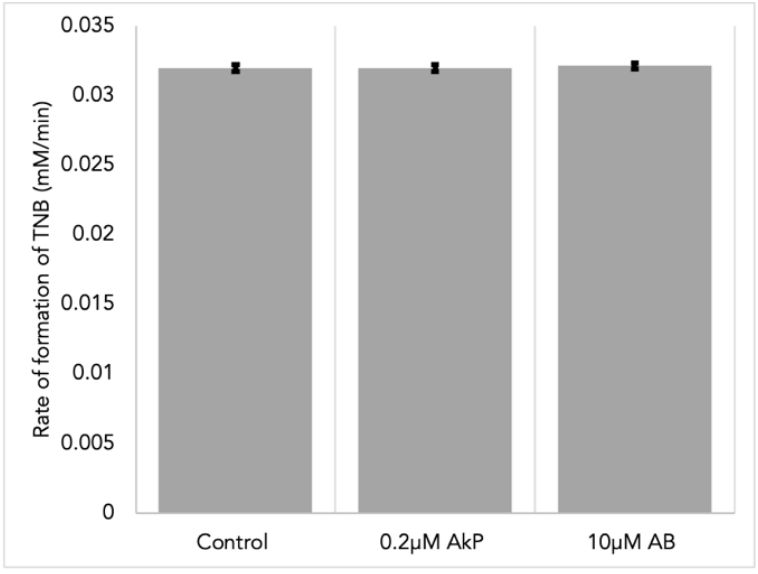

Figure 3- 7: Rate of formation of TNB due to 0.01 μM acetylcholinesterase in the presence of 10 μM amyloid β (AB) and 0.2 μM alkaline phosphatase (AkP). Results show that the rate of formation of TNB does not change upon addition of alkaline phosphatase and amyloid beta. Error bars represent the standard deviation from three trials. Activity in the presence of AkP and

AB is not significantly different ($p<0.05$) from the control. Experiments are performed in 50mM HEPES buffer.

Conditions	% Increase
Amyloid $\boldsymbol{\beta}$ (10 μM)	24
Acetylcholinesterase (0.2 μM)	23
High concentration of choline (5 mM)	44
High concentration of acetylcholine (5 mM)	43

Table 3- 1: Range of bovine intestinal mucosa alkaline phosphatase activity enhancements observed in our experiments under different conditions.

3.3 Conclusion

In conclusion, we have demonstrated that there is an interaction between amyloid β and alkaline phosphatase which causes an increase in the activity of alkaline phosphatase. We saw a 24% increase in activity due to 10 μM amyloid β which is comparable to the increases observed in previous studies in AD and cognitive impairment (Figure 3-2). We showed that this phenomenon is dependent on amyloid β concentration and not specific to a particular type of alkaline phosphatase. Thus, the increased activity of alkaline phosphatase associated with

cognitive decline and/or AD diagnosis may not be due to higher *concentration* of the enzyme[9,11,10]. We also showed that acetylcholinesterase enhances alkaline phosphatase activity and cholinesterase inhibitors used to treat AD could be affecting alkaline phosphatase activity. This increase in alkaline phosphatase activity could promote further neurodegeneration and has to be taken into account while studying AD.

Our observations suggest that molecular interactions can lead to conformational changes affecting alkaline phosphatase activity. Future studies should focus on the nature of the structural changes using alternative techniques and, in particular, attempt to identify the individual protein residues that interact with amyloid - β or acetylcholinesterase to cause the activity changes.

3.4 Materials and Methods

3.4.1 Materials

Alkaline Phosphatase from bovine intestinal mucosa, Alkaline Phosphatase from *Escherichia coli*, Acetylcholinesterase from *Electrophorus electricus* (electric eel), acetylcholine chloride, choline chloride, bovine serum albumin, acetylthiocholine chloride and para-nitro phenyl phosphate (PNPP) were purchased from Sigma Aldrich. Alexa Fluor™ 488 NHS Ester (Succinimidyl Ester) and Alexa Fluor™ 532 NHS Ester (Succinimidyl Ester) were purchased from Thermo Fisher Scientific, and 5,5-dithiobis-2-nitrobenzoic acid (DTNB) and 4-nitrophenol (PNP) was purchased from Alfa Aesar. Buffer used for all experiments was 50mM HEPES-NaOH (pH 7). Amyloid- β 1-42 was synthesized and purified by the Macro Core Facility at the Penn State University College of Medicine.

3.4.2 Methods

3. 4. 2. 1 Amyloid β solution preparation

Amyloid β was mixed with DMSO (1 mg in 30µL) and sonicated until it dissolves (about 5 minutes). This solution was then diluted with buffer to form 1 mg/mL amyloid β solution and diluted further for subsequent experiments.

3. 4. 2. 2 Alkaline phosphatase activity Measurements

Alkaline Phosphatase from bovine intestinal mucosa was used for the experiments unless specified. For these measurements, alkaline phosphatase solution was taken in a cuvette such that its final concentration was 0.2µM. Acetylcholinesterase, amyloid β, acetylcholine chloride, choline chloride, acetic acid or bovine serum albumin (BSA) were added as specified. Lastly, PNPP was added such that its final concentration was 0.5mM. Absorption at 405 nm is monitored using Thermo Fisher UV-Visible Spectrophotometer for 15 minutes with a reading taken every 0.1 minute. The slope of this graph of absorbance vs time is divided by the molar extinction coefficient of para-nitrophenol (PNP) to obtain the rate of formation of PNP. The calculation of molar extinction coefficient is shown in Appendix B.

3. 4. 2. 4 FRET experiments

Alkaline phosphatase from bovine intestinal mucosa was used for these experiments. For these experiments, we took two batches of alkaline phosphatase and mixed them with two different dyes (Alexa Fluor 488 and Alexa Fluor 532) along with 100mM sodium

bicarbonate. This solution was made in water so that the pH can be slightly basic. The solutions were shaken for 1 hour and then kept in the fridge overnight. The next morning, the solutions were shaken again for 2 hours and the tagged enzyme was purified according to procedure given in Thermo Fisher Scientific Antibody Conjugate Purification Kit. We used 50mM HEPES as the elution buffer. The starting concentration of alkaline phosphatase is 2.4 mg/mL for Alexa Fluor 488 and 1.7mg/mL for Alexa Fluor 532. The starting enzyme: dye ratios for the two enzymes were 1:3.3 (488) and 1: 1.9 (532). The ratios after tagging are given in Table 3-2. We use succinimidyl esters (NHS ester) of the two dyes. Upon tagging, these dyes become conjugated to the primary amine groups of the enzyme[22].

Enzyme and Dye	**Enzyme: Dye ratio**
Alkaline Phosphatase and Alexa Fluor 488	0.9
Alkaline Phosphatase and Alexa Fluor 532	0.7

Table 3- 2: Tagging Ratios of Alkaline Phosphatase and Alexa Fluor 488 and Alexa Fluor 532 for FRET experiments.

The FRET experiments were done on a Fluorolog JobinYvon Horiba spectrofluorometer. For the FRET Experiments, the excitation wavelength was 488 nm and the emission was captured between 500-600nm. The FRET Efficiency was calculated using the same way as described in Section 2.4, Chapter 2. The obtained FRET efficiency was normalized using the procedure given below.

3. 4. 2. 5 Normalization of FRET efficiency

To calculate the base-line corrected FRET efficiencies for the experiments, we used the FRET efficiency at 0 min of the first experiment (E_0) as a reference. For all the other experiments, we calculated α_i,

$$\alpha_i = I_0 - E_0$$

Where i corresponds to the number of the experiment, I_0 is the FRET Efficiency at 0 min for that particular experiment and E_0 is the FRET efficiency at 0 min for the first experiment.
Then, to calculate the base-line corrected FRET efficiency, we subtracted the calculated α_i for that particular trial to all the FRET efficiencies from 0 to 5 mins such that the FRET efficiency at 0 minutes is the same for all experiments. We plotted the average of the base-line corrected FRET efficiencies with respect to time. By doing so, we ensured that all the different FRET efficiencies start at the same point so that we can visualize the changes in FRET efficiencies clearly.

3. 4. 2. 6 Acetylcholinesterase Activity measurements

To assay acetylcholinesterase activity, we mixed acetylcholinesterase and acetylthiocholine chloride solutions for two minutes. After two minutes, 5,5-dithiobis-2-nitrobenzoic acid (DTNB) was added and absorption at 412 nm was measured using UV Visible Spectroscopy. The final

concentration of acetylcholinesterase, acetylthiocholine and DTNB in the experiments was 0.01 µM, 0.1 µM and 0.5 mM respectively. This absorption change was converted to the rate of formation of 2-nitro-5-thiobenzoic acid (TNB). The molar extinction coefficient of TNB at 412 nm is 14,150 M^{-1} cm^{-1} and it can be used to calculate the rate of formation of TNB which is a measure of acetylcholinesterase activity[23].

3. 4. 2. 7 Calculation of Statistical Significance

To compare the difference between two groups, we performed a two-sample unpaired t-test. Prior to conducting the t-test, the normality of the data was tested using the Shapiro-Wilk test. Also, an F-test was performed to check if the variances were equal or not. Based on the results of the F-test, the appropriate t-test was performed. The alpha value was chosen as 0.05 (5%). The two tailed P-value for the t-test is reported.

3.5 Acknowledgements

We acknowledge funding of the research by the Air Force Office of Scientific Research FA9550-20-1-0393. The amyloid β synthesis was carried out at the Macro Core Facility in the Penn State University College of Medicine RRID:SCR_020408. Any findings or conclusions expressed in this dissertation are those of the authors and do not necessarily reflect the views of the Air Force Office of Scientific Research.

3.6 References

1. Report, S., Patient, T. H. E., In, J., Era, A. N. & New, O. F. 2023 Alzheimer's disease facts and figures. *Alzheimer's Dement.* (2023) doi:10.1002/alz.13016.
2. Ross, C. A. & Poirier, M. A. Protein aggregation and neurodegenerative disease. *Nat. Med.* **10**, S10 (2004).
3. Sehar, U., Rawat, P., Reddy, A. P., Kopel, J. & Reddy, P. H. Amyloid Beta in Aging and Alzheimer's Disease. *Int. J. Mol. Sci.* **23**, (2022).
4. Murphy, M. P. & Levine, H. Alzheimer's disease and the amyloid-β peptide. *J. Alzheimer's Dis.* **19**, 311–323 (2010).
5. Zheng, W. H., Bastianetto, S., Mennicken, F., Ma, W. & Kar, S. Amyloid β peptide induces tau phosphorylation and loss of cholinergic neurons in rat primary septal cultures. *Neuroscience* **115**, 201–211 (2002).
6. Díaz-Hernández, M. *et al.* Tissue-nonspecific alkaline phosphatase promotes the neurotoxicity effect of extracellular tau. *J. Biol. Chem.* **285**, 32539–32548 (2010).
7. Ju, Y. & Tam, K. Pathological mechanisms and therapeutic strategies for Alzheimer's disease. *Neural Regen. Res.* **17**, 543–549 (2022).
8. Nho, K. *et al.* Association of Altered Liver Enzymes With Alzheimer Disease Diagnosis, Cognition, Neuroimaging Measures, and Cerebrospinal Fluid Biomarkers. *JAMA Netw. Open* **2**, 1–20 (2019).
9. Kellett, K. A. B., Williams, J., Vardy, E. R. L. C., Smith, A. D. & Hooper, N. M. Plasma alkaline phosphatase is elevated in Alzheimer's disease and inversely correlates with cognitive function. *Int. J. Mol. Epidemiol. Genet.* **2**, 114–121 (2011).
10. Boccardi, V. *et al.* Serum alkaline phosphatase is elevated and inversely correlated with

cognitive functions in subjective cognitive decline: results from the ReGAl 2.0 project. *Aging Clin. Exp. Res.* **33**, 603–609 (2020).

11. Vardy, E. R. L. C., Kellett, K. A. B., Cocklin, S. L. & Hooper, N. M. Alkaline Phosphatase Is Increased in both Brain and Plasma in Alzheimer's Disease. *Neurodegener. Dis.* **9**, 31–37 (2011).
12. Miguel Diaz-Hernandez, Felix Hernandez, M. T. M.-P. and J. A. Neuronal Tissue-Nonspecific Alkaline Phosphatase (TNAP). in *Neuronal Tissue-Nonspecific Alkaline Phosphatase (TNAP)* (2015).
13. Gómez-Ramos, A., Díaz-Hernández, M., Rubio, A., Miras-Portugal, M. T. & Avila, J. Extracellular tau promotes intracellular calcium increase through M1 and M3 muscarinic receptors in neuronal cells. *Mol. Cell. Neurosci.* **37**, 673–681 (2008).
14. Sebastián-Serrano, Á. *et al.* Tissue-nonspecific Alkaline Phosphatase Regulates Purinergic Transmission in the Central Nervous System during Development and Disease. *Comput. Struct. Biotechnol. J.* **13**, 95–100 (2015).
15. Raskatov, J. A. What Is the "Relevant" Amyloid β42 Concentration? *ChemBioChem* **20**, 1725–1726 (2019).
16. Sharma, K. Cholinesterase inhibitors as Alzheimer's therapeutics (Review). *Mol. Med. Rep.* **20**, 1479–1487 (2019).
17. Giacobini, E., Cuello, A. C. & Fisher, A. Reimagining cholinergic therapy for Alzheimer's disease. *Brain* **145**, 2250–2275 (2022).
18. Dobbertin, A. *et al.* Targeting of acetylcholinesterase in neurons in vivo: A dual processing function for the proline-rich membrane anchor subunit and the attachment domain on the catalytic subunit. *J. Neurosci.* **29**, 4519–4530 (2009).

19. Marucci, G. *et al.* Efficacy of acetylcholinesterase inhibitors in Alzheimer's disease. *Neuropharmacology* **190**, 2013 (2021).

20. Nirogi, R., Mudigonda, K., Kandikere, V. & Ponnamaneni, R. Quantification of acetylcholine, an essential neurotransmitter, in brain microdialysis samples by liquid chromatography mass spectrometry. *Biomed. Chromatogr.* **24**, 39–48 (2010).

21. Haubrich, D. R., Gerber, N., Pflueger, A. B. & Zweig, M. Tissue Choline Studied Using a Simple Chemical Assay. *J. Neurochem.* **36**, 1409–1417 (1981).

22. Nanda, J. S. & Lorsch, J. R. *Labeling a protein with fluorophores using NHS ester derivitization*. *Methods in Enzymology* vol. 536 (Elsevier Inc., 2014).

23. Peter Eyer, Franz Worek, Daniela Kiderlen, Goran Sinko, Anita Stuglin, Vera Simeon-Rudolf, cand E. R. Molar absorption coefficients for the reduced Ellman reagent: reassessment. *Anal. Biochem.* **312**, 224–227 (2003).

Chapter 4

4 Protein-mediated Aggregation of Liposomes

4.1 Introduction

Liposomes are spherical, cell-membrane-like structures made of phospholipid bilayers. They can form spontaneously in aqueous solutions and the properties of the liposomes can be controlled by varying the lipid composition, size, polydispersity and the contents of the liposomes. In literature, liposomes ranging from small sizes (nm) to giant (μM) have been synthesized[1]. Due to their spherical structure and compartmentalization ability, they are commonly used for drug delivery applications[2,3,4].

Targeted drug delivery involves transporting a drug to a specific location in the body and releasing the drug directly at that particular location[5]. Doing so will minimize side effects since the drug will not interact with healthy cells and the amount of drug required will be lower. Targeted delivery is achieved by using drug delivery vehicles that can enclose the drug within them, travel to the desired site and release the drug upon cues at the particular location. Liposomes have been used for this purpose and they can deliver both hydrophilic and hydrophobic molecules[6]. The first

nanosized liposome encapsulated drug Doxil was approved by the Food and Drug Administration (FDA) in 1995[7]. Since then, a number of drugs with liposome-based delivery systems have been approved by the FDA. However, there are a variety of challenges in the usage of liposomes for targeted drug delivery that still need to be tackled.

To use liposomes for targeted drug delivery, it is important for them to have various functionalities. We need control over their directional movement, assembly, as well as release. Controlling the aggregation of liposomes is important for their stability as well as for their use in drug delivery. By making liposomes that carry drugs aggregate selectively at a particular point such as a cancer tissue, it can help transport, gather and release the drug directly to that tissue. Liposome aggregation has been controlled by using various methods. Liposomes whose surface has been coated with DNA which can crosslink upon photoirradiation and cause aggregation of liposomes[8]. The aggregation of liposomes and superparamagnetic iron oxide nanoparticles (SPIONs) can also be controlled using radiofrequency stimulation[9]. In this work, we want to control the aggregation of liposomes using methods that are not only biocompatible, but can also help us give the liposome multiple functionalities. Protein-coating is an ideal solution because it is biocompatible and it has been used to achieve control over the directional movement and enhanced diffusion of liposomes[10,11]. In this paper we demonstrate that we can also use protein-coating to control the aggregation of liposomes.

Here, we use protein-coating to control the aggregation of liposomes in the presence of zinc and calcium ions. Zinc ions play a huge role in various cell processes and are required by over 300 enzymes in the body[12]. Although the concentration of zinc in cells is fairly low (0.2-0.3mM)[13], it is known that zinc concentration is higher in certain cancer tissues[14]. Also, higher concentration of calcium in blood has been observed for people with cancer[15]. Thus, drug delivery vehicles that

can aggregate at locations with higher zinc and calcium concentrations can help reduce side effects and ensure targeted drug delivery. By attaching proteins to liposomes and studying their aggregation using Dynamic Light Scattering (DLS) and confocal microscopy, we demonstrate that we can achieve control over the aggregation of liposomes by varying the proteins attached and the concentration of the salts.

4.2 Results and Discussions

4.2.1 Aggregation of uncoated liposomes

To begin, we synthesized liposomes using the thin-film hydration method and extruded them using a 100 nm membrane filter. Our lipid composition is 99% POPC and 1% Biotin-cap-PE and the liposomes are made in 50mM HEPES buffer (pH 7). More details about the liposome synthesis are given in Section 4.4. Before adding any proteins, we studied the aggregation of liposomes in the presence of 50mM zinc nitrate and 50mM calcium nitrate by monitoring their size using Dynamic Light Scattering (DLS). (Figure 4-1)

(a) (b)

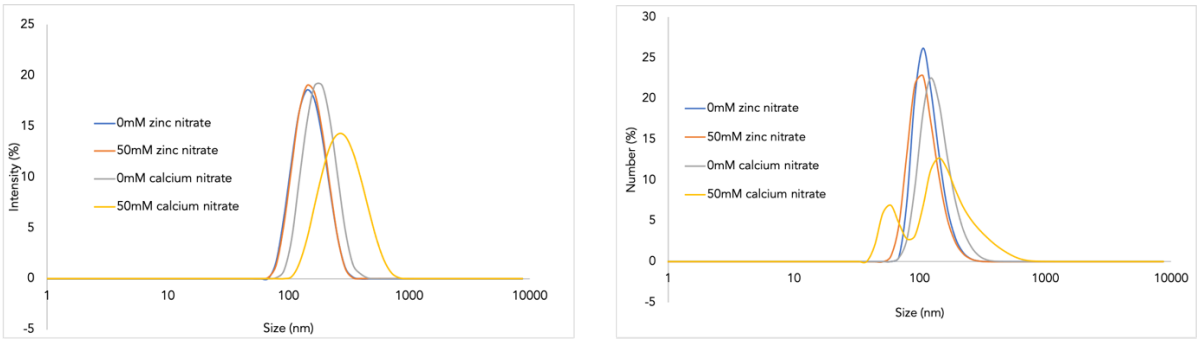

Sample Name	Z-average (nm)	PDI	Derived Count Rate (kcps)
0mM zinc nitrate	142.4	0.071	1416.7
50mM zinc nitrate	144.3	0.056	1416.5
0mM calcium nitrate	172.9	0.06	1385.5
50mM calcium nitrate	258	0.153	2300.6

Figure 4- 1: DLS measurements showing (a) Intensity (%) vs size (nm) and (b) Number (%) vs size for uncoated liposomes in the presence of 0mM zinc nitrate (blue), 50mM zinc nitrate (orange), 0mM calcium nitrate (gray) and 50mM calcium nitrate (yellow). The table below the image shows the Z-average, polydispersity index (PDI) and count rate for the samples. These curves are averages of three readings for the samples.

As expected, DLS measurements of Z-Average, polydispersity index (PDI) and count rate show that these uncoated liposomes are monodisperse and around 100 nm in size. The liposomes did not show any aggregation due to zinc and calcium nitrate. We. also tested with 50mM magnesium nitrate and the liposomes showed aggregation in the presence of 50mM magnesium nitrate (Appendix C, Figure C-1). We hypothesize that this aggregation occurs due to an interaction between the lipid membranes and magnesium ions. Interestingly, a previous study has shown molecular differences between the binding of Ca^{2+} and Mg^{2+} with a phosphatidylserine (PS^{-}) phospholipid bilayer[16]. Using molecular dynamics, they show that due to binding differences between the cations and the carboxylate and phosphate groups in the lipids, upon interaction, these

two cations are present in different areas of the phospholipid membranes and show different hydration behavior. We hypothesize that similar differences in binding of calcium and magnesium ions is causing a difference in their aggregation behavior for liposomes with phosphatidylcholine (PC) membrane. Since our aim was to study the aggregation due to proteins in the presence of high salt concentrations, we decided to exclude magnesium ions from our experiments. Therefore, in subsequent experiments, we focus purely on the effect of zinc and calcium ions.

For zinc nitrate and calcium nitrate, we also investigated whether the liposomes would remain unaggregated in the presence of different concentrations of these salt solutions using DLS. (Figure 4-2). The intensity vs. size graphs for these experiments are shown in Appendix C, Figure C-2.

(a)

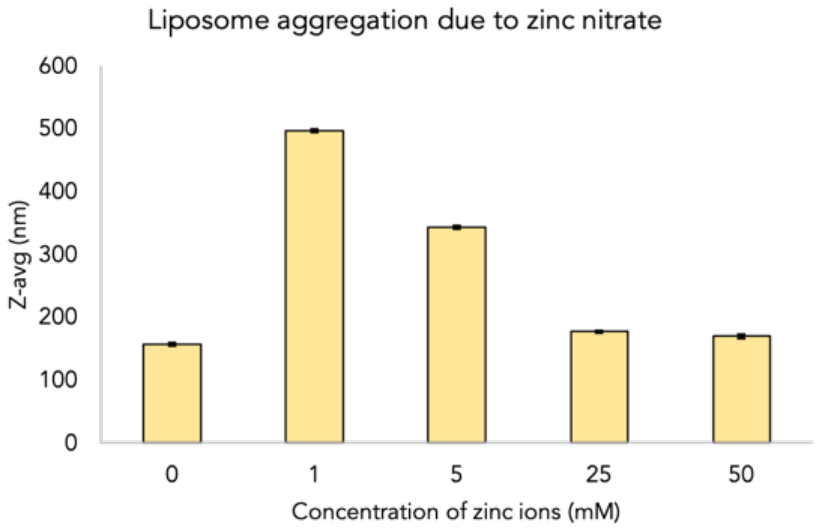

(b)

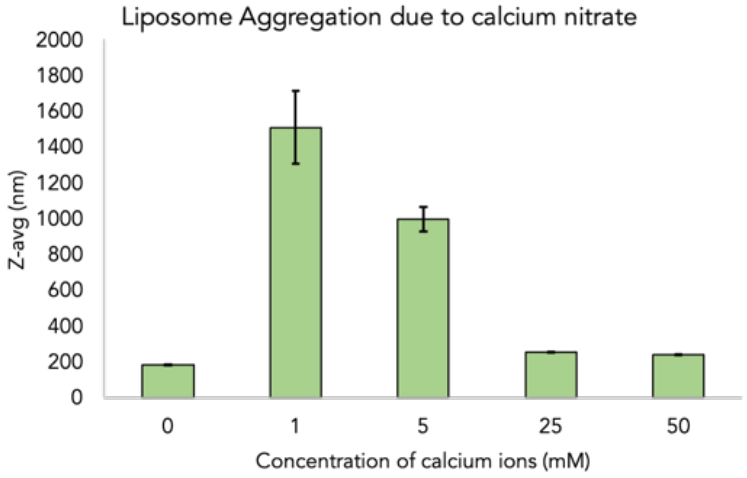

Figure 4- 2: Z-average from DLS measurements of uncoated liposomes in 0, 1, 5, 25 and 50mM concentrations of (a) zinc nitrate and (b) calcium nitrate. These uncoated liposomes show aggregation in the presence of low concentrations of zinc and calcium ions but no aggregation in the presence of high concentrations of these ions. Z-average values are the average and error bars are the standard deviations from three readings of the samples. This experiment is performed in 50mM HEPES buffer (pH 7).

Interestingly, our results showed that while this was true for higher concentrations, the liposomes aggregated at concentrations lower than 25mM which went down as the concentration of zinc nitrate and calcium nitrate increased. Although the size of the aggregates varied on different days of these experiments, the trend remained the same. We believe that this phenomenon occurs because Zn^{2+} and Ca^{2+} ions form a complex with the negatively charged lipid and stabilize the liposomes at higher concentrations, thus preventing aggregation. However, this shielding effect of zinc and calcium cations is eliminated upon addition of proteins.

4.2.2 Aggregation of protein-coated liposomes

In this study, we use two model proteins, namely streptavidin and avidin. Streptavidin is a negatively charged, 53kDa protein that is derived from bacteria while avidin is a positively charged 66kDa protein that is found in egg whites. These two proteins are chosen due to their high binding affinity to biotin. The dissociation constant for streptavidin and avidin with biotin is 4×10^{-14} M and 1.3×10^{-15} M respectively[17,18]. Before attaching them to liposomes, we studied the aggregation of streptavidin using Fluorescence Resonance Energy Transfer (FRET) (Figure 4-3). We tagged one batch of streptavidin with the donor dye, Alexa Fluor 488 and another batch with the acceptor dye, Alexa Fluor 532. Then, we mixed the two batches and measured emission spectra upon excitation at 488nm, which is the excitation of the donor. We converted this to FRET efficiency which is a measure of aggregation between the two batches. Details about the FRET experiments and analysis are given in Section 4.4. We found that streptavidin aggregates in the presence of 10 μM zinc nitrate. Also, interestingly, the aggregation is reversible and the protein de-aggregates upon addition of 10 μM EDTA.

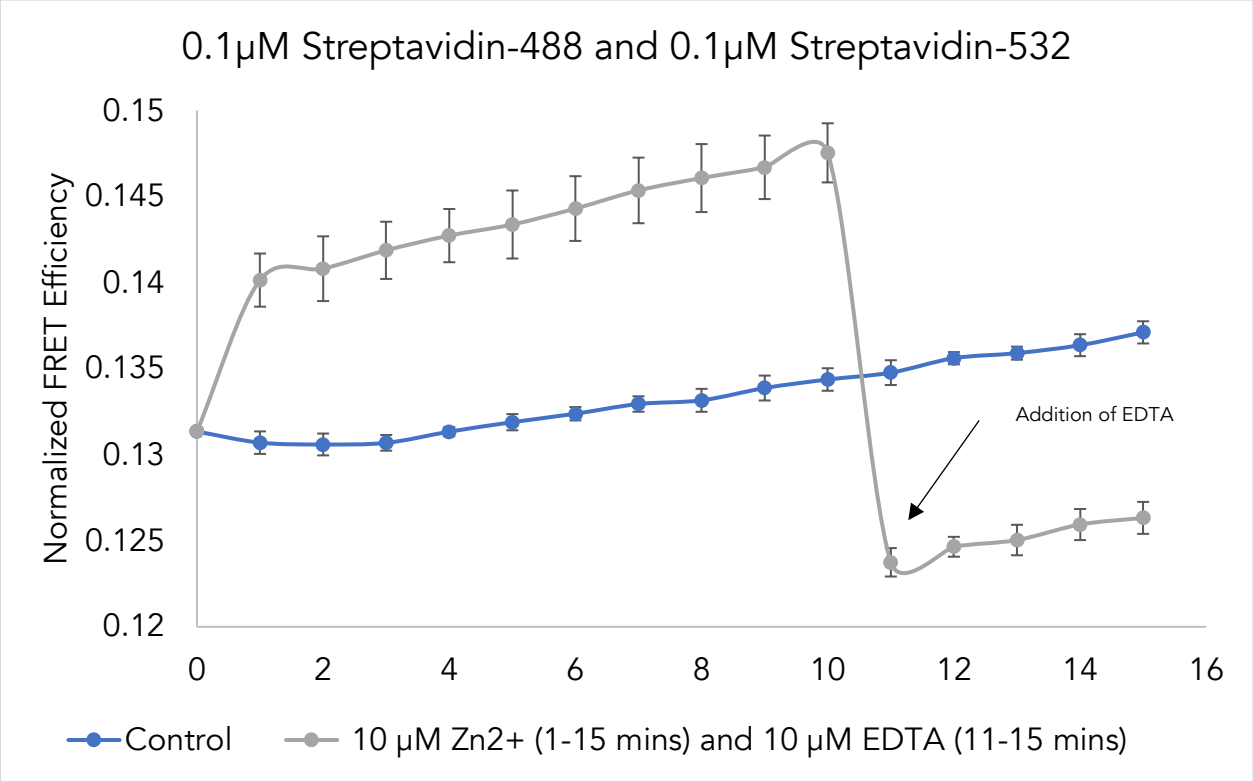

Figure 4- 3: Normalized FRET efficiency vs time for 0.1µM Streptavidin tagged with AF 488 and 0.1µM streptavidin tagged with AF 532 (blue), 0.1µM Streptavidin tagged with AF 488 and 0.1µM streptavidin tagged with AF 532 after addition of 4X filtered zinc nitrate such that its final concentration is 10 µM and ethylene diamine tetra acetic acid (EDTA) after 10 minutes such that its final concentration is 10 µM (gray). These results show that streptavidin aggregates upon addition of zinc nitrate which can be reversed upon addition of EDTA. Results are the average and error bars are the standard deviation from three trials. This experiment is performed in 50mM HEPES buffer (pH 7).

Next, we attached these proteins to the outside of liposomes and studied their aggregation using DLS. To attach the proteins, we mixed the liposomes that contain 1% biotinylated lipid with streptavidin or avidin. After mixing for an hour, we filter out the excess protein using centrifuge filtering. We found that, streptavidin coated liposomes aggregated in the presence of zinc nitrate and calcium nitrate similar to the native protein. (Figure 4-4).

(a) (b)

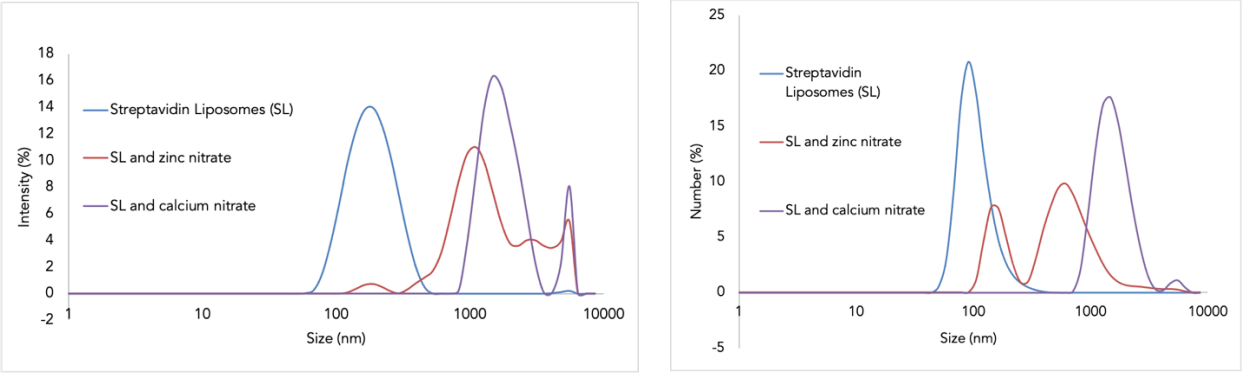

Sample Name	Z-average (nm)	PDI	Derived Count Rate (kcps)
Streptavidin Liposomes (SL)	167.9	0.141	220
SL and zinc nitrate	1383	0.564	320
SL and calcium nitrate	2598	0.406	635.8

Figure 4- 4: DLS measurements showing (a) Intensity (%) vs size (nm) and (b) Number (%) vs size (nm) for streptavidin coated liposomes by themselves (blue) in the presence of 50mM zinc nitrate (red) and 50mM calcium nitrate (violet). Table below shows the Z-average values, polydispersity index (PdI) and count rate for these readings. These liposomes show aggregation in the presence of high concentrations of zinc and calcium nitrate. Curves are the average of three readings. This experiment is performed in 50mM HEPES buffer (pH 7).

We also studied this aggregation using confocal microscopy. We used fluorescent Cy5 streptavidin for these experiments and imaged the solution in the presence of 50mM zinc nitrate and calcium nitrate (Figure 4-5). The confocal images of Cy5 streptavidin coated liposomes also show that these liposomes aggregate in the presence of zinc and calcium nitrate.

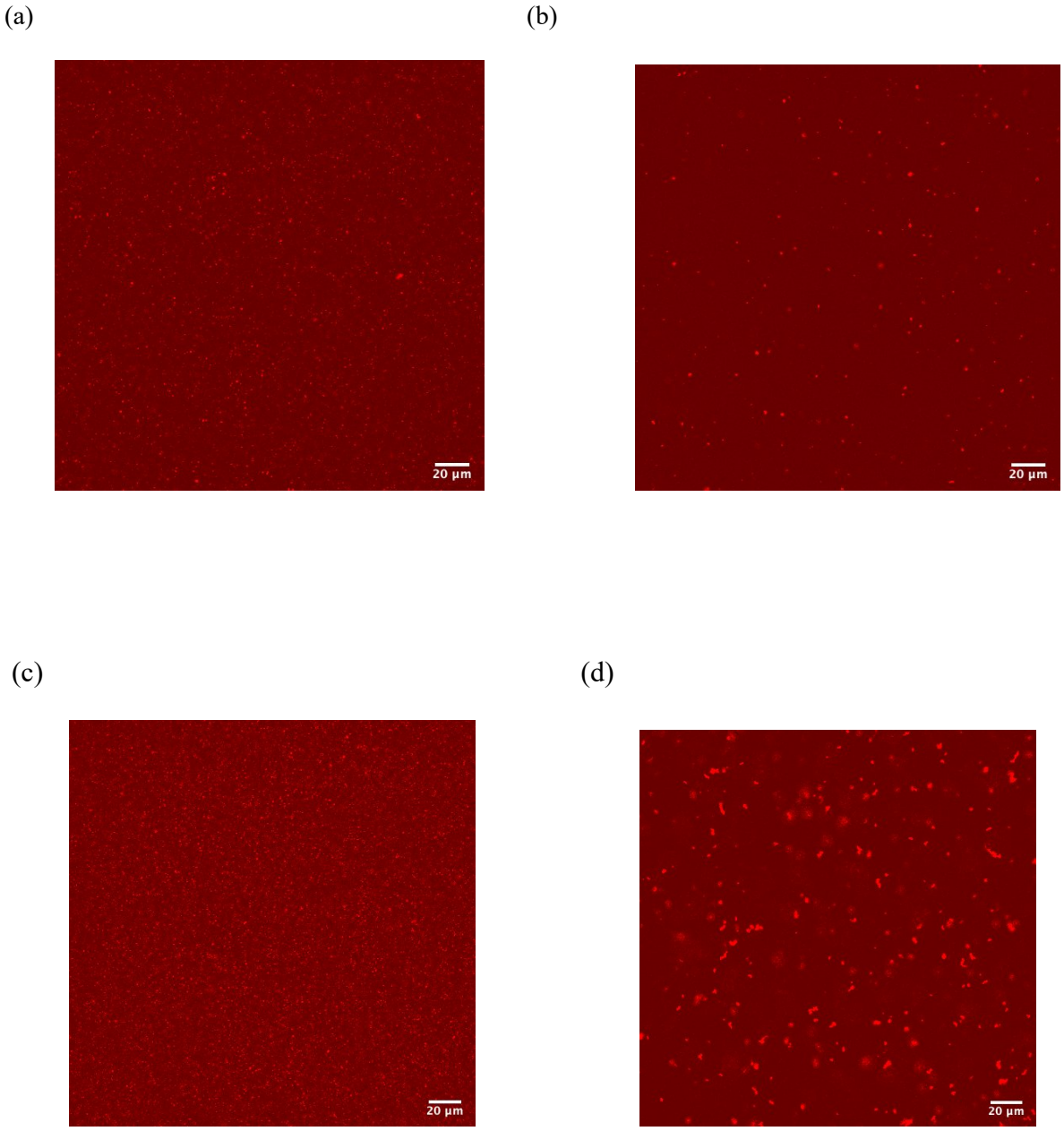

Figure 4- 5: Confocal Microscope images (brightness increased) of Cy5 streptavidin coated liposomes (a) in buffer (b) in a solution of 50mM zinc nitrate (c) in buffer (d) in a solution of 50mM calcium nitrate. The brightness of these images was increased using Fiji so that the aggregates can be observed clearly. These images show that Cy5 streptavidin coated liposomes aggregate in the presence of zinc and calcium nitrate. The scale bars are 20um.

We also did a concentration-dependent measurement (Figure 4-6) and we observe that unlike the uncoated liposomes, streptavidin-coated liposomes aggregate at higher concentrations of zinc nitrate and calcium nitrate but not at lower concentrations. The intensity vs. size graphs for these experiments are shown in Appendix C, Figure C-3. This means that the interaction between the liposomes and the cation changes upon coating the liposome with proteins.

(a)

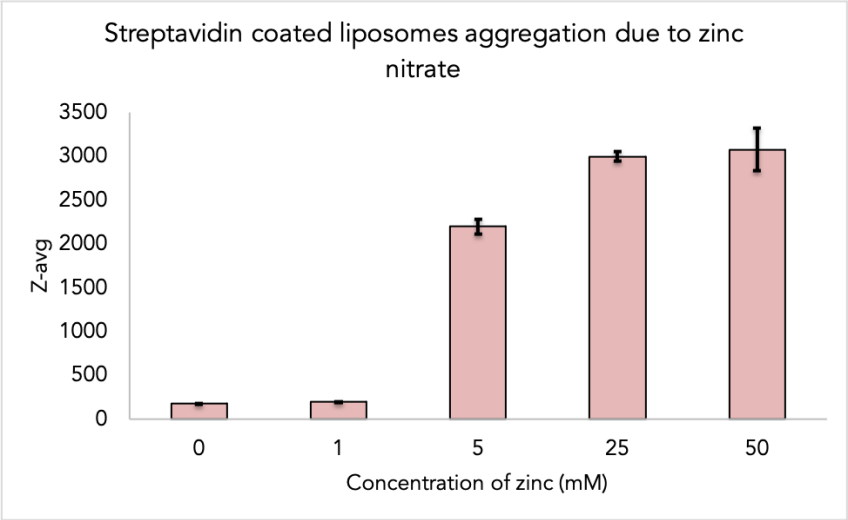

(b)

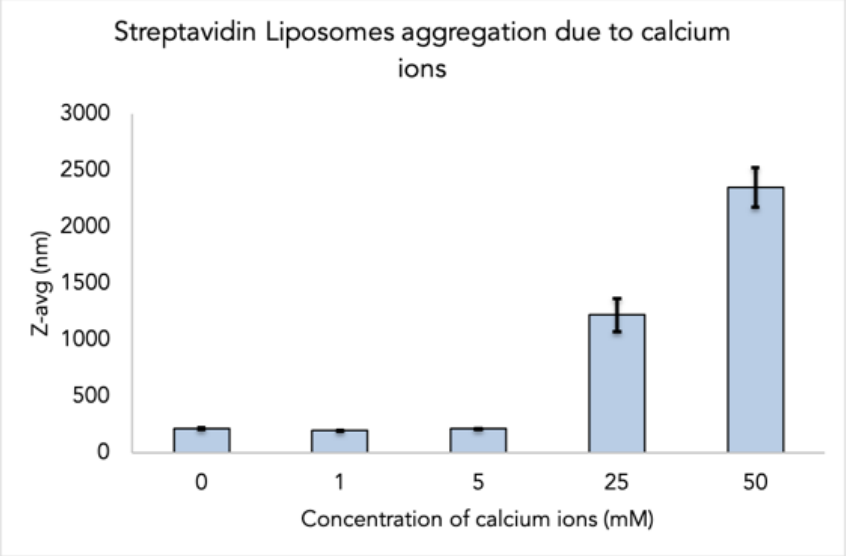

Figure 4- 6: Z-average from DLS measurements of streptavidin coated liposomes in 0, 1, 5, 25, 50mM concentrations of (a) zinc nitrate and (b) calcium nitrate. These streptavidin-coated liposomes show aggregation in the presence of high concentrations of zinc and calcium ions but no aggregation in the presence of low concentrations of these ions. Z-average values are the average and error bars are the standard deviations from three readings of the samples. This experiment is performed in 50mM HEPES buffer (pH 7).

To figure out if this effect is based on the charge of proteins, we also studied the effect of avidin, which is positively charged. Avidin-coated liposomes also show similar patterns of aggregation in the presence of zinc nitrate and calcium nitrate. (Figure 4-7). The intensity vs. size graphs for these experiments are shown in Appendix C, Figure C-4. These results demonstrate that aggregation does not depend on the charge of the protein.

(a)

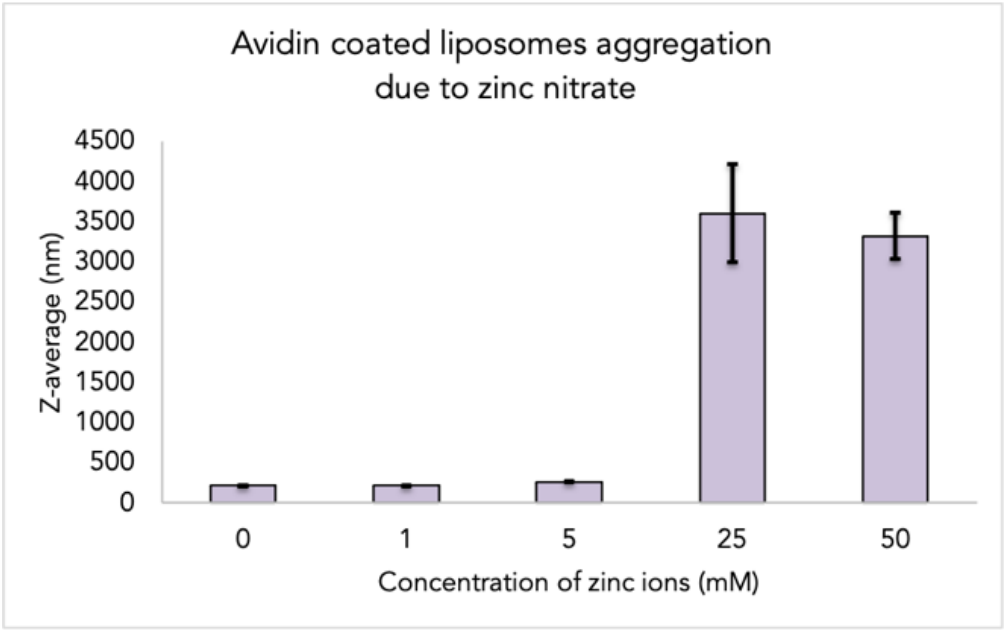

(b)

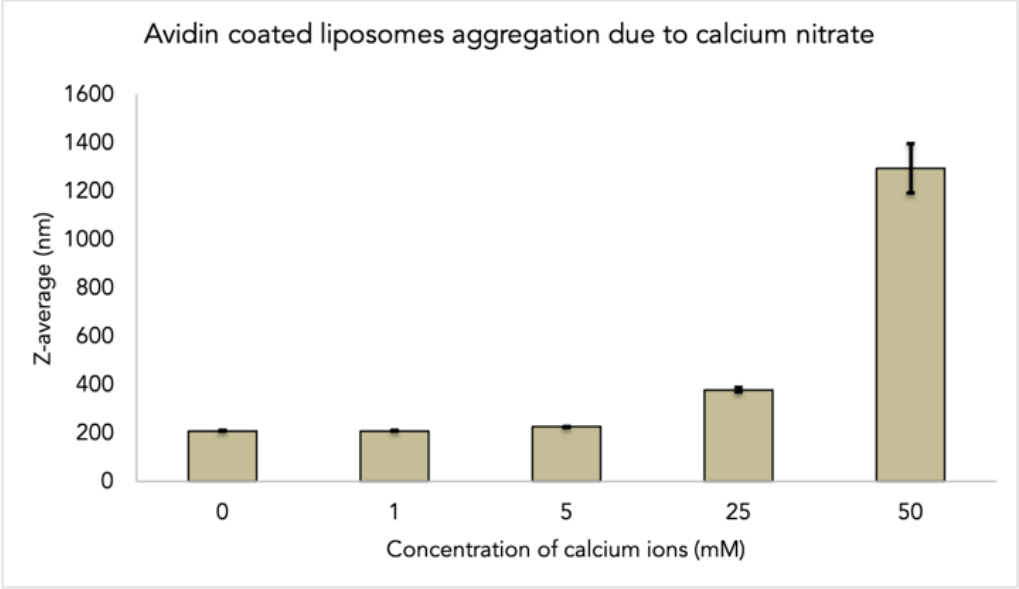

Figure 4- 7: Z-average from DLS measurements of avidin coated liposomes in 0, 1, 5, 25, 50mM concentrations of (a) zinc nitrate and (b) calcium nitrate These avidin-coated liposomes show aggregation in the presence of high concentrations of zinc and calcium ions but no aggregation in the presence of low

concentrations of these ions. Z-average values are the average and error bars are the standard deviations from three readings of the samples.

4.2.3 Aggregation of Nanoparticles

We also studied the aggregation of protein-coated polystyrene nanoparticles in the presence of zinc and calcium ions. For these experiments, we used 0.196 µm streptavidin coated microspheres. The size of these microspheres by themselves and in 50mM salt solutions was analyzed using DLS (Figure 4-8). As expected, by themselves, the beads showed a size average of around 200 nm. The results for the salt solutions show that these streptavidin-coated microspheres aggregate in the presence of high concentrations of zinc nitrate but not in the presence of high concentrations of calcium nitrate. These results are interesting because they prove that the aggregation pattern of streptavidin coated liposomes and nanoparticles are not identical. Based on these results, we hypothesize that the aggregation of streptavidin coated liposomes due to calcium involves an interaction between the lipids, protein and salt solution while the aggregation of streptavidin-coated liposomes due to zinc nitrate is driven purely by protein aggregation of streptavidin.

(a) (b)

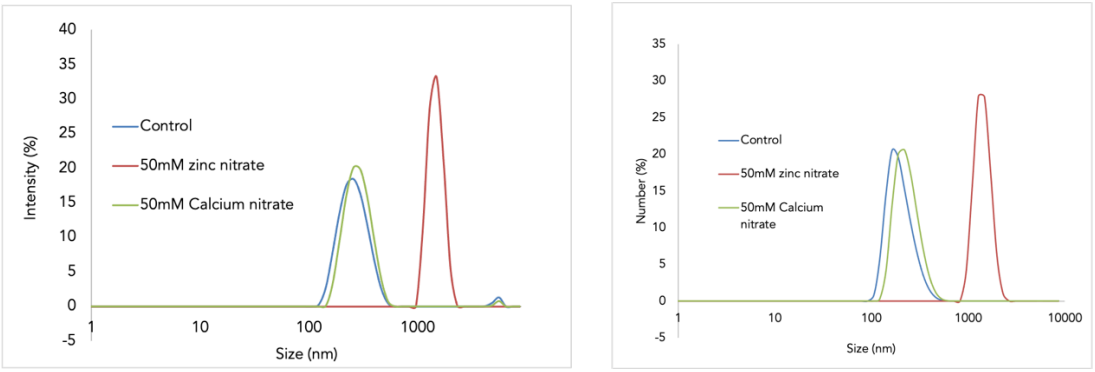

Sample Name	Z-average (nm)	PDI	Derived Count Rate (kcps)
Control	261.6	0.217	46.6
50mM zinc nitrate	2680	0.502	41.3
50mM calcium nitrate	300.4	0.253	49.3

Figure 4- 8: DLS measurements showing (a) Intensity (%) vs size (nm) and (b) Number (%) vs size (nm) for control - streptavidin coated microspheres by themselves, (blue) in the presence of 50mM zinc nitrate (red) and 50mM calcium nitrate (green). Table below shows the Z-average values, polydispersity index (PDI) and count rate for these readings. Curves are the average of three readings.

4.3 Conclusions and Future Work

In conclusion, we have demonstrated that we can control the aggregation of liposomes based on the protein attached to the liposomes and the concentration of the salt solution added. We have shown that, by themselves, liposomes can aggregate in the presence of low concentrations of zinc and calcium nitrate. When proteins such as streptavidin or avidin are attached to them through the biotin-streptavidin linkage, these liposomes aggregate in the presence of high concentration of zinc and calcium nitrate. This can be observed by performing size analysis using DLS and imaging using confocal microscopy. FRET experiments show that streptavidin aggregates in the presence of zinc ions which can be reversed upon addition of a chelator such as EDTA. We also observe that nanoparticles coated with streptavidin only aggregate upon addition of zinc nitrate but not

calcium nitrate. These results indicate the presence of interactions between the lipids, proteins and the salts. This interaction can be used for fine-tuning the motion and assembly of liposomes for targeted drug delivery applications.

Our results suggest that protein aggregation can be used as a driving force for aggregation of cargo such as liposomes and nanoparticles. Future studies can focus on optimizing this aspect and designing liposomes with protein coatings that can enable better targeted drug delivery by control of the motion, assembly, release and degradation of vesicles.

4.4 Materials and Methods

4.4.1 Materials

Streptavidin Coated Microspheres, 0.196 μm, 1% Solids were purchased from Bangs Laboratories, Inc. 1-palmitoyl-2-oleoyl-glycero-3-phosphocholine (POPC) and 1,2-dioleoyl-sn-glycero-3-phosphoethanolamine-N-(cap biotinyl) (sodium salt) (Biotin-cap-PE) were purchased from Avanti Polar Lipids. Cy5 streptavidin was purchased from Thermo Fisher Scientific. Zinc nitrate hexahydrate, magnesium nitrate, calcium nitrate, Avidin from egg white and HEPES buffer were purchased from Sigma Aldrich.

4.4.2 Methods

4.4.2.1 Nanoparticle Aggregation Experiments

50μL of streptavidin coated microspheres were taken in a centrifuge tube and centrifuged at 7000rcf for 8 mins. The supernatant was removed and replaced with 1mL of 50mM HEPES

buffer (pH 7). This process was repeated 2 more times to wash the beads. Then, the beads were sonicated for 20 minutes to break down aggregates. 1μL of this solution was diluted to 1mL in buffer solution or 50mM salt solution. DLS measurements were taken for these samples.

4.4.2.2 Synthesis of Protein- coated liposomes

POPC and Biotin-cap-PE dissolved in chloroform were added to a glass vial and the chloroform was evaporated under a stream of nitrogen. This vial was kept under vacuum for 1 hour to ensure that all the chloroform is evaporated. Then, 1mL of HEPES buffer is added to the vial and the liposomes are formed due to self-assembly. This solution is vortexed and then sonicated for 2 minutes. After sonicating, it is extruded using a 100nm membrane filter in a mini-extruder until the solution is clear. Then, 500 μL of liposome solution is mixed with 5 μL of 1mg/mL protein (streptavidin, avidin or Cy5 streptavidin) solution and shaken for 1 hour. After shaking, the excess protein is removed using a 100kDa centrifuge filter. The sample is centrifuged 3 times at 1800 rpm for 5 minutes to remove excess protein. These protein-coated liposomes are then used for subsequent experiments.

4.4.2.3 Dynamic Light Scattering (DLS) experiments

Particle size measurements are taken on the Malvern Zetasizer ZS90 (red laser). The sample is taken in a quartz cuvette and incubated for 2 minutes before measurements are taken. The temperature is set to 25° C. The results shown in the paper are the average of 3 readings for the sample.

4.4.2.4 Preparation of salt solutions

All salt solutions are filtered 6X using a 0.2-micron cellulose acetate syringe filter before being used for DLS and confocal experiments.

4.4.2.5 FRET Experiments

The procedure for FRET experiments, analysis and normalization is similar to the procedure given in Section 3.4.2.4 and Section 3.4.2.5 in Chapter 3. Instead of alkaline phosphatase, we use streptavidin. We use a starting concentration of 1mg/mL of streptavidin for the protein tagging and the starting protein to dye ratios are 1:1.06 for streptavidin and Alexa Fluor 532 and 1:2.13 for Alexa Fluor 488. and the protein to dye ratios for our experiments are shown in Table 4-1.

Sample	Protein: Dye Ratio
Streptavidin and Alexa Fluor 488	0.51
Streptavidin and Alexa Fluor 532	0.52

Table 4- 1: Tagging Ratio of streptavidin with Alexa Fluor 488 and Alexa Fluor 532 for FRET experiments.

4.4.2.6 Confocal Microscope Experiments

The confocal images are taken on a Leica TCS SP5 laser scanning confocal inverted microscope (LSCM, Leica Microsystems) with a 63× oil objective (HCX PL APOCS, 1.40 NA).

The samples are excited using the 633nm laser and emission between 670 to 770nm is measured. The liposomes are imaged and then the salt solution is added and mixed. After waiting for 5 minutes, the solution is imaged again.

4.4.2.7 Confocal Image Analysis

Image Analysis was done using ImageJ. To ensure that the aggregates are seen clearly, the brightness of the image was increased from 0 to 255 to -95 to 160 using the image adjustment function in ImageJ.

4.5 Acknowledgements

We acknowledge funding of the research by the Air Force Office of Scientific Research FA9550-20-1-0393. We also thank Prof. Andrew Zydney (Penn State) and Prof. Christine Keating (Penn State) for letting us use instruments in their lab. Thank you to Niladri, Jiaqi and other Sen lab members for helpful discussions. Any findings or conclusions expressed in this dissertation are those of the authors and do not necessarily reflect the views of the Air Force Office of Scientific Research.

4.6 References

1. Rideau, E., Dimova, R., Schwille, P., Wurm, F. R. & Landfester, K. Liposomes and polymersomes: a comparative review towards cell mimicking. *Chem. Soc. Rev.* **47**, 8572–8610 (2018).

2. Liu, P., Chen, G. & Zhang, J. A Review of Liposomes as a Drug Delivery System : Current. *Molecules* **27**, 1372 (2022).

3. Vemuri, S. & Rhodes, C. T. Preparation and characterization of liposomes as therapeutic delivery systems: a review. *Pharm. Acta Helv.* **70**, 95–111 (1995).

4. Alavi, M., Karimi, N. & Safaei, M. Application of various types of liposomes in drug delivery systems. *Adv. Pharm. Bull.* **7**, 3–9 (2017).

5. Singh, R. & Lillard, J. W. Nanoparticle-based targeted drug delivery. *Exp. Mol. Pathol.* **86**, 215–223 (2009).

6. Akbarzadeh, A., Rezaei-sadabady, R., Davaran, S., Joo, S. W. & Zarghami, N. Liposome : classification , prepNew aspects of liposomesaration , and applications. *Nanoscale Res. Lett.* **8**, 1–9 (2013).

7. Beltrán-Gracia, E., López-Camacho, A., Higuera-Ciapara, I., Velázquez-Fernández, J. B. & Vallejo-Cardona, A. A. *Nanomedicine review: Clinical developments in liposomal applications*. *Cancer Nanotechnology* vol. 10 (Springer Vienna, 2019).

8. Fujimoto, K., Ichikawa, M. & Nakamura, S. Photoinduced aggregation of liposome modified with DNA containing ultrafast DNA photo-cross-linker. *J. Chem. Technol. Biotechnol.* **97**, 295–298 (2022).

9. Haša, J., Hanuš, J. & Štěpánek, F. Magnetically Controlled Liposome Aggregates for On-Demand Release of Reactive Payloads. *ACS Appl. Mater. Interfaces* **10**, 20306–20314 (2018).

10. Somasundar, A. *et al.* Positive and negative chemotaxis of enzyme-coated liposome motors. *Nat. Nanotechnol.* **14**, 1129–1134 (2019).

11. Ghosh, S. *et al.* Motility of Enzyme-Powered Vesicles. *Nano Lett.* **19**, 6019–6026 (2019).

12. Hambidge, M., Cousins, R. J. & Costello, R. B. Zinc and health: Current status and future directions: Introduction. *J. Nutr.* **130**, (2000).

13. Maret, W. Analyzing free zinc(II) ion concentrations in cell biology with fluorescent chelating molecules. *Metallomics* **7**, 202–211 (2015).

14. Rusch, P. *et al.* Zinc distribution within breast cancer tissue of different intrinsic subtypes. *Arch. Gynecol. Obstet.* **303**, 195–205 (2021).

15. Seccareccia, D. & Mclsc, C. E. M. Palliative Care Files Cancer-related hypercalcemia Dori Seccareccia MD CCFP(EM) MClSc. *Palliat. Care Files* **56**, 244–246 (2010).

16. Martín-Molina, A., Rodríguez-Beas, C. & Faraudo, J. Effect of calcium and magnesium on phosphatidylserine membranes: Experiments and all-atomic simulations. *Biophys. J.* **102**, 2095–2103 (2012).

17. Haugland, R. P. & You, W. W. Coupling of antibodies with biotin. *Methods Mol. Biol.* **418**, 13–23 (2007).

18. Marangoni, J. M., Wu, S. C., Fogen, D., Wong, S. L. & Ng, K. K. S. Engineering a disulfide-gated switch in streptavidin enables reversible binding without sacrificing binding affinity. *Sci. Rep.* **10**, 1–15 (2020).

Chapter 5

5 Conclusions and Future Directions

5.1 Summary and Conclusions

Through the work in this thesis, I have answered fundamental questions about proteins, their interactions as well as the role that they play in our body. I have also studied the application of protein aggregation in drug delivery by studying the aggregation of protein-coated targeted drug delivery systems such as liposomes. In this thesis, I have answered the following specific questions.

1. Do enzymes aggregate or fragment while catalyzing reactions?
2. What causes the activity of alkaline phosphatase to increase during Alzheimer's disease?
3. Can protein aggregation be used to precisely control the aggregation of liposomes?

In this chapter, I provide a summary and discuss the conclusions from my thesis. I will also discuss possible future directions and research questions that arise from the studies mentioned in this thesis. Lastly, I also aim to provide a perspective about the broad field of protein aggregation.

In Chapter 1, I provide an introduction to this work. Protein aggregation is a broad term that could refer to a variety of protein associations due to varied mechanisms[1]. The study of protein aggregation can be challenging due to their dynamic nature, microscopic size of aggregates and sample alteration caused by components in commonly used techniques[2]. Scientists and researchers are constantly innovating and discovering new ways to solve these problems and understand protein aggregation. Protein aggregation plays a fundamental role in numerous diseases associated with neurodegeneration and understanding the role of proteins in these diseases will immensely help the search for cures[3]. Although protein aggregation is a well-established research field, surprisingly, the aggregation and fragmentation of enzymes in particular is a relatively new field and has not been studied in detail. The motivation to study it stems from recent evidence showing the formation of metabolons as well as the study of enzyme enhanced diffusion[4,5]. An outline about the use of protein aggregation in drug delivery systems is also provided in this chapter. The study of protein aggregation is a critical field of research and has meaningful benefits for human health and wellness.

Chapter 2 explores the question about change in the hydrodynamic diameter of enzymes during catalysis due to their aggregation or fragmentation. In this study, we demonstrate that D-Glucose fragments the enzyme glucose oxidase. Interestingly, this enzyme only fragments in the presence of its substrate. It does not show fragmentation upon addition of L-Glucose. Using Fluorescence Resonance Energy Transfer (FRET) experiments, I also identify the concentration required for the fragmentation to occur. 0.3mM or higher concentrations of D-Glucose induce

fragmentation. Glucose oxidase also de-aggregates from other enzymes if D-Glucose is added to the solution and aggregates upon addition of adenosine triphosphate (ATP) and magnesium ions. This work demonstrates that enzymes can undergo aggregation or fragmentation upon interaction with chemicals that play a role in its catalysis.

In Chapter 3, I explore the role of one of the enzymes, alkaline phosphatase in the body. As described in the Chapter 1, it has come to light in recent years that higher alkaline phosphatase levels are observed in Alzheimer's disease[6]. Using UV-Visible spectroscopy as well as FRET, I investigated this activity increase. I showed that the activity is higher due to interactions with the peptide, amyloid - β and the enzyme, acetylcholinesterase. Since higher activity of alkaline phosphatase plays a role in neurodegeneration, it is important to understand these increases in activity. Activity increases could also occur due to high concentrations of choline or acetylcholine. All of these species are present in the brain and play an important role in the disease.

In Chapter 4, I demonstrate the use of protein aggregation to control the clustering of liposomes. Using techniques such as DLS as well as confocal microscopy, we observe that liposomes coated with proteins aggregate in the presence of metal salts. The aggregation profile in the presence of different concentrations of salt changes upon coating the liposomes with proteins. We use streptavidin and avidin coated liposomes and observe that they both aggregate when high concentrations of zinc and calcium nitrate are added. Interestingly, we also observe that microspheres coated with the same protein (streptavidin) shows aggregation in the presence of zinc nitrate but not in the presence of calcium nitrate. Through this study, we demonstrate that protein-protein interactions can dictate movement and aggregation of cargo attached to the proteins which has applications in targeted drug delivery systems.

5.2 Broader Perspectives and Future Work

Protein aggregation is an important field of research. Understanding and controlling protein aggregation provides tremendous benefits in the fields of enzymology, neurodegenerative diseases, drug delivery, formulation chemistry and synthetic biology. Although these fields have been studied extensively, there is still a lot that we do not understand and some questions still remain unanswered. Future research in this field can take a variety of different directions. In this section, I will give a broader perspective of the field and how my work fits into that. The results of the studies done in this thesis give rise to new areas of research and brings up more questions that can be explored. Hence, in this section, I will also give specific examples of future directions of research that can be pursued based on my research.

5.2.1 Understanding the Mechanism of Enzyme Aggregation

In Chapter 2, we investigated the aggregation and fragmentation of enzymes and showed that the size of enzymes could change due to aggregation or fragmentation while catalyzing reactions. This observation is important as it elucidates that we cannot make assumptions that the native structure of the enzyme is retained during catalysis. Although the observations are interesting, they raise more questions about the mechanism behind this phenomenon. To better understand enzyme aggregation and fragmentation, it is important to investigate the mechanism behind it. While studying these, we had 2 major hypotheses about the mechanisms. The first one involved a change in the conformation of the enzyme while the enzyme is catalyzing the reaction. The second mechanism involved assembling and disassembling of the multimeric structures of

enzymes that is causing aggregation or fragmentation[7]. Further studies need to test these hypotheses to figure out the mechanism.

Conformational changes in enzyme structure can be investigated experimentally as well as computationally. Determining the X-ray crystal structure of these enzymes by themselves and under catalytic conditions can help us understand whether there is a structural change in the enzyme before and after substrate binding[8,9,10]. According to the induced fit theory of enzymes which was proposed in 1985 by Koshland[11], it is believed that enzymes undergo conformational changes to increase the strength of their binding with the substrate. In the future, it would be interesting to investigate whether conformational changes in glucose oxidase, invertase and maltase while binding to their substrate or ligands is causing the aggregation or fragmentation that we have observed in Chapter 2. This can also be investigated for other enzymes that show aggregation and fragmentation such as alkaline phosphatase and hexokinase. Structural dynamics of these enzymes can also be studied using molecular dynamics simulations. Molecular Dynamics (MD) models the motion of atoms and molecules[12]. MD simulations that can help elucidate structural changes in the enzyme while binding to substrate or catalyzing reactions can be extremely valuable in figuring out whether conformational changes are causing enzyme aggregation and fragmentation[13].

To test the second hypothesis and figure out whether there are changes in the multimeric structures of enzymes, we can conduct similar FRET experiments where the two dyes are on two monomers of the same enzyme rather than different batches of enzymes[14,15]. These FRET experiments can help us determine if the two monomers are dissociating or exchanging while the enzyme undergoes catalysis. Another way is to find out details about the protein structure. For example, if disulfide bonds are part of the protein structure, they can be broken down using

reducing agents such as beta - mercaptoethanol (BME) or dithiothreitol (DTT)[16]. Thus, it would be interesting to investigate if reduction of these disulfide bonds using these reducing agents helps the enzyme bind to the substrate or catalyze the reaction. These studies can give us an insight into the mechanism behind the observed aggregation and fragmentation and help us understand this phenomenon better.

5.2.2 Aggregation between Multiple Enzymes

The two enzyme experiments (glucose oxidase and invertase; glucose oxidase and maltase) in Chapter 2 show that enzymes can aggregate or de-aggregate with other enzymes in the presence of chemicals related to its catalytic reaction. In the future, it would be interesting to study the aggregation and de-aggregation between two enzymes upon addition of species related to each of their catalysis. For example, preliminary results show that hexokinase and alkaline phosphatase aggregate together upon addition of 20mM ATP and 20mM magnesium ions (Figure 5-1). This procedure for the experiment and analysis is similar to the procedure used for FRET experiments in Chapter 2 and is described in Section 2.4 in Chapter 2. Understanding these patterns of aggregation and de-aggregation can help us understand the formation of enzyme metabolons. Furthermore, although the two enzyme experiments done in Chapter 2 looked at cascade enzymes, the result shown in Figure 5-1 indicate that there could be association and disassociation between opposing enzymes such as kinases and phosphatases. This can be explored using FRET as well as other methods using in Chapter 2 such as DLS and AFM. Studying these associations will help us understand the working of these enzymes better and also answer questions about the formation and breaking of enzyme clusters in the body.

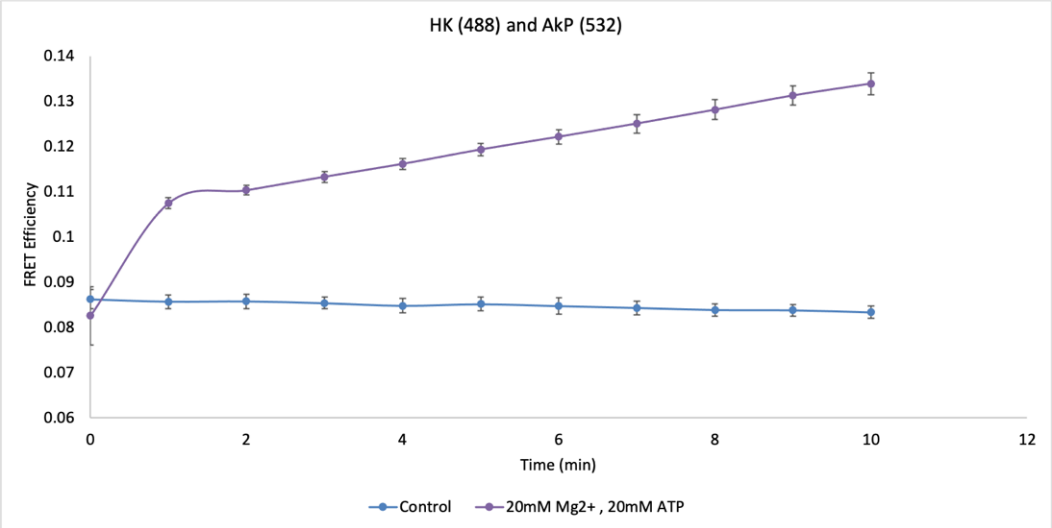

Figure 5- 1: FRET efficiency with respect to time for 0.1 micromolar hexokinase (HK) tagged with Alexa Fluor-488 and 0.1 micromolar M alkaline phosphatase (AkP) tagged with Alexa Fluor 532 (blue) and 0.1 micromolar hexokinase (HK) tagged with Alexa Fluor-488 and 0.1 micromolar alkaline phosphatase (AkP) tagged with Alexa Fluor 532 in the presence of 20mM magnesium chloride and 20mM adenosine triphosphate (ATP). Results show that hexokinase and alkaline phosphatase aggregate upon addition of ATP and magnesium chloride. Results are the average and error bars are the standard deviation from three trials. Experiments are performed in 50mM HEPES buffer.

5.2.3 Interaction between Alkaline Phosphatase and Amyloid beta

In Chapter 3, using FRET, we have shown that the presence of amyloid - β de-aggregates alkaline phosphatase. Investigating the specific interaction between these two can help us understand the role of alkaline phosphatase in Alzheimer's disease better. These studies can try to identify the specific residues that are involved in this interaction. Synthesizing mutations can help us identify these amino acid residues. Knowing these residues can help us understand the nature of the interaction between the two. We can also test the de-aggregation of alkaline phosphatase in the presence of other peptides of amyloid - β such as A β-18, A β-40 and so on. It would also be interesting to test this interaction in the presence of amyloid - β in oligomeric and fibrillar state to see if the tertiary structure of the peptide plays a role in this interaction. Another approach would be to investigate what chemical phenomenon is causing this interaction. For example, if the

interaction is ionic, we would observe a difference upon addition of large amounts of salts. Using these techniques, we can identify what is causing the de-aggregation of alkaline phosphatase upon addition of amyloid - β.

Another strategy will involve fluorescently tagging amyloid - β and investigating if alkaline phosphatase aggregates with amyloid - β which causes de-aggregation of alkaline phosphatase with itself. Although fluorescent tagging of the peptide has been challenging for us in the past, a thorough study could identify the right kind of functional groups on the dye that are needed for it to be attached to amyloid - β peptide. More FRET experiments can also help us identify the aggregation of amyloid - β and see if there is any change in amyloid - β aggregation upon addition of alkaline phosphatase. These studies will be useful in understanding the specific interactions between the two species that can help us understand Alzheimer's disease better.

5.2.3 Effect of Protein-protein Interactions on Enzyme Activity

In Chapter 3, we also showed that amyloid - β and acetylcholinesterase can affect alkaline phosphatase activity. In general, the most common causes of increase in enzymatic activity are generally believed to be changes in pH, temperature, substrate concentration etc. However, our study showed that other proteins can also act as enhancers of enzymatic activity. These results shed light on the phenomenon that enzymatic activity for certain enzymes can be affected by their interaction with other enzymes, proteins, or peptides. This phenomenon has also been shown before for enzyme metabolons. We know that enzymes in cascades aggregate together to form metabolons which causes substrate channeling. By attaching cascade enzymes on microspheres and studying their colocalization and activity, Xiong and co-authors have shown that enzyme activity increases upon colocalization of the cascade enzymes[17]. The effect of these interactions

on enzymatic activity can be investigated further by assaying enzyme activity for commonly used enzymes such as urease, catalase, glucose oxidase etc. in the presence of other proteins that are present in cells. We know that the cell is a crowded environment. Scientists have estimated that there are 2-4 million proteins per cubic micron in a cell[18]. Hence, it is possible that these enzymes interact with other proteins present in the cell which causes changes in their catalytic activity. Studying these interactions will help us understand and discover associations between proteins.

Another research direction could involve studying whether this phenomenon is general for all phosphatases. There are numerous protein phosphatases in the body[19]. It would be interesting to study whether the activity and interaction state of other phosphatases such as acid phosphatase change in the presence of amyloid - β and acetylcholinesterase. These studies will not only help us understand the specific nature of the interactions that we have observed but also answer general questions about how protein-protein interactions influence the rate at which enzymes catalyze reactions.

5.2.4 Liposome Aggregation and Chemotaxis for Drug Delivery Applications

Undesired liposome aggregation is considered harmful and researchers have been trying to figure out ways to increase the stability of liposomes to prevent their aggregation[20]. However, our study as well as other similar studies have pointed out that by figuring out a way to control liposome aggregation, it can be used to our advantage to give additional functionalities to drug delivery vehicles[21,22] . We show that based on the salt concentration and the protein attached to the vesicles, we can control their aggregation. In the future, it would be interesting to study if these liposomes also show chemotaxis towards these salt solutions. Since uncoated liposomes aggregate in the presence of low concentration of zinc ions while streptavidin coated liposomes aggregate in

the presence of high concentrations, it would be interesting to study the chemotactic behavior of uncoated and protein-coated liposomes in the presence of different concentrations of salts. This can be done by using a 3-inlet-1 outlet microfluidic channel that has previously been used by our group[23].

Additionally, since we want to potentially understand this aggregation in a physiological environment, studying aggregation in the presence of a crowded environment will be useful to understand aggregation of liposomes in the body. This can be done by studying aggregation in the presence of Ficoll which can mimic the crowded cytosolic environment in the cell[24]. Finding new functionalities and improving drug delivery systems can help treatment of diseases and improve human lives.

5.3 References

1. Philo, J. & Arakawa, T. Mechanisms of Protein Aggregation. *Curr. Pharm. Biotechnol.* **10**, 348–351 (2009).
2. Housmans, J. A. J., Wu, G., Schymkowitz, J. & Rousseau, F. A guide to studying protein aggregation. *FEBS J.* **290**, 554–583 (2023).
3. Ross, C. A. & Poirier, M. A. Protein aggregation and neurodegenerative disease. *Nat. Med.* **10**, S10 (2004).
4. Zhang, Y. & Hess, H. Enhanced Diffusion of Catalytically Active Enzymes. *ACS Cent. Sci.* **5**, 939–948 (2019).
5. Zhao, X. *et al.* Substrate-driven chemotactic assembly in an enzyme cascade. *Nat. Chem.* **10**, 311–317 (2018).

6. Vardy, E. R. L. C., Kellett, K. A. B., Cocklin, S. L. & Hooper, N. M. Alkaline Phosphatase Is Increased in both Brain and Plasma in Alzheimer's Disease. *Neurodegener. Dis.* **9**, 31–37 (2011).

7. Fernandez-Lafuente, R. Stabilization of multimeric enzymes: Strategies to prevent subunit dissociation. *Enzyme Microb. Technol.* **45**, 405–418 (2009).

8. Fraser, J. S. *et al.* Accessing protein conformational ensembles using room-temperature X-ray crystallography. *Proc. Natl. Acad. Sci. U. S. A.* **108**, 16247–16252 (2011).

9. Rejto, P. A. & Freer, S. T. Protein conformational substates from X-ray crystallography. *Prog. Biophys. Mol. Biol.* **66**, 167–196 (1996).

10. Grant, B. J., Gorfe, A. A. & McCammon, J. A. Large conformational changes in proteins: Signaling and other functions. *Curr. Opin. Struct. Biol.* **20**, 142–147 (2010).

11. Koshland, D. E. The Key–Lock Theory and the Induced Fit Theory. *Angew. Chemie Int. Ed. English* **33**, 2375–2378 (1995).

12. Patodia, S. Molecular Dynamics Simulation of Proteins: A Brief Overview. *J. Phys. Chem. Biophys.* **4**, 4–7 (2014).

13. Ye, F. *et al.* Biochemical Studies and Molecular Dynamic Simulations Reveal the Molecular Basis of Conformational Changes in DNA Methyltransferase-1. *ACS Chem. Biol.* **13**, 772–781 (2018).

14. Heyduk, T. Measuring protein conformational changes by FRET / LRET Tomasz Heyduk. *Curr. Opin. Biotechnol.* **13**, 292–296 (2002).

15. Kim, H. D. *et al.* Mg2+-dependent conformational change of RNA studied by fluorescence correlation and FRET on immobilized single molecules. *Proc. Natl. Acad. Sci. U. S. A.* **99**, 4284–4289 (2002).

16. Mthembu, S. N., Sharma, A., Albericio, F. & de la Torre, B. G. Breaking a Couple: Disulfide Reducing Agents. *ChemBioChem* **21**, 1947–1954 (2020).

17. Xiong, Y., Tsitkov, S., Hess, H., Gang, O. & Zhang, Y. Microscale Colocalization of Cascade Enzymes Yields Activity Enhancement. *ACS Nano* **16**, 10383–10391 (2022).

18. Milo, R. What is the total number of protein molecules per cell volume? A call to rethink some published values. *BioEssays* **35**, 1050–1055 (2013).

19. Chen, M. J., Dixon, J. E. & Manning, G. Genomics and evolution of protein phosphatases. *Sci. Signal.* **10**, 1–18 (2017).

20. Akbarzadeh, A., Rezaei-sadabady, R., Davaran, S., Joo, S. W. & Zarghami, N. Liposome : classification , prepNew aspects of liposomesaration , and applications. *Nanoscale Res. Lett.* **8**, 1–9 (2013).

21. Haša, J., Hanuš, J. & Štěpánek, F. Magnetically Controlled Liposome Aggregates for On-Demand Release of Reactive Payloads. *ACS Appl. Mater. Interfaces* **10**, 20306–20314 (2018).

22. Lombardo, D., Calandra, P., Barreca, D., Magazù, S. & Kiselev, M. A. Soft interaction in liposome nanocarriers for therapeutic drug delivery. *Nanomaterials* **6**, (2016).

23. Somasundar, A. *et al.* Positive and negative chemotaxis of enzyme-coated liposome motors. *Nat. Nanotechnol.* **14**, 1129–1134 (2019).

24. Zhao, X. *et al.* Substrate-driven chemotactic assembly in an enzyme cascade. *Nat. Chem.* **10**, 311–317 (2018).

Appendix A

Supporting Information for Chapter 2

A.1 Supplementary Texts

Thank you to Kayla Gentile for the calculation of Förster Radius and FRET efficiencies in this section

A.1.2 Calculation of FRET Efficiencies

We have calculated FRET efficiency using the following equation (Equation A-1).

$$\text{FRET Efficiency} = \frac{F_{555} - \gamma F_{515}}{F_{515} + (F_{555} - \gamma F_{515})} \qquad \text{(A-1)}$$

In this equation, F_{515} and F_{555} denotes the fluorescence emission values at 510 to 520 nm and 550 to 560 nm, respectively when excited at 488 nm, when both dyes are used in the experiment, and γ is the correction factor that corrects for the emission of the donor at 560 nm. This FRET efficiency describes the portion of enzymes in the sample that are within a distance of 6 nm of each other.

γ is the correction factor and it is calculated using the following equation.

$$\gamma = \frac{F_{555}Donor}{F_{515}Donor} \quad \text{(A-2)}$$

In this equation, $F_{515}Donor$ and $F_{555}Donor$ denote the fluorescence emission values for the donor dye Alexa Fluor 488 from 510 to 520 nm (average of all 3 values) and 550 to 560 nm (average of all 3 values) respectively when the sample is excited at 488 nm. In this case, only the donor dye (AF488) is present in the experiment. We take average of emissions from 510 to 520 and 550 to 560 so that the noise in the system is minimized.

A.1.1 Förster Radius Calculation for the two dyes: Alexa Fluor 488 and Alexa Fluor 532

Föster radius is defined as the distance between the two FRET dyes for 50% efficient energy transfer. For our experiments, we used the two dyes- Alexa Fluor 488 and Alexa Fluor 532. The Förster radius for our experiments between these two dyes is calculated as shown below[1].

$$R_0 = 0.211\sqrt[6]{\kappa^2 n^{-4} Q_D J(\lambda)} \quad \text{(A-3)}$$

In this equation, R_0 denotes the Förster radius, κ^2 denotes the orientation factor, n denotes the fluid refractive index, Q_D denotes the quantum yield of the donor and $J(\lambda)$ denotes the overlap integral. Q_D and $J(\lambda)$ values were obtained from https://www.fpbase.org/fret/.

$$R_0 = 0.211\sqrt[6]{0.667(1.33)^{-4}(0.92)(3.44e^{15}\ M^{-1}cm^{-1}nm^4)} \quad \text{(A-4)}$$

$$R_0 = 62.5\ \dot{A}$$

These equations show that the distance between the donor (Alexa Fluor 488) and the acceptor (Alexa Fluor 532) has to be <6.25nm for the energy transfer to happen. Thus, the sample only shows FRET when the two dyes are within 6 nanometers of each other. If the distance is more than that, the sample will not show FRET and we will not see emission of the acceptor due to excitation of the donor.

A.2 Supplementary Tables

Enzyme	**Starting Conc.**	**Starting Enzyme:488 Dye Ratio**	**Starting Enzyme: 532 Dye Ratio**	**Final Mol Dye: Mol Protein**
Glucose oxidase	12.5 µM	1:10	1:5	~ 1.1 (488) ~1.1 (532)
Invertase	22.2 µM	N/A	1.1:1	N/A 1.4 (532)
Maltase	31.7 µM	N/A	1.6:1	N/A 1.5 (532)

Table C- 1: Table showing the details for tagging of glucose oxidase, invertase and maltase with the donor and acceptor dyes (Alexa Fluor 488 and Alexa Fluor 532) for FRET experiments. In this table, we show the starting concentration and enzyme to dye ratio as well as the final dye to protein ratio obtained after tagging.

A.3 Supplementary Figures

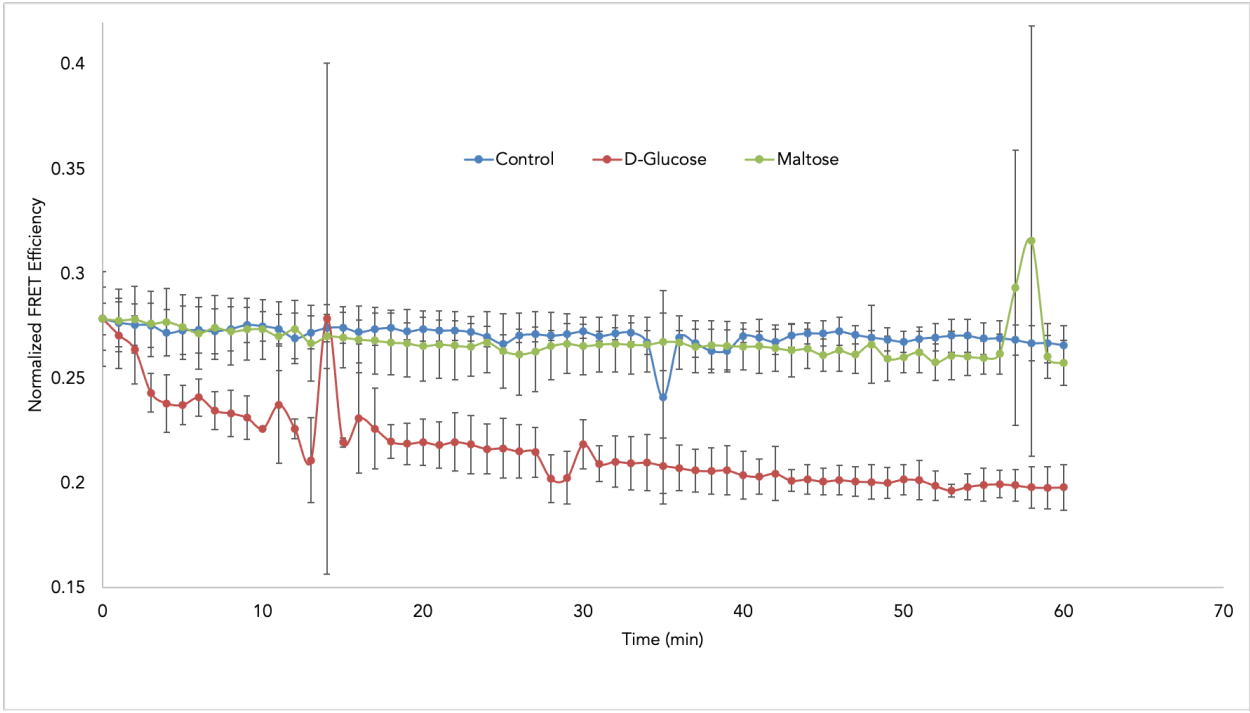

Figure A- 1: This figure shows the same data as Figure 2-8 but includes outliers. Normalized FRET efficiency with respect to time for 0.1 µM glucose oxidase tagged with Alexa Fluor 488 and 0.1 µM maltase tagged with Alexa Fluor 532 (blue); 0.1 µM glucose oxidase tagged with Alexa Fluor 488 and 0.1 µM maltase tagged with Alexa Fluor 532, 1mM D-Glucose (red), 0.1 µM glucose oxidase tagged with Alexa Fluor 488 and 0.1 µM maltase tagged with Alexa Fluor 532, 1mM Maltose (green). The buffer that was used to make all solutions for the experiment was 50 mM MES (pH 6). Values are the average and error bars are the standard deviation from three trials.

A.4 References

1. Wu, P.G. and Brand, L., 1994. Resonance energy transfer: methods and applications. *Analytical biochemistry*, *218*(1), pp.1-13.

Appendix B

B Supporting Information for Chapter 3

B.1 Supplementary Text

B.1.1 Calculation of molar extinction coefficient

To calculate the molar extinction coefficient of p-nitrophenol (PNP), we measured the absorbance at 405 nm of different concentrations of PNP. (Figure B-1). The slope of line (5400 $M^{-1}cm^{-1}$) is the molar extinction coefficient used for our experiments.

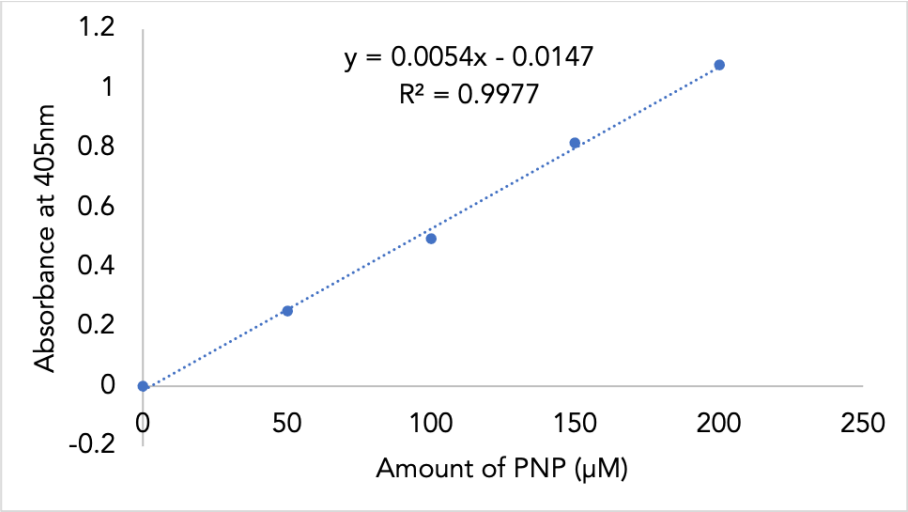

Figure B- 1: Absorbance at 405 nm measured for concentrations of 0, 50, 100, 150, 200 µM of 4-nitrophenol. The linear trendline for the data is shown. The equation for the trendline is y = 0.0054x – 0.0147 and the R^2 value is 0.9977. Experiments are carried out in 50mM HEPES buffer (pH 7).

B.1.2 Synthesis of Amyloid – β

Thanks to Suja Rani Maddukuri for the peptide synthesis and MALDI-TOF in this section.

The amyloid - β peptide was synthesized by the Macromolecular Synthesis Core at Penn State. It is a 42 amino acid peptide. The peptide sequence and MALDI-TOF (Figure B-2) is given below.

Peptide Sequence: H-Asp-Ala-Glu-Phe-Arg-His-Asp-Ser-Gly-Tyr-Glu-Val-His-His-Gln-Lys-Leu-Val-Phe-Phe-Ala-Glu-Asp-Val-Gly-Ser-Asn-Lys-Gly-Ala-Ile-Ile-Gly-Leu-Met-Val-Gly-Gly-Val-Val-Ile-Ala-OH.

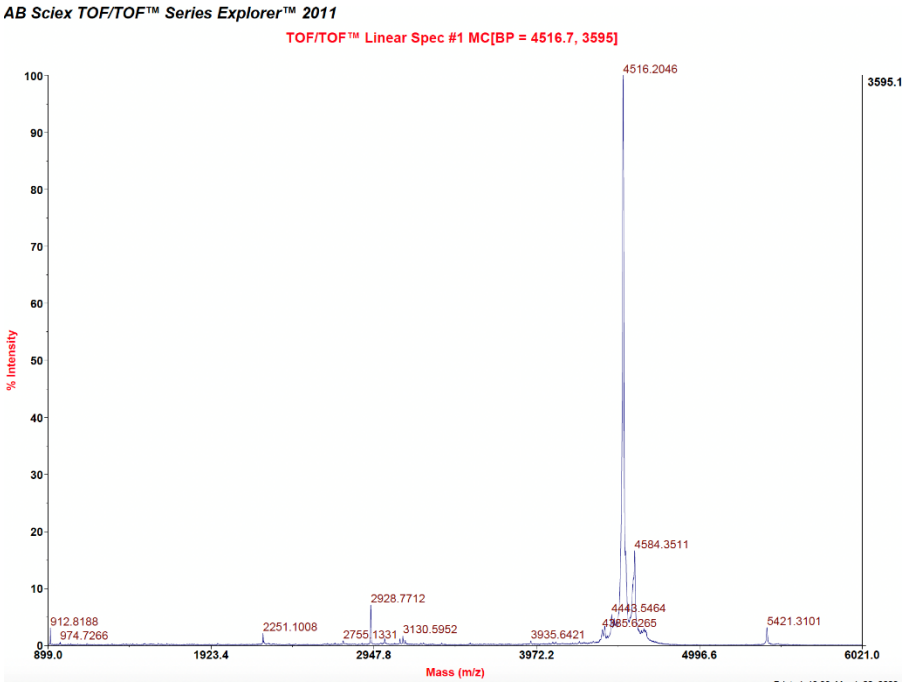

Figure B- 2: MALDI-TOF of the synthesized amyloid β peptide taken in linear mode at the Macro Core Facility at Penn State. The graph shows % Intensity vs Mass (m/z). The highest peak is at a Mass (m/z) value of 4516.2046.

B.2 Supplementary Figures

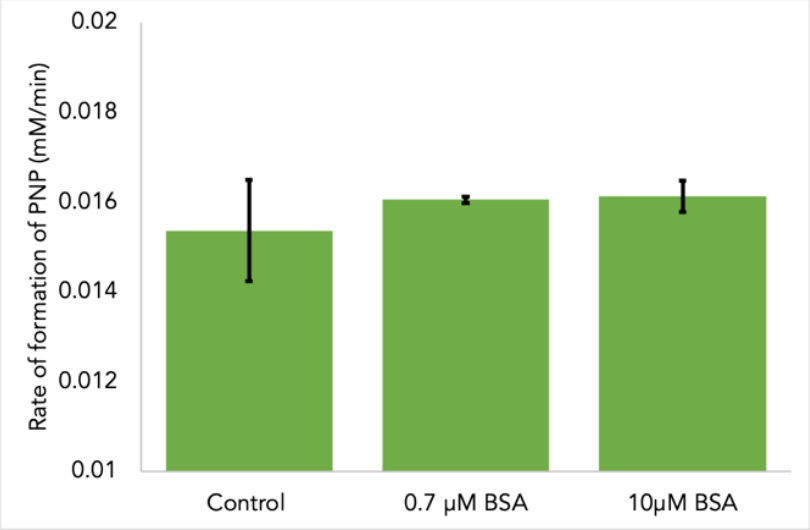

Figure B- 3: Rate of formation of p-nitrophenol (PNP) measured using UV Visible spectroscopy in the presence of 0.7 µM and 10 µM concentrations of bovine serum albumin (BSA) due to 0.2µM alkaline phosphatase. These results show that the rate of formation of PNP does not change due to the addition of BSA. Results are the average and error bars represent the standard deviation of four trials for control and three trials for 10 and 0.7 µM BSA. Experiments are carried out in 50mM HEPES buffer (pH 7).

(a)

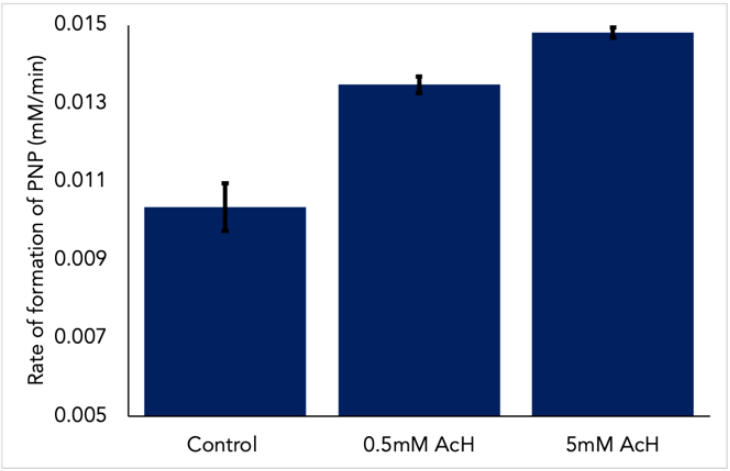

(b)

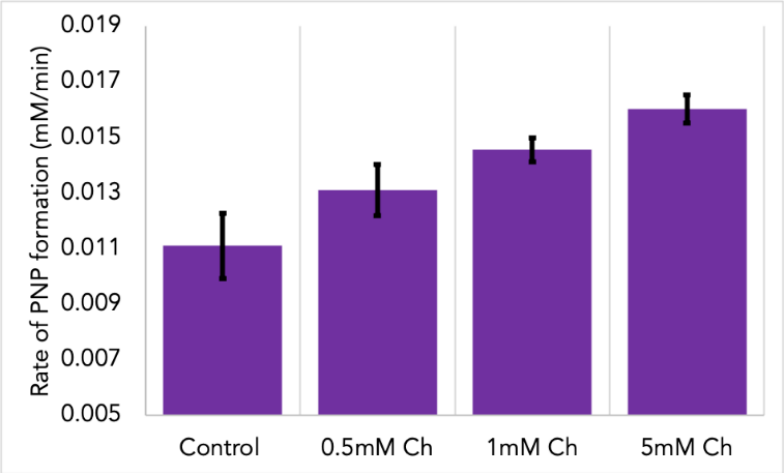

Figure B- 4: Rate of formation of PNP measured using UV Visible spectroscopy in the presence of (a) 0, 0.5 and 5mM acetylcholine chloride (AcH) and (b) 0, 0.5, 1, 5 mM Choline chloride (Ch) due to 0.2 μM alkaline phosphatase. Results are the average and error bars represent the standard deviation from three trials. These results show that acetylcholine chloride and choline chloride in millimolar concentrations increases the rate of formation of PNP. As the concentration of AcH or Ch increases, the rate of formation of PNP also increases. Experiments are carried out in 50mM HEPES buffer (pH 7).

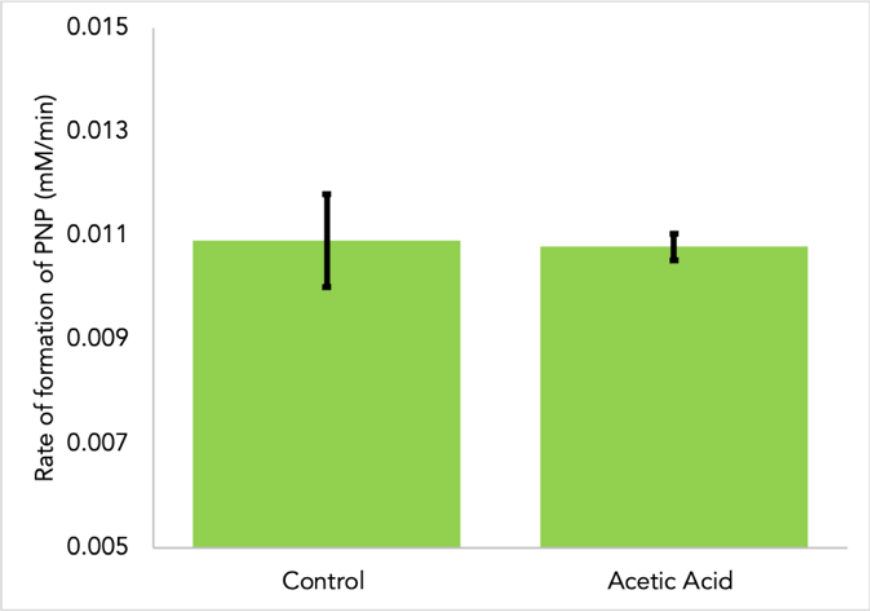

Figure B- 5: Rate of formation of PNP measured using UV Visible spectroscopy in the presence of 0.5 mM acetic acid due to 0.2 µM alkaline phosphatase. These results show that the rate of formation of PNP does not change upon addition of 0.5mM acetic acid. Results are the average and error bars represent the standard deviation from 3 trials. Experiments are carried out in 50mM HEPES buffer (pH 7).

Appendix C

C Supporting Information for Chapter 4

C.1 Supplementary Figures

C.1.1 Aggregation of Uncoated Liposomes

(a) (b)

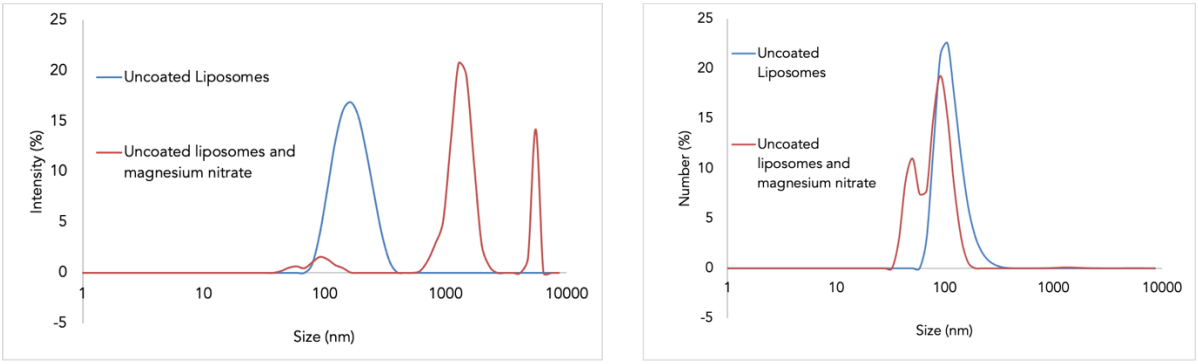

Sample	Z-average (nm)	PDI	Derived Count Rate (kcps)
Uncoated Liposomes	156.8	0.098	1317.8
Uncoated Liposomes and magnesium nitrate	4249	0.591	1106.8

Figure C- 1: DLS measurements showing (a) Intensity (%) vs size (nm) and (b) Number (%) vs size for uncoated liposomes without (blue) and with 50mM magnesium nitrate (red). The table below the image shows the Z-average, polydispersity index (PDI) and count rate for the samples. These curves are averages of three readings for the samples. These experiments were performed in 50mM HEPES (pH 7) buffer.

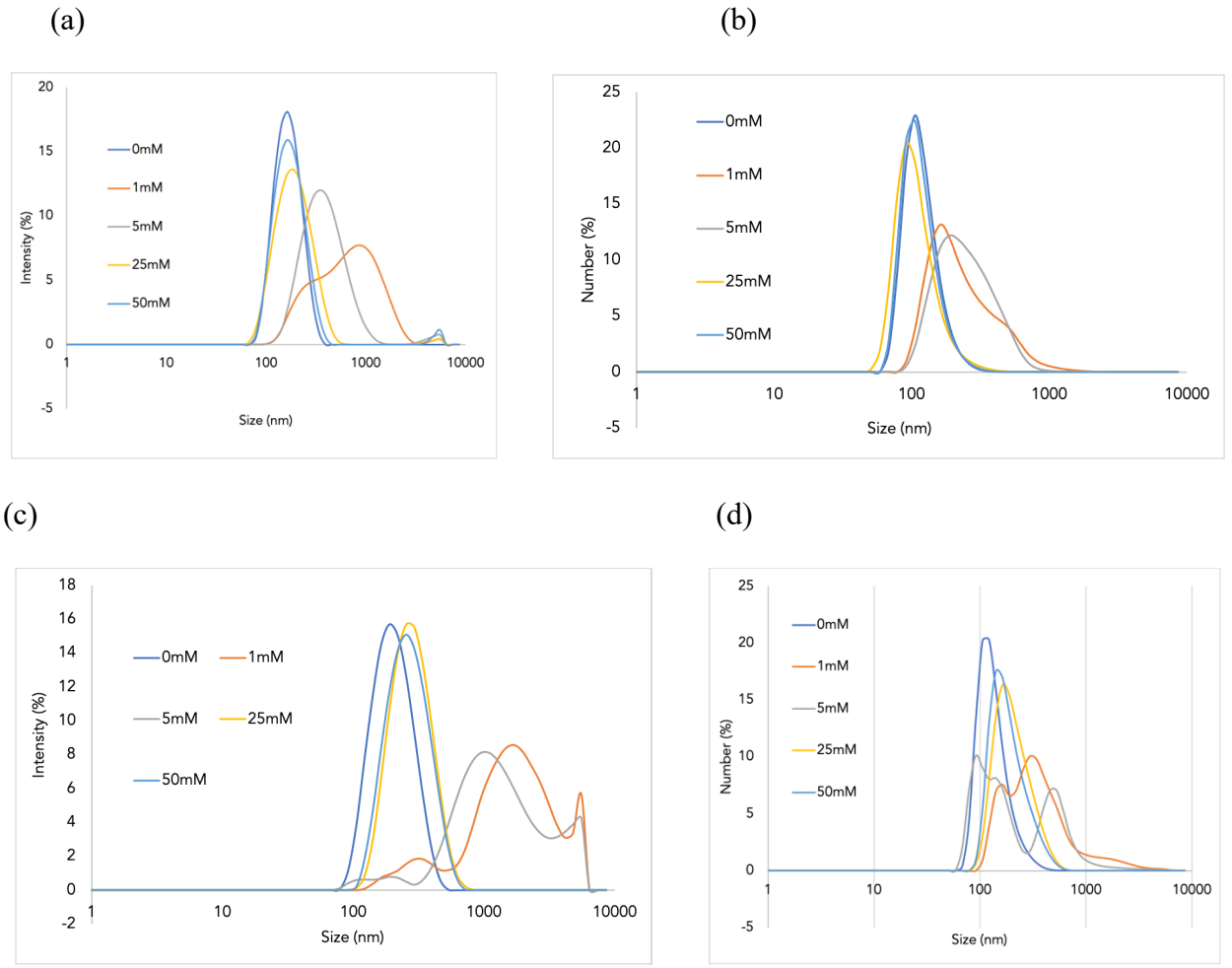

Figure C- 2: DLS measurements showing (a) Intensity (%) vs size (nm) and (b) Number (%) vs size for uncoated liposomes in the presence of 0mM (blue), 1 mM (orange), 5mM (gray), 25mM (yellow) and 50mM (light blue) zinc nitrate and (c) Intensity (%) vs size (nm) and (d) Number (%) vs size (nm) for uncoated liposomes in the presence of 0mM (blue), 1 mM (orange), 5mM (gray), 25mM (yellow) and 50mM (light blue) calcium nitrate. These curves are averages of three readings for the samples. These experiments were performed in 50mM HEPES (pH 7) buffer.

C.1.2 Aggregation of Protein-coated liposomes

(a) (b)

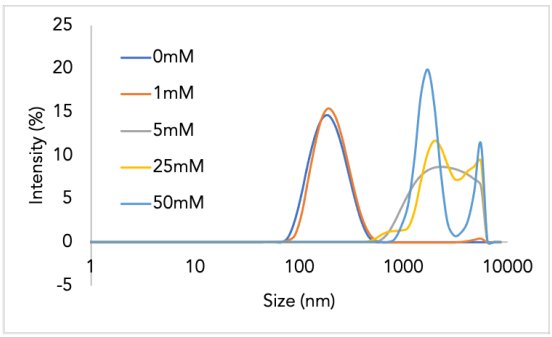

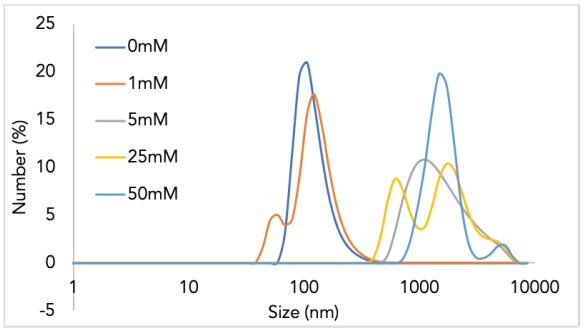

(c) (d)

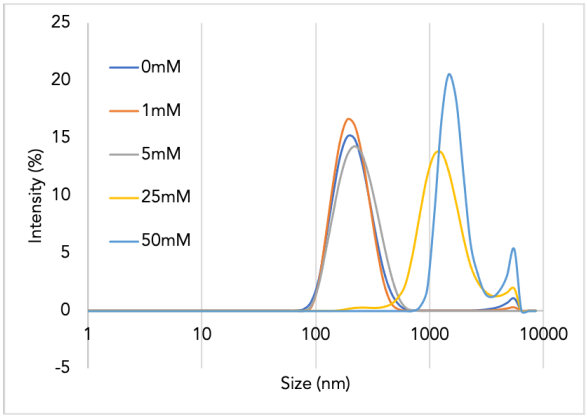

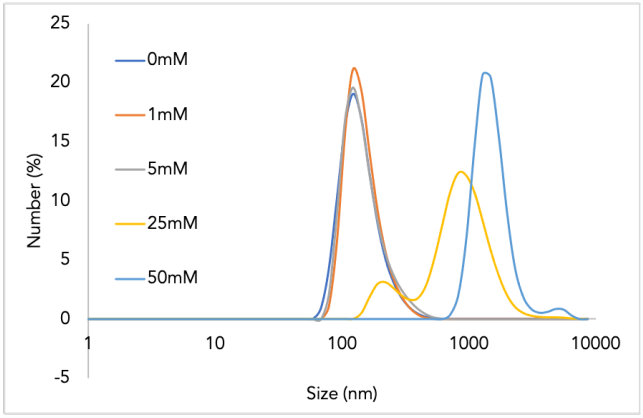

Figure C- 3: DLS measurements showing (a) Intensity (%) vs size (nm) and (b) Number (%) vs size for streptavidin coated liposomes in the presence of 0mM (blue), 1 mM (orange), 5mM (gray), 25mM (yellow) and 50mM (light blue) zinc nitrate and (c) Intensity (%) vs size (nm) and (d) Number (%) vs size (nm) for streptavidin coated liposomes in the presence of 0mM (blue), 1 mM (orange), 5mM (gray), 25mM (yellow) and 50mM (light blue) calcium nitrate. These curves are averages of three readings for the samples. These experiments were performed in 50mM HEPES (pH 7) buffer.

(a) (b)

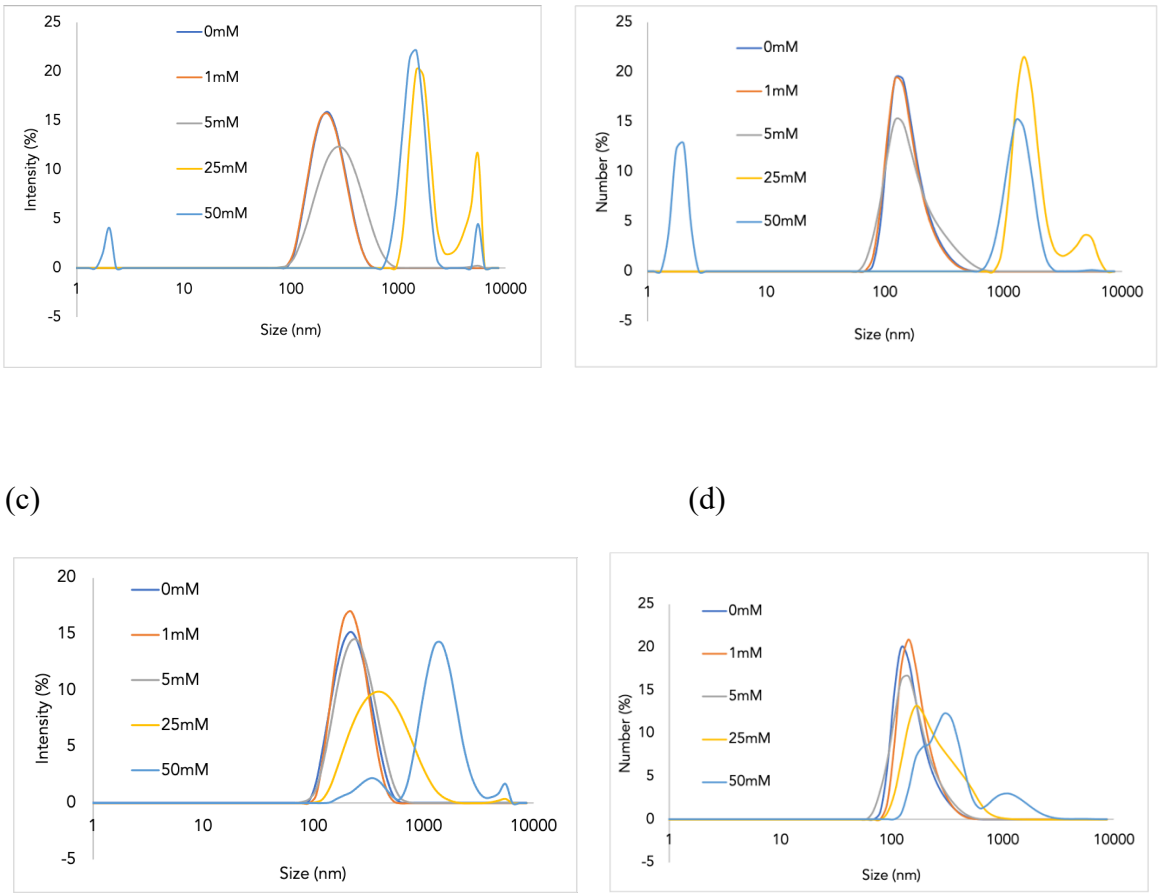

Figure C- 4: DLS measurements showing (a) Intensity (%) vs size (nm) and (b) Number (%) vs size for avidin coated liposomes in the presence of 0mM (blue), 1 mM (orange), 5mM (gray), 25mM (yellow) and 50mM (light blue) zinc nitrate and (c) Intensity (%) vs size (nm) and (d) Number (%) vs size (nm) for avidin coated liposomes in the presence of 0mM (blue), 1 mM (orange), 5mM (gray), 25mM (yellow) and 50mM (light blue) calcium nitrate. These curves are averages of three readings for the samples. These experiments were performed in 50mM HEPES (pH 7) buffer.

VITA

Ashlesha Bhide

Ashlesha grew up in Thane, India and got a Bachelor of Technology degree in Dyestuff Technology from the Institute of Chemical Technology, Mumbai in 2018. During her undergrad, she worked with Dr. Satyajit Saha to investigate the transformation of pyrazalone and its derivatives to complex intermediates. She also worked in the Research and Development department at Heubach Color Pvt. Ltd. in Ankleshwar, Gujarat in the summer of 2017. After coming to Penn State, she joined the Sen lab. In the past 5 years, she has investigated the aggregation and fragmentation of enzymes. Using spectroscopic methods, she showed that glucose oxidase fragments upon addition of D-Glucose. She also showed that alkaline phosphatase activity increases in the presence of amyloid - β and acetylcholinesterase using UV-Visible spectroscopy. After this, she also studied the aggregation of protein-coated liposomes. Apart from research, she enjoys participating in outreach events, traveling, running and cooking.